Proton and Ion Linear Accelerators

Yuri Batygin[1], Sergey Kurennoy[1], Sebastian Szustkowski[1], Salvador Sosa Guitron[1], Vyacheslav Yakovlev [2],

[1]Los Alamos National Laboratory
[2]Fermi National Accelerator Laboratory

U.S. Particle Accelerator School

July 15 – July 26, 2024

Proton and Ion Linear Accelerators

Cavity design. Linac architecture, Lecture 14

Vyacheslav Yakovlev, Fermilab

U.S. Particle Accelerator School (USPAS)

Education in Beam Physics and Accelerator Technology

July 24, 2024

RF Accelerating Structures

Outline:

🔯 **Fermilab**

Chapter 10.

SRF Cavity Design Approaches for Linear Accelerators.
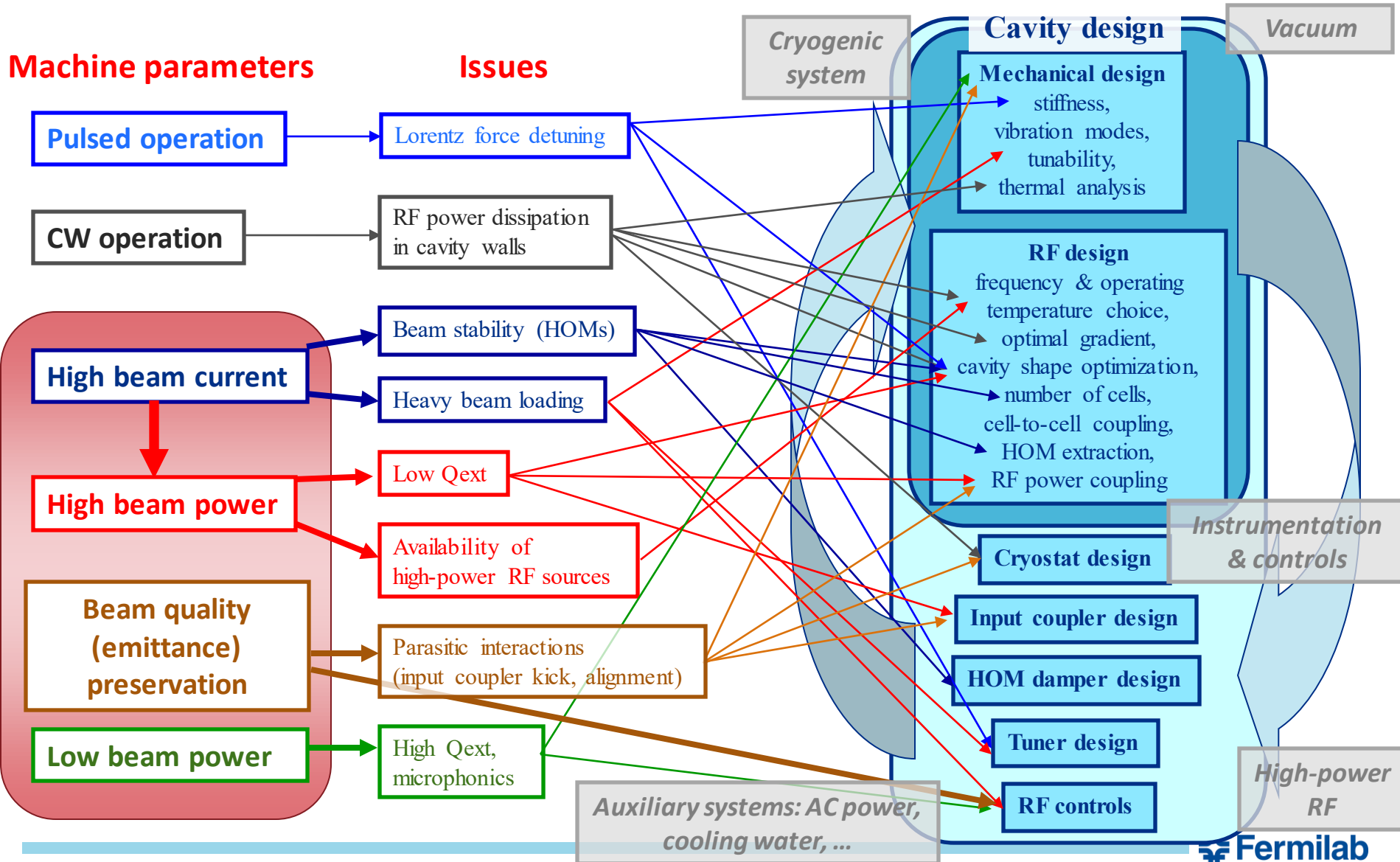a. The cavity RF design: approaches, tools;
b. SRF cavity mechanical design;
c. The cavity component design – RF couplers and tuners;
d. Cryo-module design: issues and approaches.

🐦 **Fermilab**

SRF system design interdependences

Cryomodule design

Machine parameters   **Issues**   *Cryogenic system*   Cavity design   *Vacuum*

Pulsed operation → Lorentz force detuning

CW operation → RF power dissipation in cavity walls

High beam current → Beam stability (HOMs)
High beam current → Heavy beam loading

High beam power → Low Qext
High beam power → Availability of high-power RF sources

Beam quality (emittance) preservation → Parasitic interactions (input coupler kick, alignment)

Low beam power → High Qext, microphonics

Mechanical design stiffness, vibration modes, tunability, thermal analysis

RF design frequency & operating temperature choice, optimal gradient, cavity shape optimization, number of cells, cell-to-cell coupling, HOM extraction, RF power coupling

Cryostat design

Instrumentation & controls

Input coupler design

HOM damper design

Tuner design

High-power RF

RF controls

Auxiliary systems: AC power, cooling water, ...

Fermilab

SRF cavities design issues:

- Acceleration efficiency
    - max R/Q & min surface field enhancement factors (electric & magnetic)

- High Order Modes (HOMs) dumping
    - incoherent effect (loss factors, cryogenic losses)
    - coherent effects (emittance dilution, cryo-losses)
    - collective effects (transverse & longitudinal beam instabilities)

- Operation with small beam current
    - narrow cavity bandwidth & microphonics

- Field Emission
    - multipactor & dark current

- High Gradient pulsed operation
    - Lorentz force detuning

- Input Power Coupler
    - CW operation (min RF loss & static heat load)

- Beam Instrumentation
    - Cold Beam Position Monitor (low & high relativistic beam)

V. Yakovlev | Cavity design. Linac archeticture, Lecture 14   7/24/2024

🐟 Fermilab

Tools for RF cavity simulations:

I. Field calculations:
   -Spectrum, (r/Q), G, β (coupling)
   -Field enhancement factors
   • HFSS (3D);
   • CST (3D);
   • Omega-3P (3D);
   • Analyst (3D);
   • Superfish (2D)
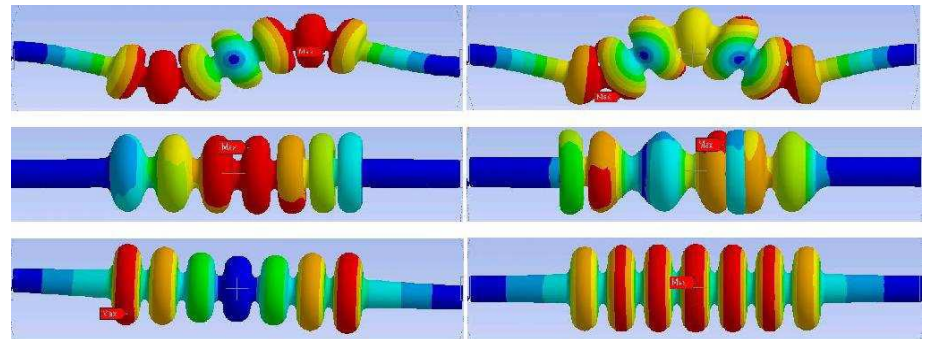   • SLANS (2D, high precision of the field calculation).
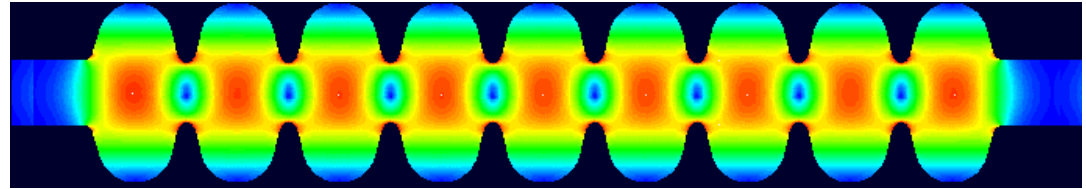
II. Multipactoring (2D, 3D)
   • Analyst;
   • CST (3D);
   • Omega-3P
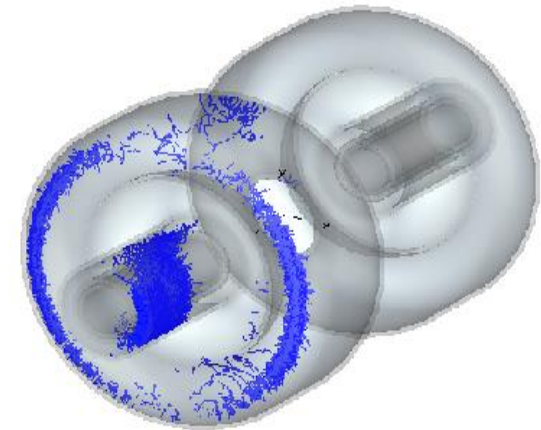
III. Wakefield simulations (2D, 3D):
   • GdfidL;
   • PBCI;
   • ECHO.

IV. Mechanical simulations:
   Lorenz force and Lorenz factor,
   Vibrations,
   Thermal deformations.

a. ANSYS

🎇 **Fermilab**

Cavity Simulation Workflow

1. **Creation of the project 3D model**
   - drawing in the CST GUI (takes time, full-parametrization, easy modification)
   - geometry import from 3rd parties CADs (quick, need special license, limited parametrization, potential mesh problem)

2. **Choosing a proper solver**
   - depends on the problem, available hardware, simulation time …

3. **Setting boundary conditions**
   - frequency, symmetries, ports, materials, beam excitation, temperature, …

4. **Checking the mesh quality**
   - generate and visualize the mesh, set initial mesh size, create sub-volumes and modify models if needed, mesh fine-tuning (curvature order, surface approximation)

5. **Solver fine-tuning**
   - direct or iterative, parallelization, special settings, …

6. **Running first simulation**
   - check the results, set postprocessing steps, tune & modify the mesh, …

7. **Setting optimization**
   - set parameters sweep, define the goal function, simplify the model

🟦 **Fermilab**

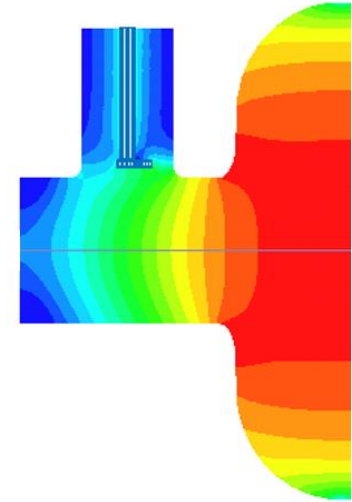V. Yakovlev | Cavity design. Linac architecture, Lecture 14   7/24/2024

Design approaches

- **Aperture choice:**
- Smaller aperture → smaller field enhancement factors, higher R/Q;
- Limitations:
  - beam losses,
  - field flatness,
  - mechanical stability,
  - surface processing,
  - Q_{load} (coupling to the main coupler)
  - HOMs (trapped modes)
  - Wakes (electron accelerators)

SNS (805 MHz):   2a=86mm (β=0.61), 2a/λ = 0.23

2a=98mm (β=0.81), 2a/λ = 0.26

HIPPI (704 MHz):   2a=80mm (β=0.47), 2a/λ = 0.19

PIP II (650 MHz):   2a=83mm (β=0.61), 2a/λ = 0.18

2a=100 mm (β=0.9), 2a/λ = 0.22

🐝 **Fermilab**

Design approaches

Cavity shape:
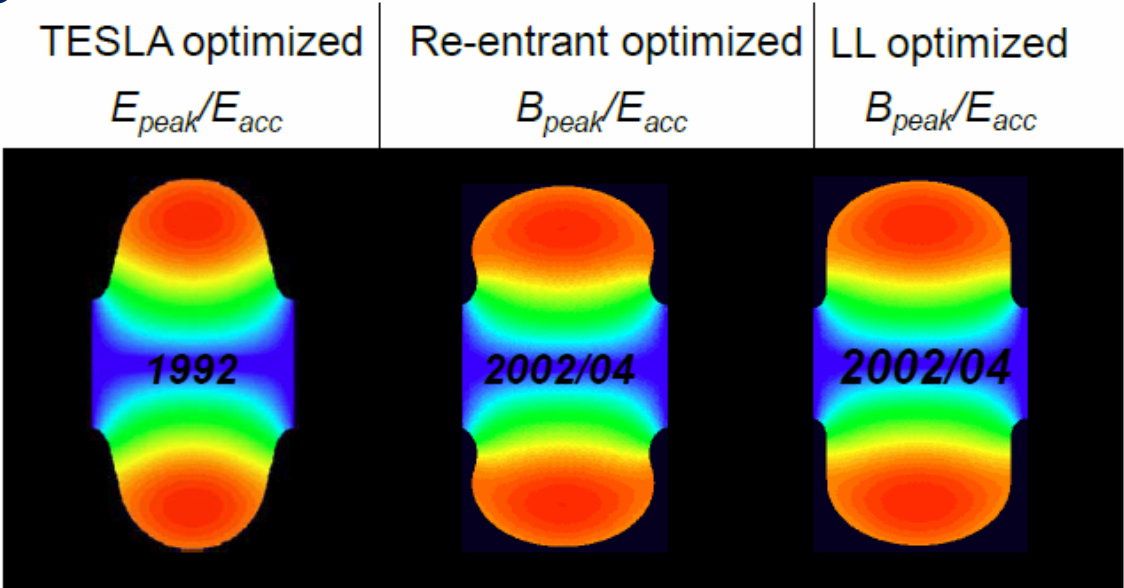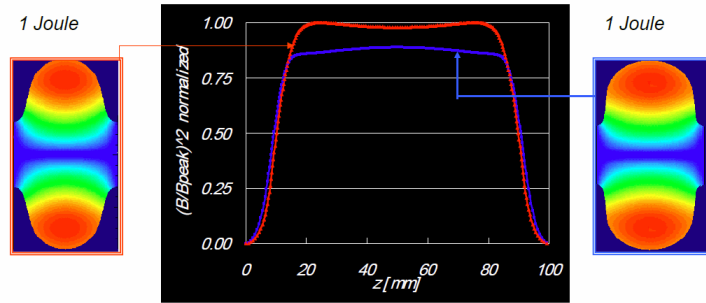
		TESLA optimized E_{peak}/E_{acc}	Re-entrant optimized B_{peak}/E_{acc}	LL optimized B_{peak}/E_{acc}
r_i	[mm]	35	30	30
k_{cc}	[%]	1.9	1.56	1.52
E_{peak}/E_{acc}	-	1.98	2.30	2.36
B_{peak}/E_{acc}	[mT/(MV/m)]	4.15	3.57	3.61
R/Q	[Ω]	113.8	135	133.7
G	[Ω]	271	284.3	284
$R/Q*G$	[Ω*Ω]	30840	38380	37970
$k_\perp$ ($\sigma_z=1mm$)	[V/pC/cm^2]	0.23	0.38	0.38
$k_\parallel$ ($\sigma_z=1mm$)	[V/pC]	1.46	1.75	1.72

Electromagnetic optimization

Fermilab

The Scope of EM-Mechanical Design (a cavity +He vessel)

- Minimize a sensitivity to microphonics because He pressure fluctuations (df/dP) and mechanical vibrations
- Minimize a Lorentz Force Detuning (LFD) coefficient
- To keep the stiffness and tuning sensitivity at suitable level to allow for tuning.
- Keep provision for slow and fast tuner integration.
- Enough strength to withstand atmospheric pressure
- "Dressed" cavity has to be qualified in 5 different load conditions by stress analysis
1. Warm Pressurization
2. Cold operation at maximum pressure
3. Cool down and tuner extension
4. Cold operation at maximum pressure and LHe weight
5. Upset condition – Insulating and beam vacuum failure

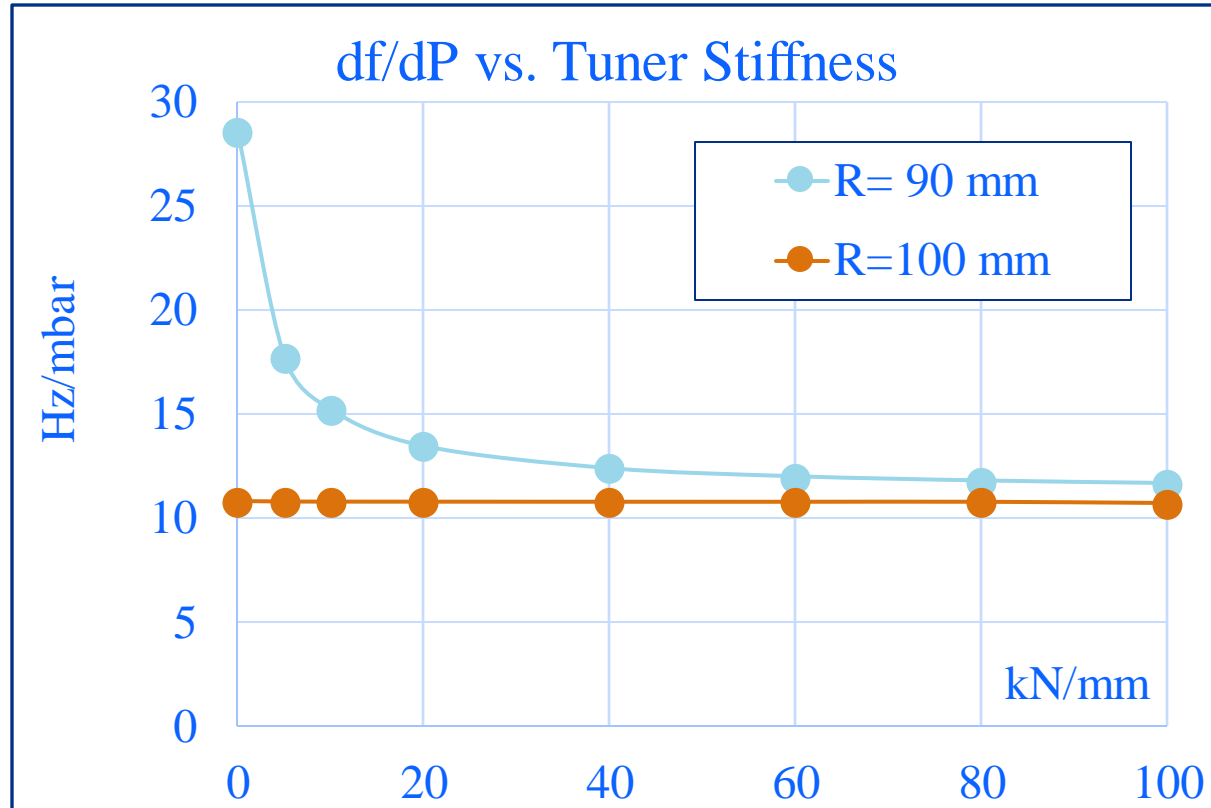# Design approaches. Mechanical stiffness
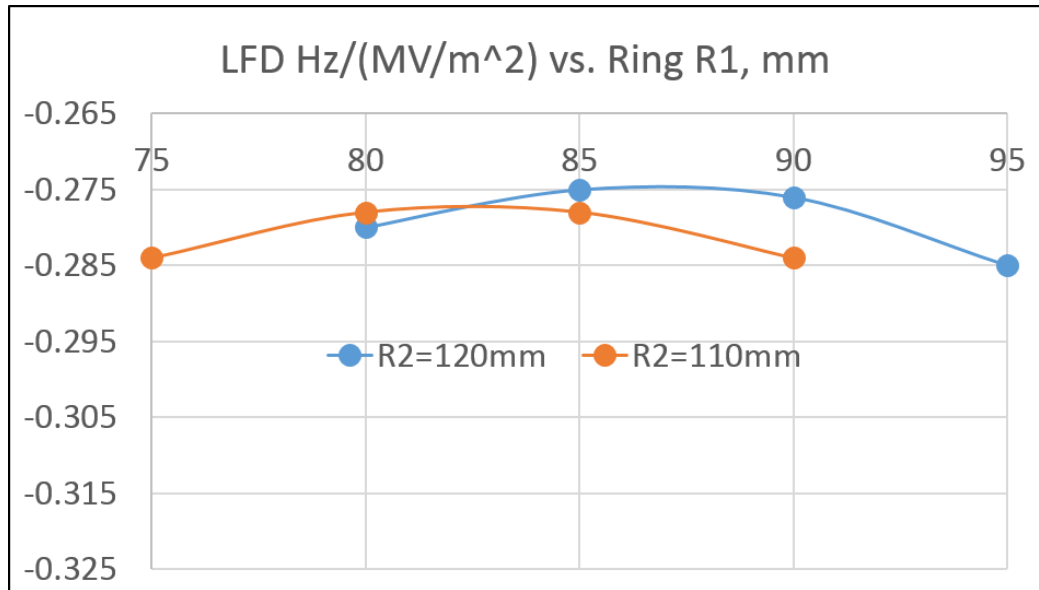

Bare cavity

Dressed cavity

He vessel

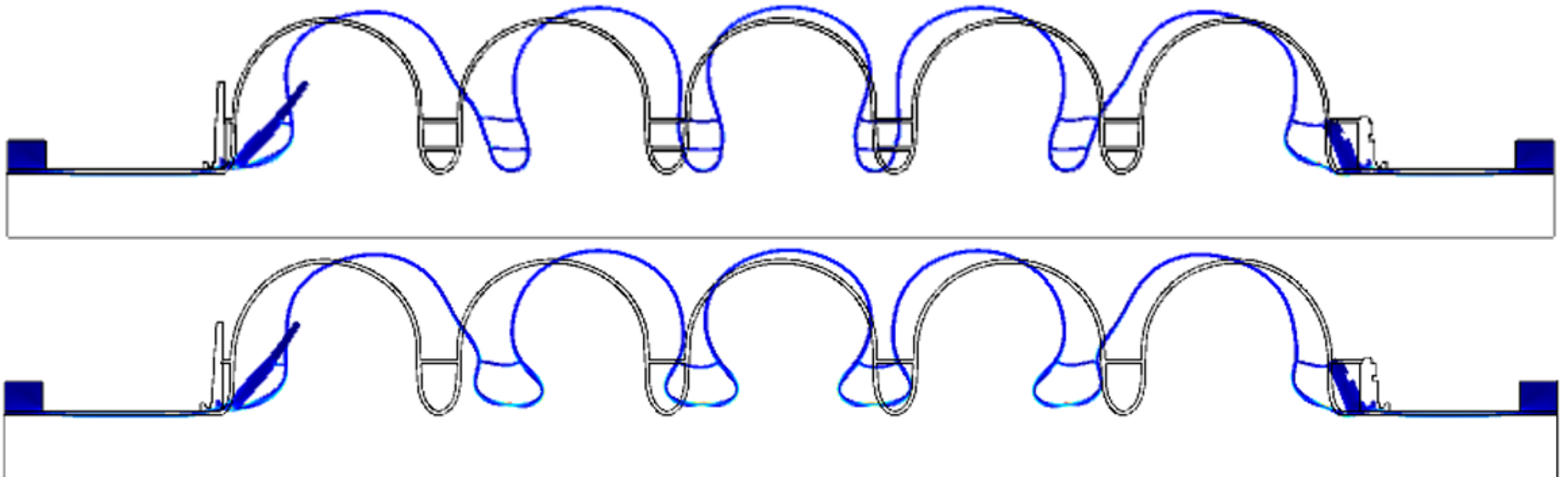Bellows

Stiffening rings

🔷 Fermilab
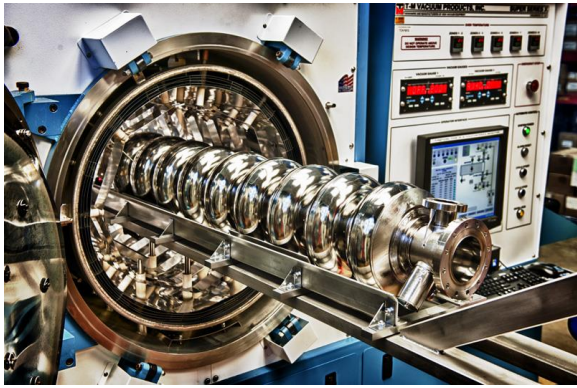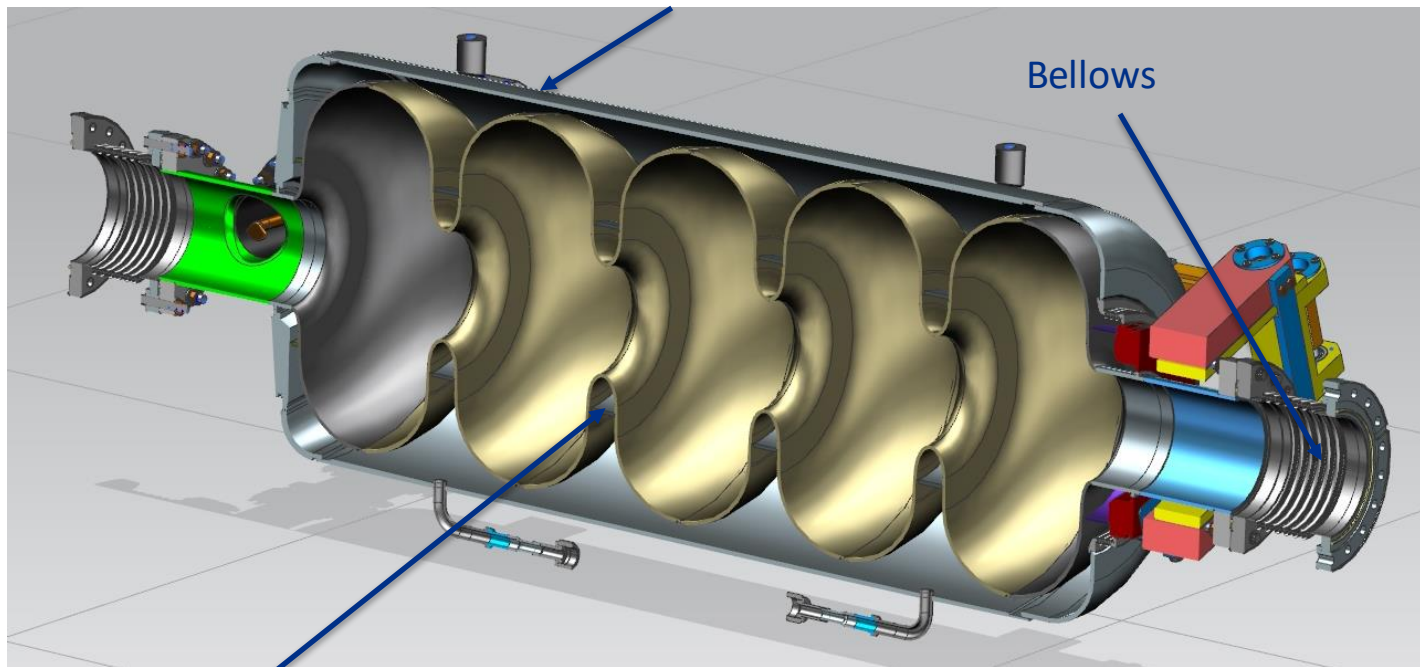
Design approaches, df/dP optimization

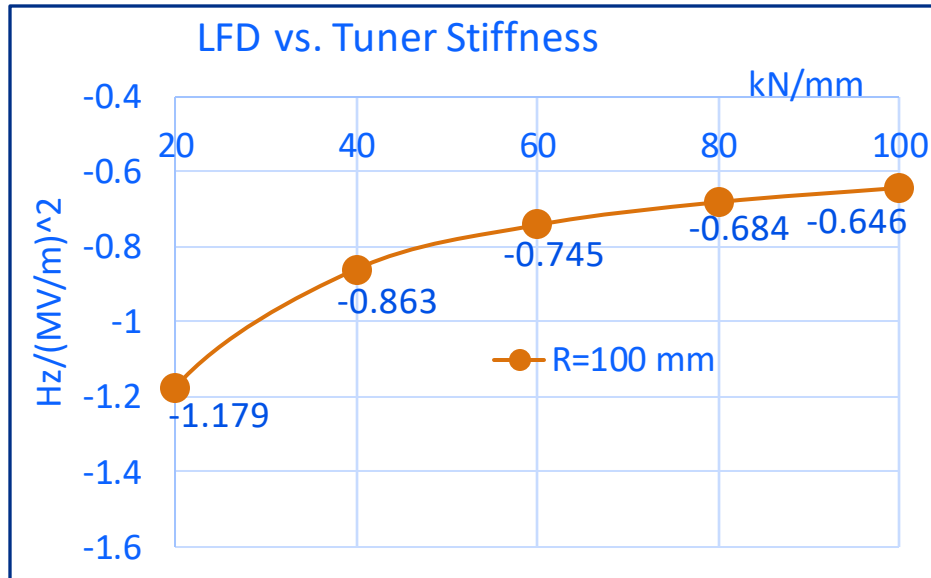df/dP for stiffening ring R = 90 mm vs. 100 mm
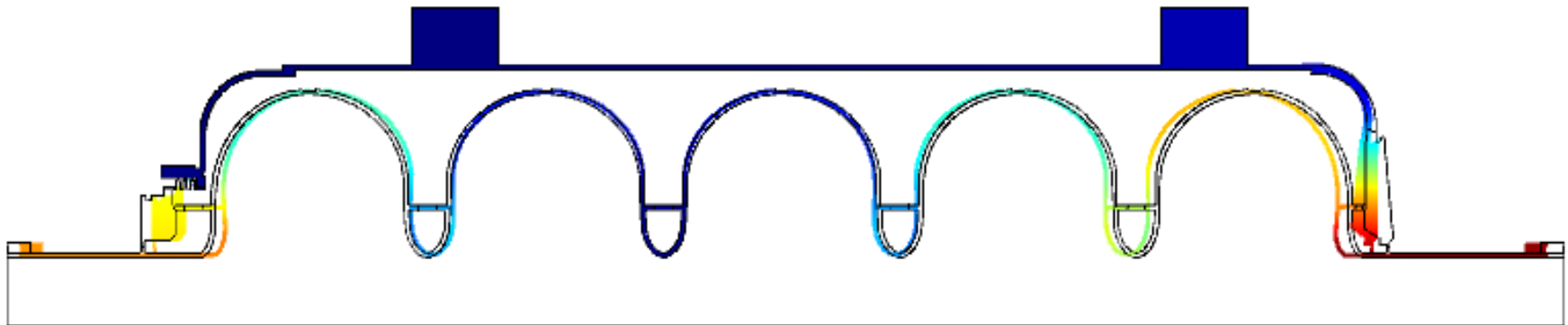Bellows radius of OD=125 mm

Design approaches, LFD minimization.

LFD Hz/(MV/m^2) vs. Ring R1, mm

R2=120mm   R2=110mm

For 2 rings LFD~-0.275 Hz/(MV/m)^2
For 1 ring LFD~-0.38 Hz/(MV/m)^2.

V. Yakovlev | Cavity design. Linac archeticture, Lecture 14

🎇 Fermilab

Design approaches, LFD optimization

LFD vs. Tuner Stiffness

LFD for dressed cavity with R=100 mm stiffening rings

V. Yakovlev | Cavity design. Linac architecture, Lecture 14

Fermilab

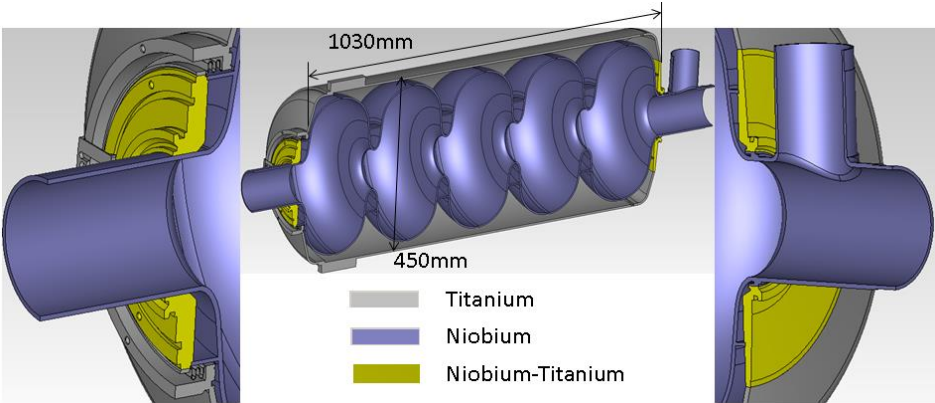# Design approaches, an elliptical cavity tuner options
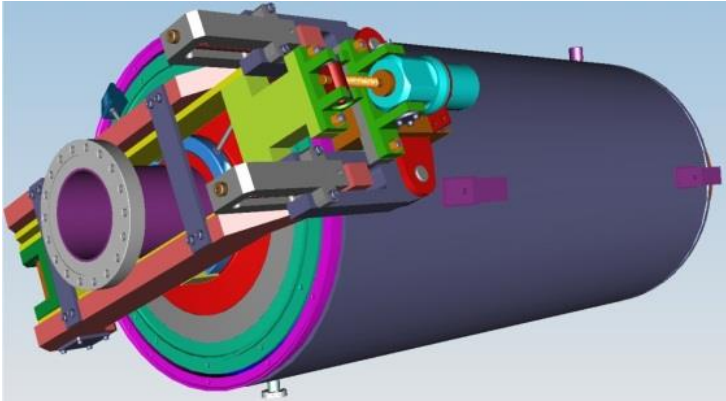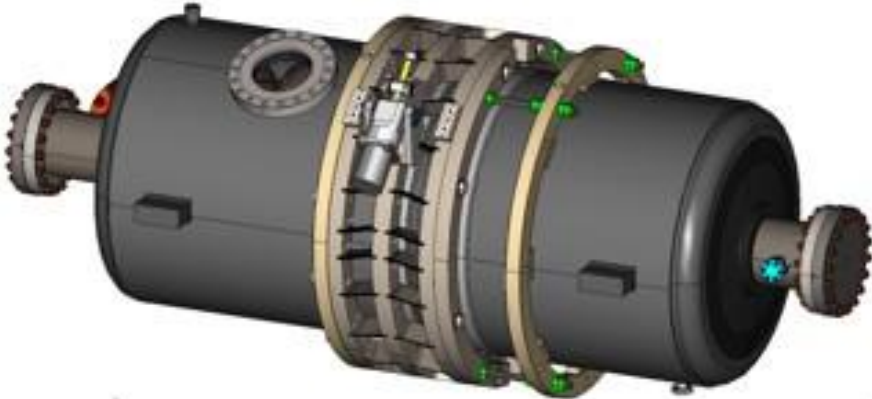
Blade Tuner – scaled ILC:
*   High df/dP,
*   Insufficient tuning efficiency ;

Lever Tuner   design:
*   Low df/dP,
*   Mechanical resonances > 60 Hz;
*   Good tunability;
*   Less expensive.

1030mm

450mm

Titanium

Niobium

Niobium-Titanium

🔷 Fermilab

Design approaches, the tuner

- Coarse tuner (step motor) – for the cavity tuning after cooldown, range ~100 kHz
- Fine tuner (piezo) – for microphonics and LFD compensation, range ~ 1kHz

Motor & power screw location

Piezo

Thin lever

Thick lever

Half model of tuner with boundary conditions

Helium vessel support location

Pivotal point 1
Pivotal point 2

Equivalent spring model

Analysis of tuner

Tuning ratio for motor ~ 20

Tuning ratio for piezo ~ 2

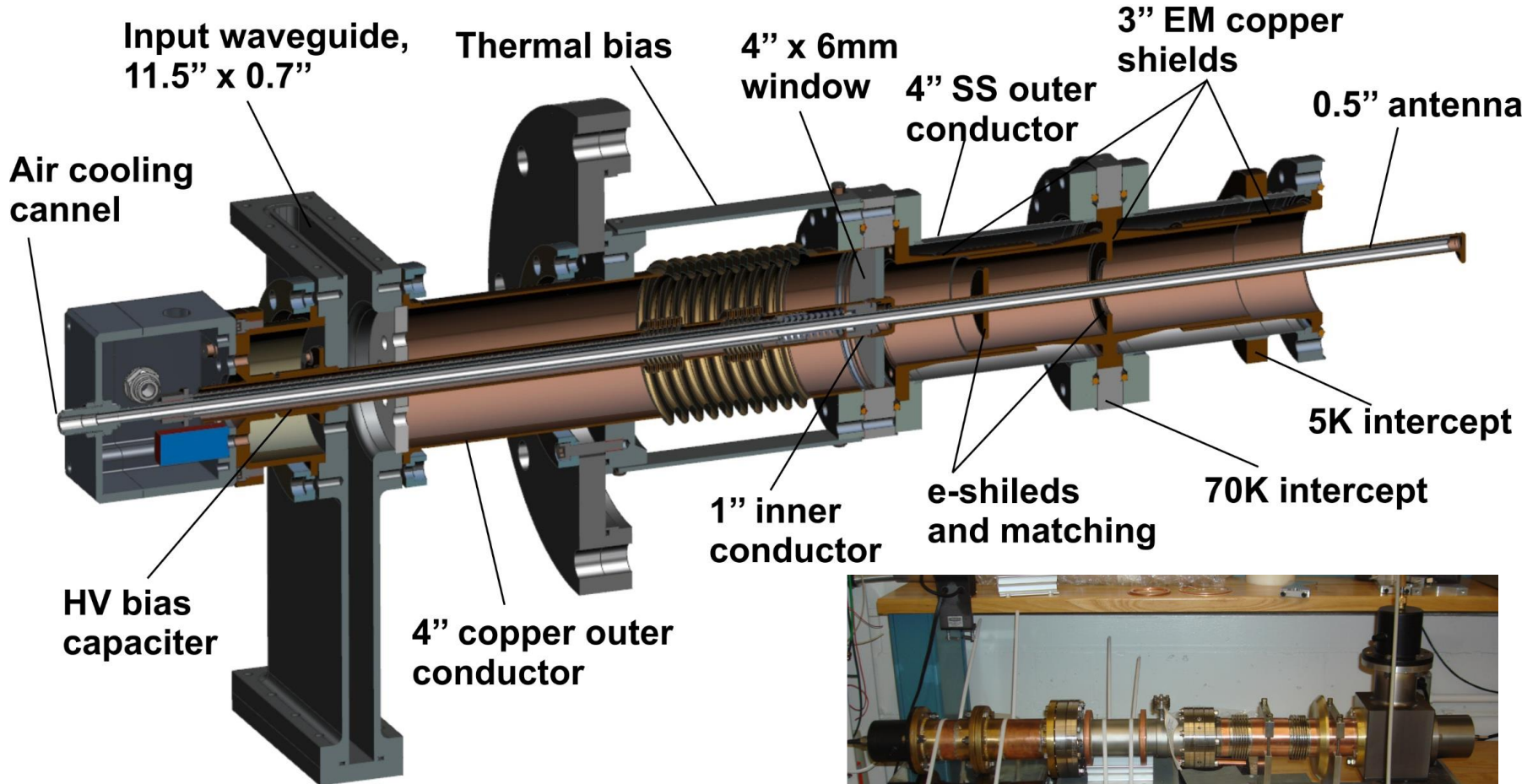Tuner Stiffness ~ 68 kN/mm

Common tuner for LB & HB cavities
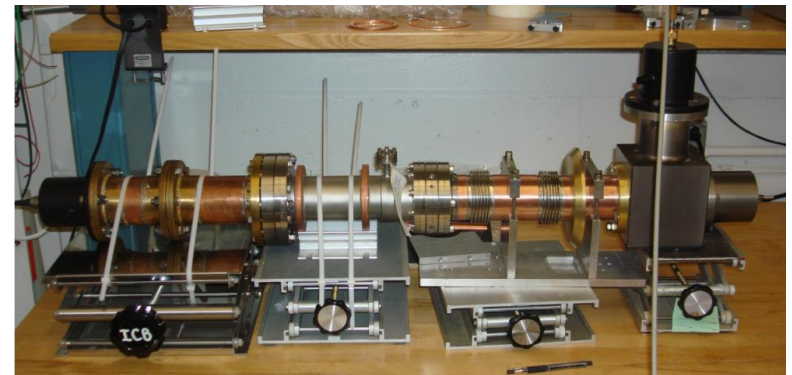
🎝 Fermilab

Couplers for SRF cavities:

❑ The couplers should transfer RF power to the cavity operating at cryo temperature

- High pulsed power (hundreds of kW for pulsed operation - SNS, ESS) $\rightarrow$ good electric strength

- High average power (up to 100 kW in CW – PIP II) $\rightarrow$ low dynamic losses, sufficient cooling (air, He)

- Low static losses

- Good vacuum properties

❑ Issues:

- MP in the vacuum part $\rightarrow$ DC bias

- Copper plating (chips)

❑ Design choices:

- One window versus two windows

- Type of cooling

‡‡ Fermilab

Couplers for SRF cavities:

Coupler for PIP II LB/HB 650

Input waveguide, 11.5" x 0.7"

Thermal bias

4" x 6mm window

4" SS outer conductor

3" EM copper shields

0.5" antenna

Air cooling cannel

HV bias capaciter

4" copper outer conductor

1" inner conductor

e-shileds and matching
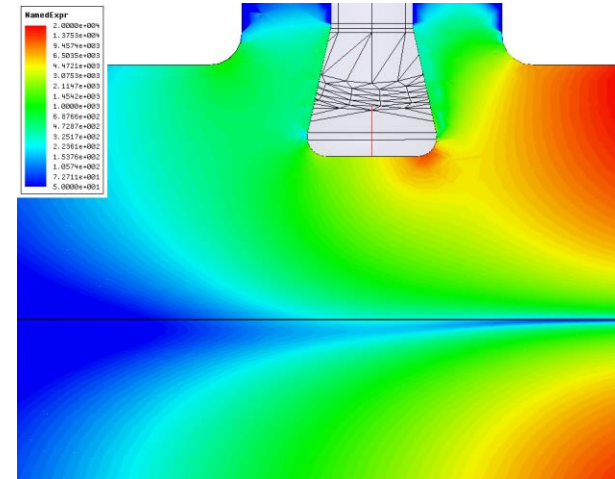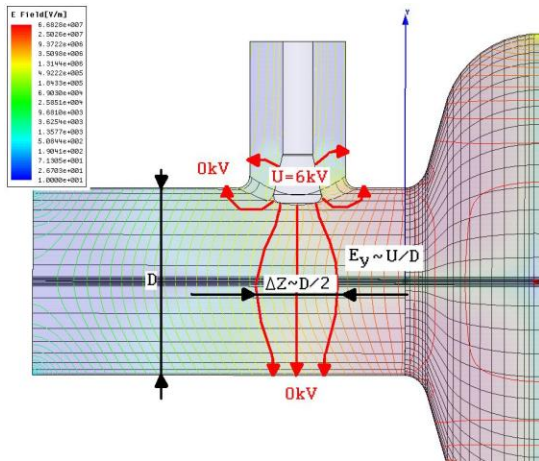
70K intercept

5K intercept

Average power up to 100 kW

Fermilab

RF kick caused by the input and HOM couplers.

Simple estimations of the transverse
fields caused by the main coupler:

RF voltage:
$U=(2PZ)^{1/2}$, Z–coax impedance;
for P=300 kW and $Z\approx70$ Ohms
$U \approx 6$ kV

Transverse kick:

$$v = \frac{\Delta p_y c}{\Delta U_{acc}} \approx \frac{U}{2U_{acc}} = \frac{6kV}{2\times30MV} = 10^{-4}$$

Transverse kick caused by the couplers acts on a bunch the same direction for all the RF cavities of the linac.

Real part may be compensated by the linac feedback system;

Imaginary part dives the beam emittance dilution (here β is beta-function, σ is the bunch length, and U_0 is the initial beam energy):

$$\gamma\varepsilon \approx \gamma(z_{max}) y_{max} y'_{max} = \frac{\pi^2 v^2 E^2 \sigma^2 \beta^3 \gamma_0}{\lambda_{RF}^2 U_0^2}$$

🔷 **Fermilab**

SRF cavity production technology

Parts: sheets, tubes → Parts QC → Half cell forming → Iris welding → Dumbbell, end ass. RF QC → Equator welding → QC

Fabrication → Quality Control → Chemical Processing → Heat Treatment → Frequency Tuning → Light Chemistry → Baking → VTS Testing

Vessel Welding → Light Chemistry → Quality Control → HTS Testing

String Assembly → Quality Control → Cryomodule Assembly → Cryomodule Testing

Fermilab

Material quality control

Typical Technical Specification to Niobium Sheets (For XFEL Cavities)

Concentration of impurities in ppm*				Mechanical properties	
Ta	≤ 500	H	≤ 2	RRR**	≥ 300
W	≤ 70	N	≤ 10	Grain size	≈ 50 μm
Ti	≤ 50	O	≤ 10	Yield strength, $\sigma_{0.2}$	$50<\sigma 0,2<100$ N/mm^2 (Mpa)
Fe	≤ 30	C	≤ 10	Tensile strength	> 100 N/mm^2 (Mpa)
Mo	≤ 50			Elongation at break	30 %
Ni	≤ 30			Vickers hardness HV 10	≤ 60

*ppm=Parts per Million
**The Residual Resistance Ratio "RRR" is the ratio of resistance at 300K (room temperature) to the resistance at 10K.
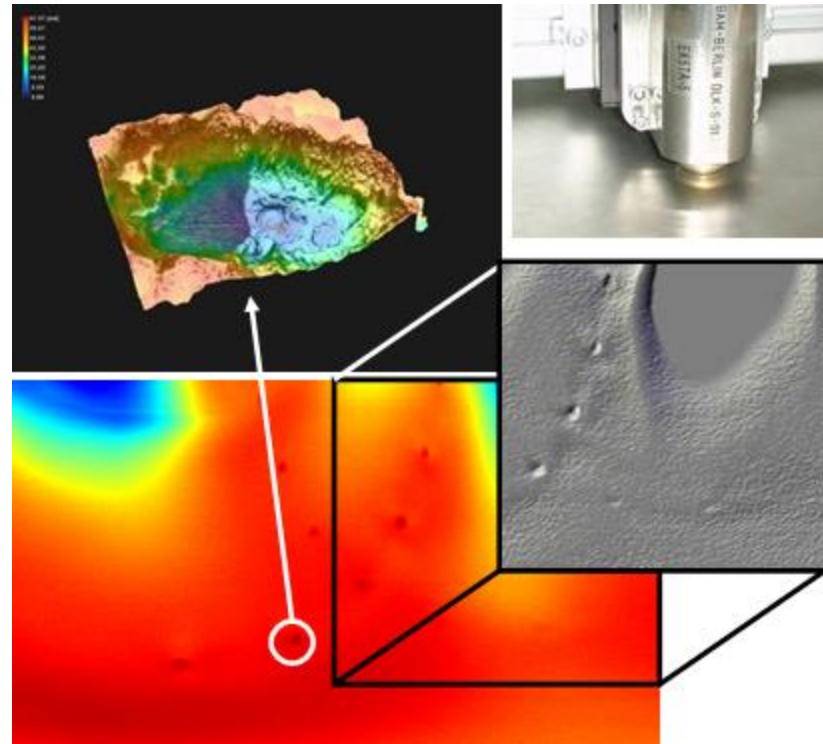
🎙 Fermilab

7/24/2024

Material quality control

Eddy current scanning
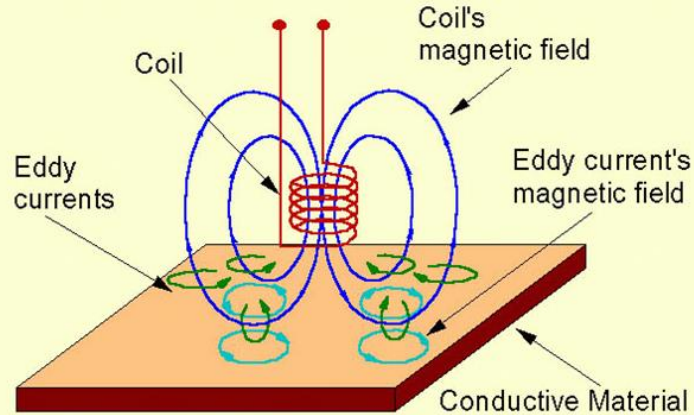
Disks are cut from high purity niobium sheet and eddy current scanned for pits, scratches or inclusions of foreign materials

Discs with inclusions of foreign materials or damage are rejected

🟦 Fermilab

Elliptical cavity production

Fabrication: Conventional fabrication (deep drawing and EB welding of fine grain Nb). Experiences of ca. 20 years of industrial cavity fabrication are available
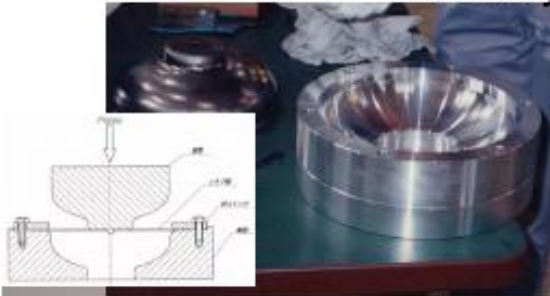
Half cells are produced by deep drawing.

Dumb bells are formed by electron beam welding.

After proper cleaning eight dumb bells and two end group sections welded by electron beam together

Important: clean conditions on all steps shape accuracy, preparation and EB welding

🎄 Fermilab

Elliptical cavity production

Cavity welding: the general way
There are differences of welding processes in industry

1   1 pieces

2   8 pieces

3   1 piece
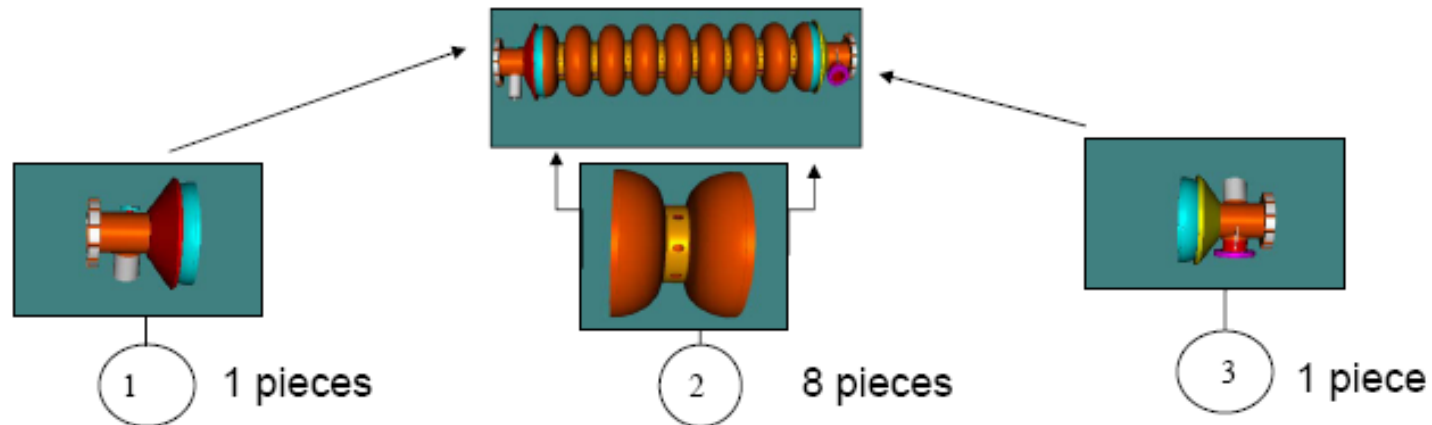
1. Degreasing and rinsing of parts
2. Drying under clean condition
3. Chemical etching at the welding area (Equator)
4. Careful and intensive rinsing with ultra pure water
5. Dry under clean conditions
6. Install parts to fixture under clean conditions
7. Install parts into electron beam (eb) welding chamber
    (no contamination on the weld area allowed)
8. Install vacuum in the eb welding chamber <= 1E-5 mbar
9. Welding and cool down of Nb to T< 60 C before venting
10. Leak check of weld

Fermilab

Elliptical cavity production
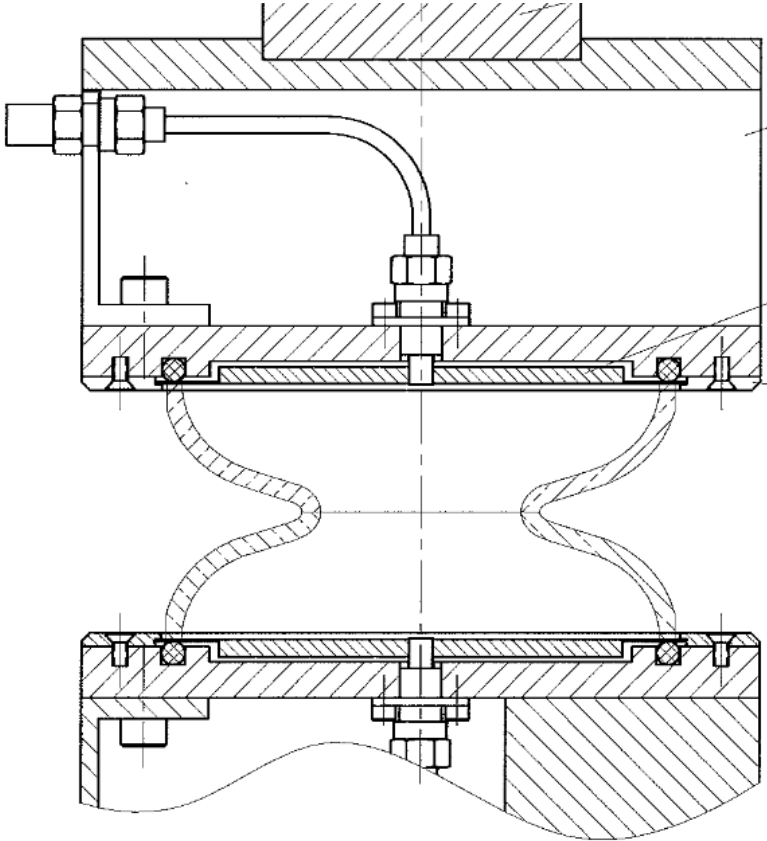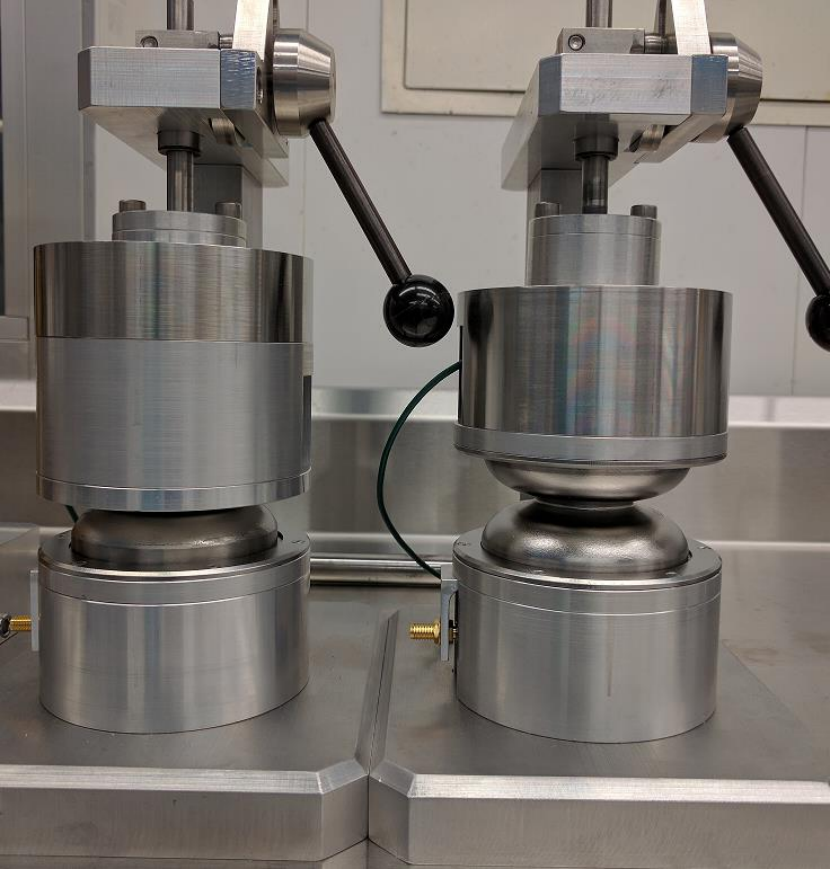
MEASURING OF DUMBELL

3.9 GHz half cells and dumbbell measurement fixture

🔷 **Fermilab**

Elliptical cavity production

Cavity production steps:

-Eddy current scanning of Nb shits.

-Cut disk blanks with hole in the center

-Flow forming of half-cell and trimming iris and equator area with extra length for tuning and welding shrinkage compensation. No extra length for a tuning in mid-cells. If pass visual inspection:

-Frequency and length measurements. Sensitivity of the frequency to extra length is 14 MHz/mm at iris and -55 MHz/mm at equator.

-EB welding of two half-cell at iris to form dumbbell. Partial penetration welding from both sides. If pass visual inspection:

-Frequency and length measurements of the dumbbells. Both mode frequencies F_0 and F_{pi} measured 3 times: 1) without perturbation F0 and F1, 2) with perturbation in 1st half cell F_{01} and F_{11} 3) with perturbation in 2nd half cell F_{02} and F_{12}. Difference of the frequencies of two half cell can be calculated from these data:

$$dF=F_2-F_1=(F_{01} - F_{11} +F_{12} -F_{02})/(F_{01} +F_{11}- F_{02} -F_{12}))*k*F0$$

Where $k\sim4(F_{pi} - F_0)/(F_{pi} + F_0)$, for a 3rd harmonic cavity $k\sim0.08$ MHz

-Trimming calculations:

-Equator trimming

-Equator welding

-Mechanical and RF QC of the new cavity.

-Bulk BCP and 800C baking,

-RF tuning of the cavity

Dumbbell F vs Length, Pi-mode.

🟦 Fermilab
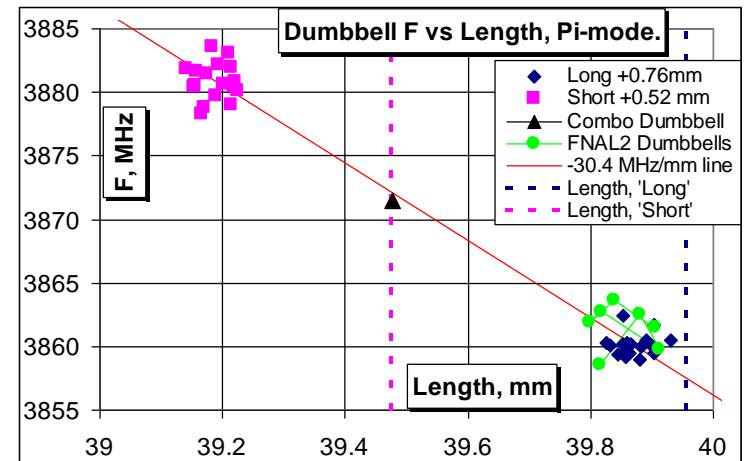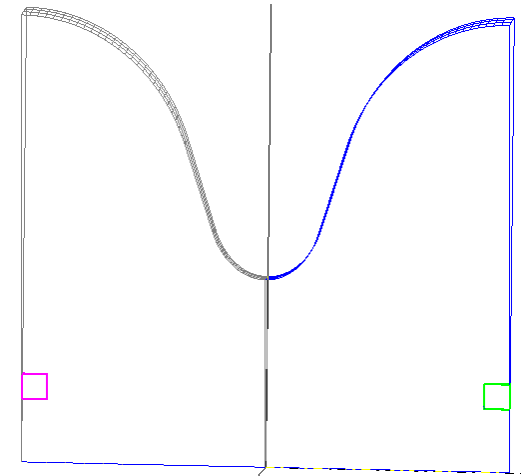
Multi-cell cavity field flatness tuning

FNAL elliptical 9 cell cavity tuning procedure. This technique based on bead-pull measurements of field distribution on operating (π-mode). Amplitudes of E-field in the center of each cell used for frequency of individual cells.

Normalized field distribution is uniform, $A_i=1$ for i=1,2, … 8, 9, if frequency of each cell are same. When frequency of the cell #n is shifted by dF_n field distribution will change by dA_i.

$$dA_i = K_{in} * dF_n$$

Perturbation of frequency of each will change field distribution:

Let us solve this equation to find frequency perturbation from field distribution:

$$dA = K * dF \Rightarrow K^{-1} * dA = K^{-1} K * dF = dF$$

Where sensitivity coefficients matrix K calculated from HFSS simulations.

During RF tuning of the cavity, we need to tune its operating mode frequency F_9. Also, we can not measure individual cell frequency but can measure F_9. Tuning of cell #n by dF_n shifts also cavity frequency by $dF_9 \sim dF_n/9$. If design frequency is $F_9 0$ tuning of the cell should be done by shifting operating mode frequency by:

$$dF_9 = (F_9 0 - F_9 - dF_n)/9$$

This technique works best when field flatness of the cavity is close to ideal. Because it linear and based on small perturbations. Tuning is better to start with most perturbed cell. If field flatness still not acceptable the additional tuning cycle should be done.
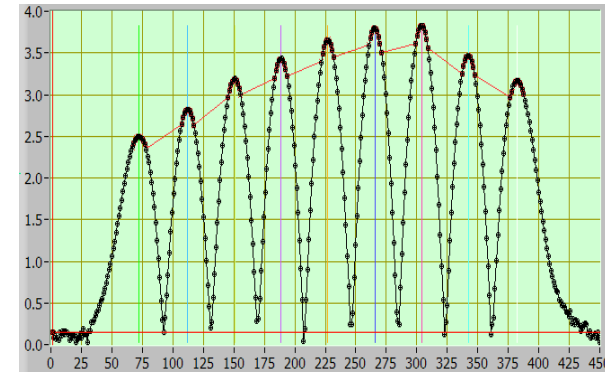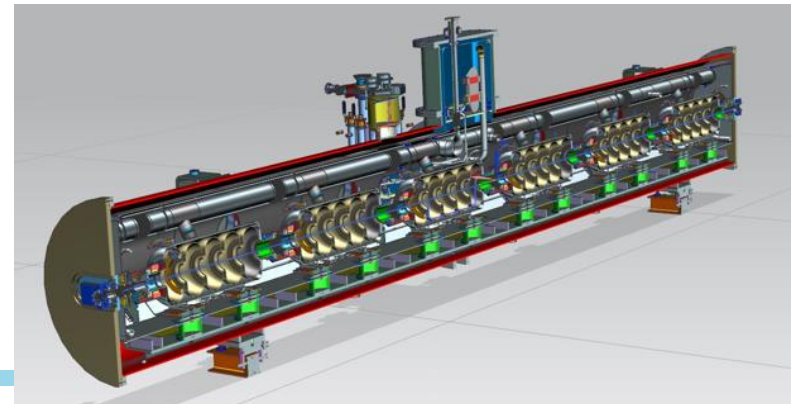

Before tuning. FF 65%, slope +28 %
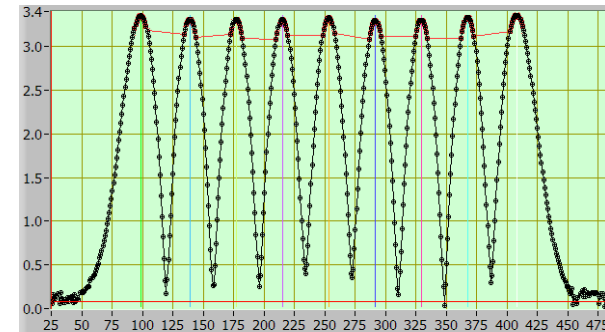
After tuning. FF 98%, slope +0.64 %

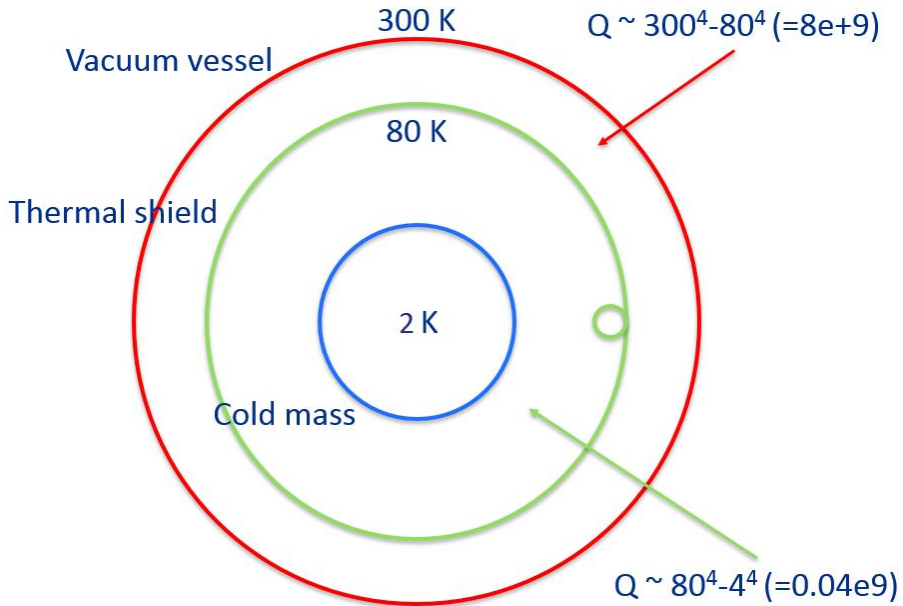‡‡ **Fermilab**

ICL Cavity Tuning Machine

Vacuum vessels

- The outermost cryostat component that:
  - Contains the insulating vacuum.
  - Serves as the major structural element to which all other systems are attached to the accelerator tunnel floor.
  - Serves as a pressure containment vessel in the event of a failure in an internal cryogen line.

- The design for internal and external pressure are addressed by the ASME Boiler and Pressure Vessel Code, Section VIII, Divisions 1 and 2 and specific workplace codes.

- Insulating vacuum is generally in the $1e10^{-6}$ torr range, but can be as low as $1e10^{-4}$. The lower the better.

Vacuum vessel and thermal shields

300 K

$Q \sim 300^4 - 80^4 \,(=8e+9)$

Vacuum vessel

80 K

Thermal shield

2 K

Cold mass

$Q \sim 80^4 - 4^4 \,(=0.04e9)$
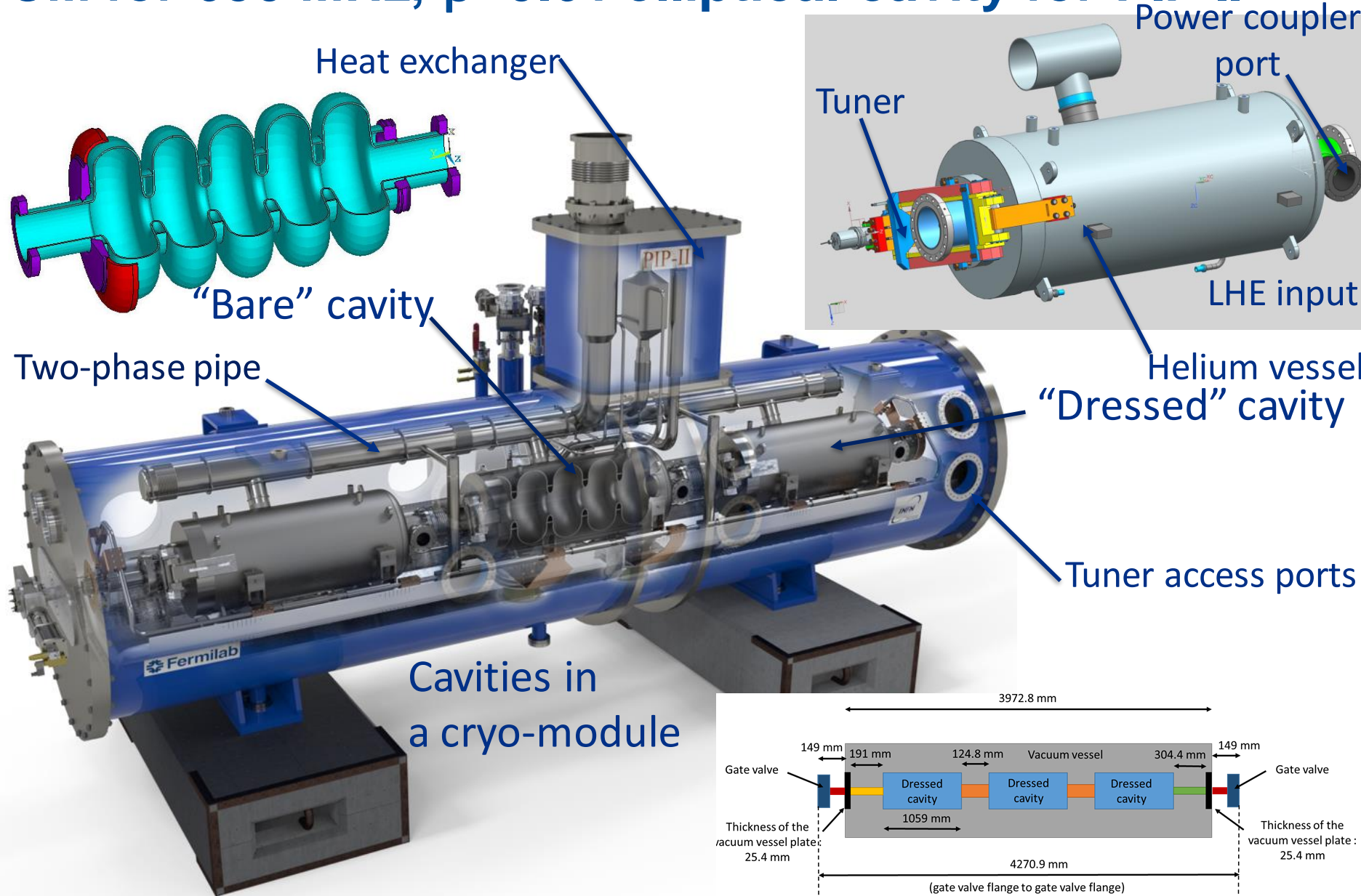

2/26/2004

❖ Fermilab
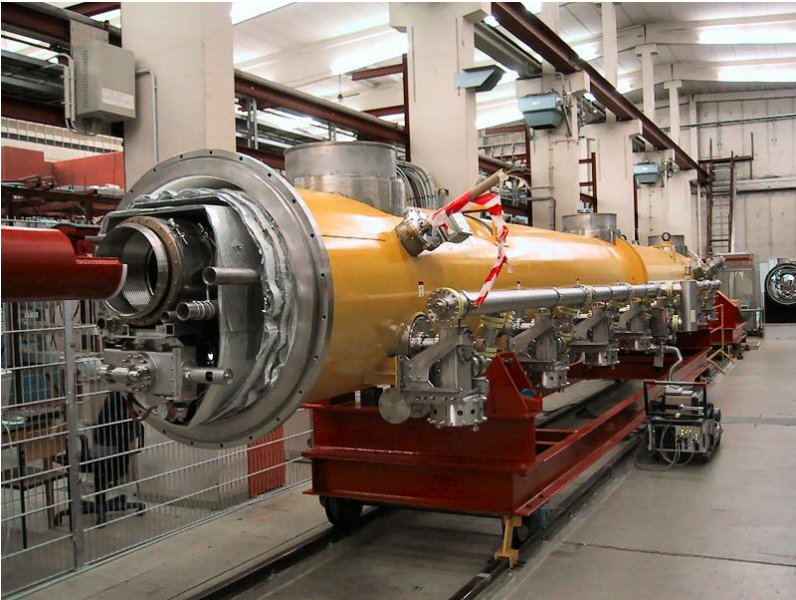
Insulation

- Multi-layer insulation (MLI) reflects radiation heat transfer back toward its source.

- Usually mounted on the outside of the colder surface, e.g. the thermal shield or cold mass.

- Consists of alternating layers of reflector and spacer material:

  – Reflector is usually double-aluminized mylar sheets 6-12 μm thick aluminum-coated on both sides with a minimum of 300 Å.

  – Spacer is usually a polyester net, fiberglass net or other similar material compatible with the environment.

  – The reflector can be perforated to facilitate pumpout.

- The number of layers varies but is usually from 30-60 layers on a thermal shield nominally at 80 K and 10-15 layers on a lower temperature shield or cold mass.

- It must be in vacuum – 1e10^{-4} torr or lower.

- To estimate the total heat load due to radiation and residual gas conduction, realistic values are ~1.5 W/m^2 at 80 K and ~0.15 W/m^2 at 4.5 K.

🎇 Fermilab

CM for 650 MHz, β=0.61 elliptical cavity for PIP II

Power coupler port

Heat exchanger

Tuner

"Bare" cavity

Two-phase pipe

LHE input

Helium vessel

"Dressed" cavity

Tuner access ports

Cavities in a cryo-module

3972.8 mm

149 mm | 191 mm | 124.8 mm | Vacuum vessel | 304.4 mm | 149 mm

Gate valve | Dressed cavity | Dressed cavity | Dressed cavity | Gate valve

1059 mm

Thickness of the vacuum vessel plate 25.4 mm

Thickness of the vacuum vessel plate : 25.4 mm

4270.9 mm

(gate valve flange to gate valve flange)

🔷 Fermilab

CM for 650 MHz, β=0.9 elliptical cavity for PIP II

Tuner

Internal magnetic shield

Supports

🔷 Fermilab
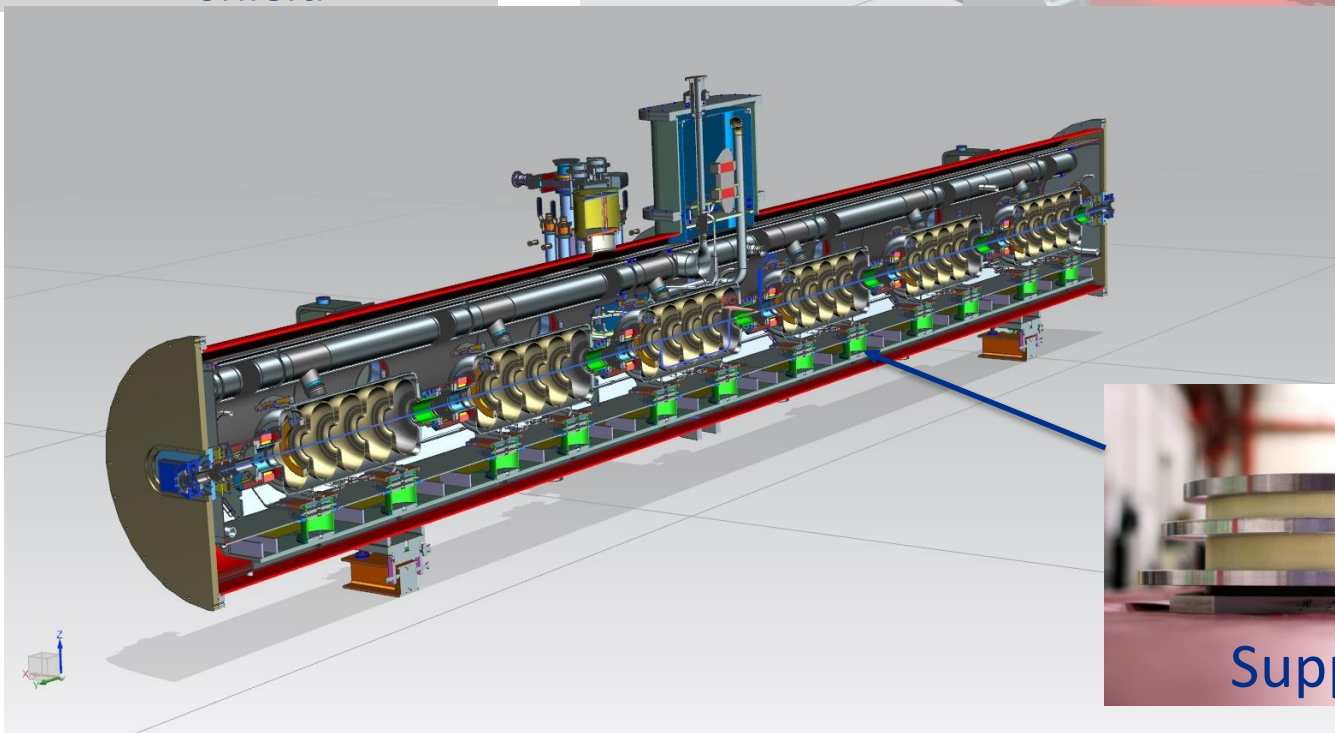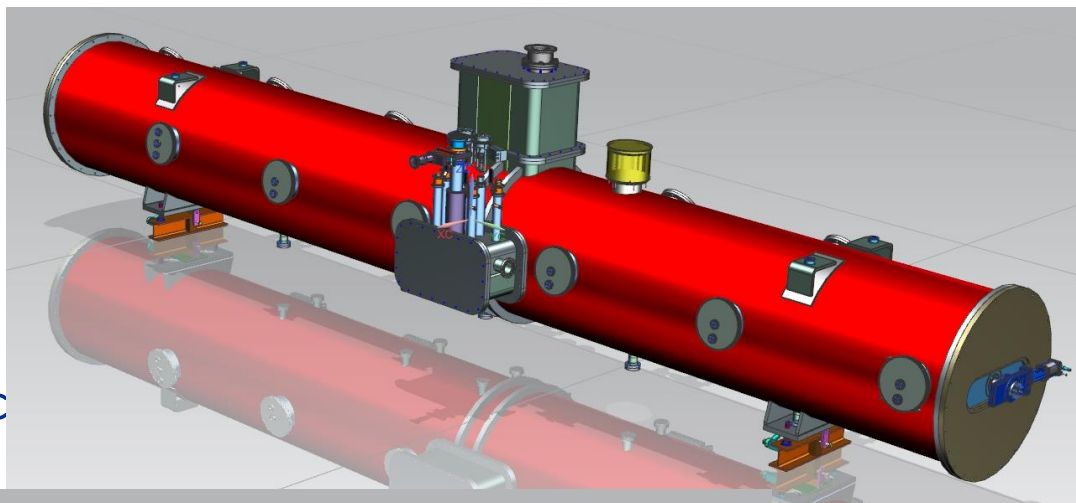
CM for 3.9 GHz elliptical cavity for LCLS II

🔶 Fermilab
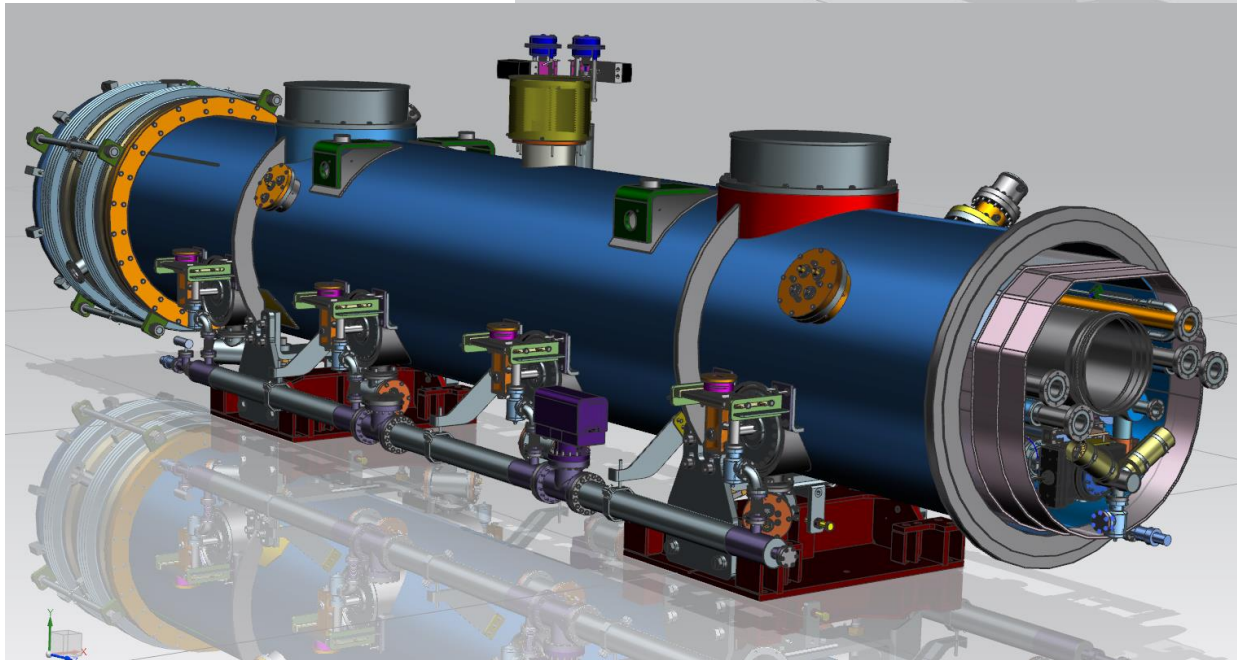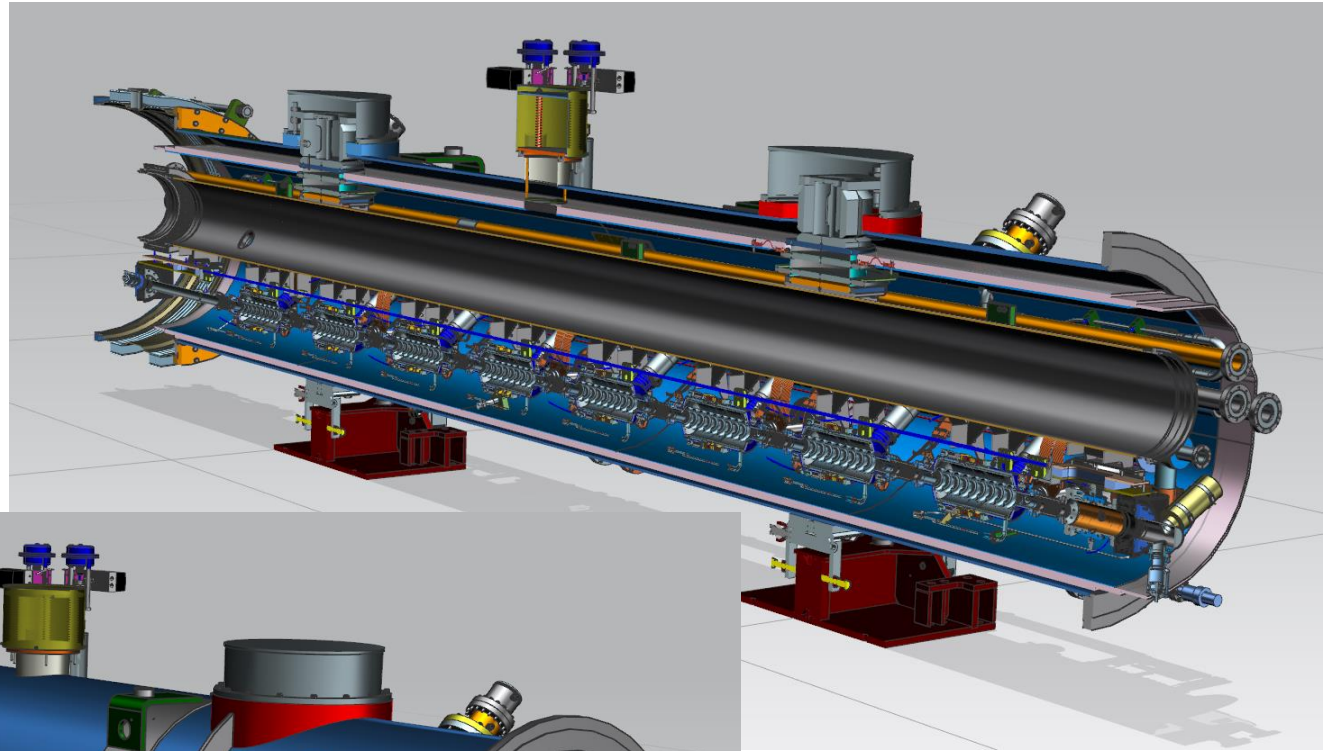
Cavities supported by High-power couplers

Elliptical Cryomodules – CEA/IPNO

Helium tank

5-cell elliptical cavity

Cold tuning System

Power coupler

Space frame

Figure 4.120: Helium vessel with hanging rod

🔷 Fermilab

CM for 325 MHz HWR cavities for PIP II (developed by ANL)

cavities

solenoids

🟣 Fermilab

Cavities alignment

Cavity fiducials

Strongback fiducials

Transverse cavity alignment, mm RMS <±1
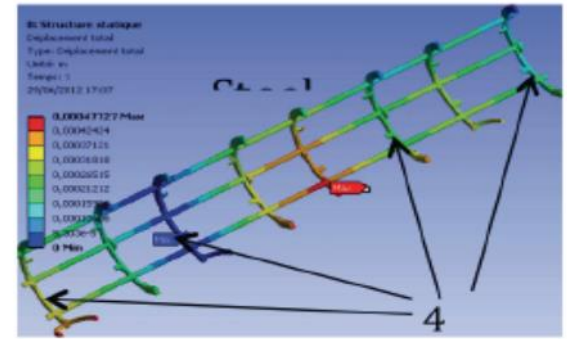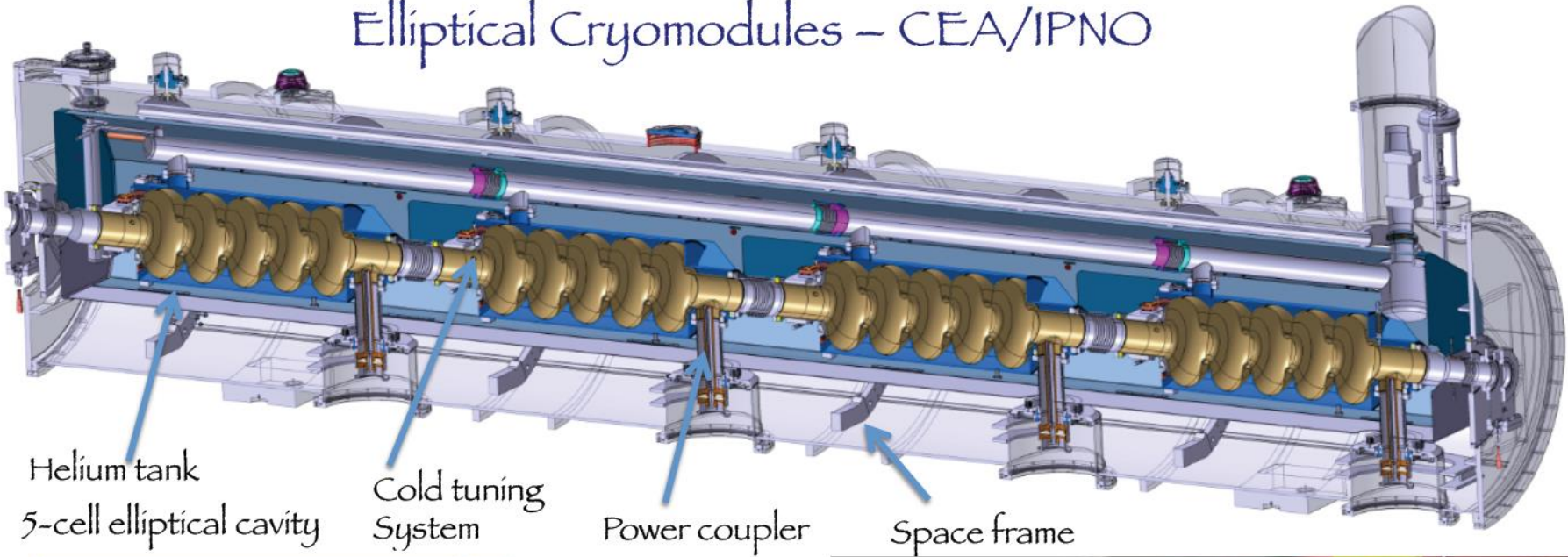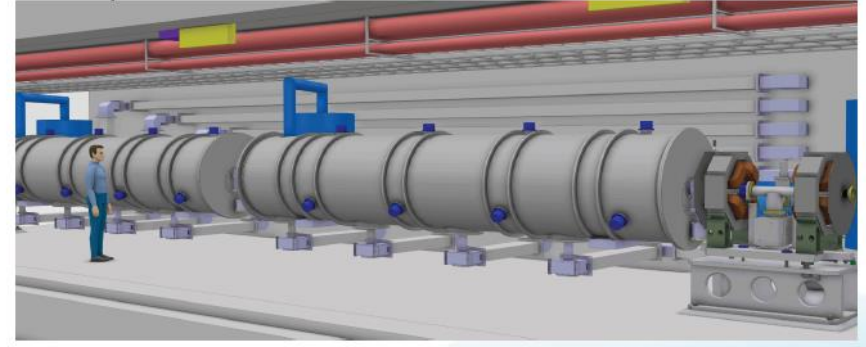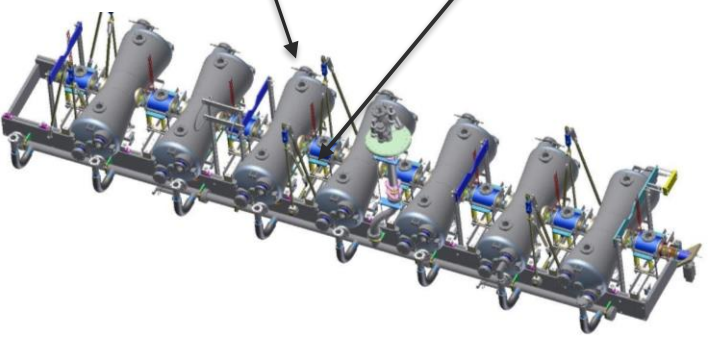Angular alignment, mrad RMS   ≤±10

- The cavity string is aligned in warm state with an offset to compensate for thermal shrinking.
- Laser Trackers and precision optical and electronic levels is used as instrumentation for the alignment of cavity string
- After completion of cavity string alignment and transfer to the strongback referencing points, the cavities and solenoids temporary fiducials, as well as the fiducials on both sides of the strongback, can be removed

❑ Beam – base alignment (BPM, HOMs)

- Special alignment wire target panels (4 per each component, 1 upstream and 1 downstream on each left-right side) – used for relative optical measurement with respect to external reference points
- Each panel has two intersecting wires forming a crosshair along the diagonal, creating 24 configurations

Alignment wire targets system

Wire target panels

Alignment viewport

Strongback fiducials

Cryomodule fiducials

🔷 Fermilab

Cryogenics and thermoacoustic oscillations

- LCLS-II is a low-beam-current SRF linac → cavities have very narrow bandwidth, ~10 Hz.

- During acceptance testing of the prototype LCLS-II cryomodule, unexpectedly high level of microphonics was encountered preventing stable operation of the cavities in a GDR mode.

- The problem was traced to thermoacoustic oscillations in the supply JT valves.

- Thermoacoustic oscillations generally occur in long gas-filled tubes with a large temperature gradient.

- Acoustic modes couple to mass transport up and down column especially well when gas density is strongly tied to temperature. E.g. warm gas from the top of a valve column moving to the cold bottom contracts, reducing pressure at warm region, driving the now cold gas back.

- These oscillations are generally important for the tremendous heat leaks they can represent, not microphonics.

Normal Operation / Low Pressure Operation

o Low pressure operation consistently eliminated icing on the supply valves (JT, bypass)

o Indicates *suppression* of thermo-acoustic oscillations

J. Holzbauer, "1.3 GHz Microphonics measurement and mitigations," MRCW18

🧲 Fermilab

Beam Diagnostics

- *Beam Position and Phase Measurement System (button –type or stripline BPMs)*
- *Beam Loss Measurement System (ionization chambers).*
- *Beam Intensity Measurement System (DC current transformers and beam toroids)*
- *Beam Transverse Profile Measurement System (traditional wire scanner or photo-disassociation of H^- by laser radiation)*
- *Beam Transverse Emittance Measurements (Allison-Type Emittance Scanners or Laser-Based Emittance Scanners)*

"Don't try to save on the beam diagnostics!"

🐝 **Fermilab**

Beam Diagnostics in CM, beam position monitors (BPM)

Ø36 mm

50Ω line

Voltage Monitor
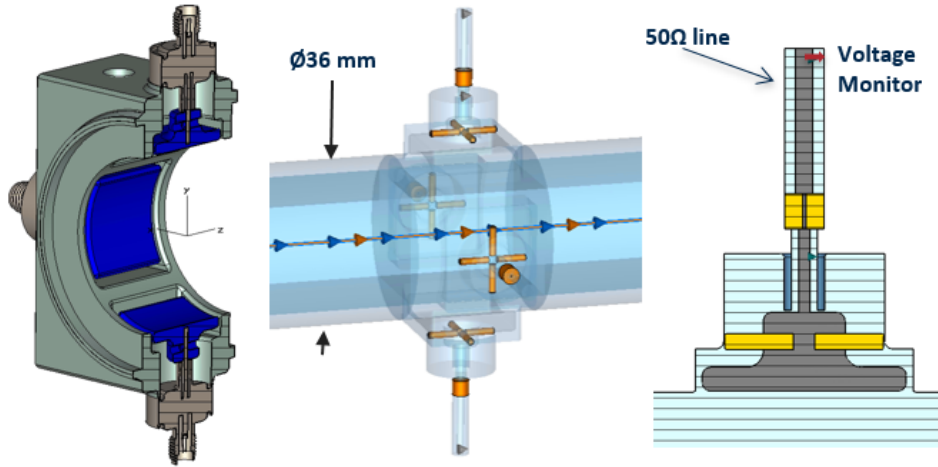
BPM signals produced by the 4 mm rms bunch

Instant Electric Field induced by the 4 mm bunch (β =1)
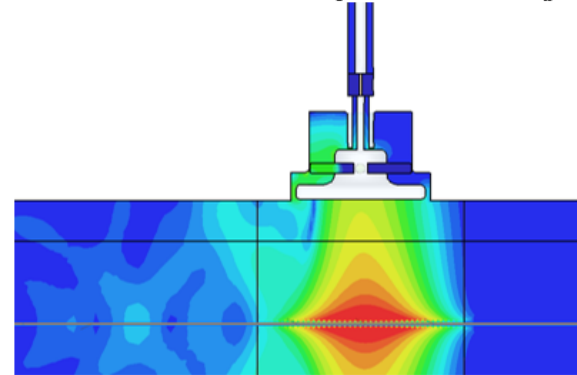
BPM signals spectral densities for various bunch lengths

- Hermetic feedthrough welding is finished.
- Next step = fit the electrodes and electron beam weld them into position.

BPMs for HWR cryomodule, prototype (top) and production (bottom) units

BPMs for SSR1 cryomodule

P.Ostroumov, PIP-II MAC meeting, 03/10/15

1

BPMs are mounted to the focusing elements:

ring pickup

🔷 **Fermilab**
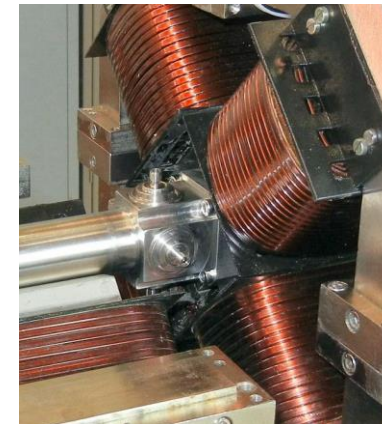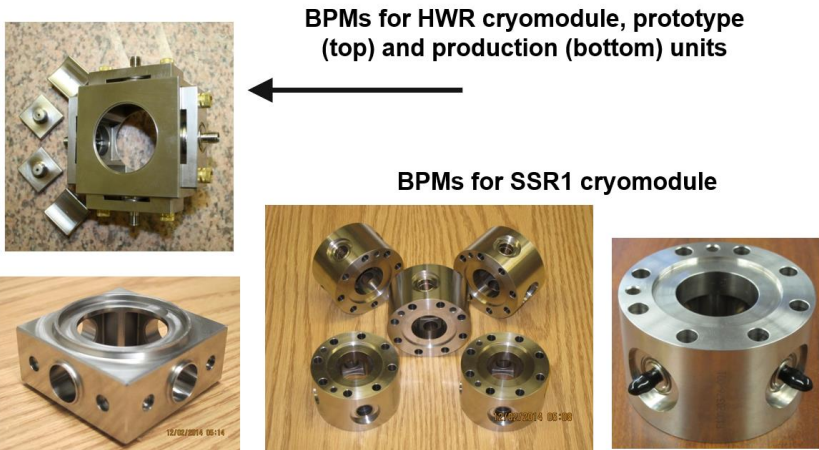
Summary:

❑ RF design of the cavity is based on
- the accelerator operation regime – pulsed or CW;
- the beam power and energy;
- the beam quality requirements.

❑ RF cavity parameter optimization includes:
- frequency,
- RT versus SRF
- operating temperature choice for SRF,
- optimal gradient,
- cavity shape optimization,
- number of cells,
- cell-to-cell coupling,
- HOM extraction,
- RF power coupling

❑ RF linac is self-consistent system and its subsystem are interconnected; therefore, the RF cavity design is an iterative process.

❑ RF cavity design includes:
- RF parameter optimization;
- MP analysis
- Mechanical optimization.

🐝 Fermilab

Summary (cont):

❑ The SRF cavity component design includes:
- the input power design;
- the cavity tuner design;
- The He vessel design.

❑ The SRF cavity manufacturing process contains a lot of operations and requires high technological culture:
- material quality control;
- cell manufacturing and pre-tune;
- final assembly;
- surface processing;
- welding into the He vessel;
- component assembly;
- Cavity string assembly;
- cryo-module assembly;
- alignment

❑ The cryo-module:
- Contains the insulating vacuum.
- Serves as the major structural element to which all other systems are attached to the accelerator tunnel floor.
- Serves as a pressure containment vessel in the event of a failure in an internal cryogen line.

🔹 Fermilab

Chapter 11.

Architecture of SRF accelerators.

a. proton/ion SRF linacs:

- RT or SRF front end?

- choice of beamline elements;

- lattice design.

b. electron SRF linacs.

V. Yakovlev | Cavity design. Linac archeticture, Lecture 14

🔱 **Fermilab**

Architecture of a GeV–range proton SRF accelerator:
Layout of typical modern proton SRF accelerator.
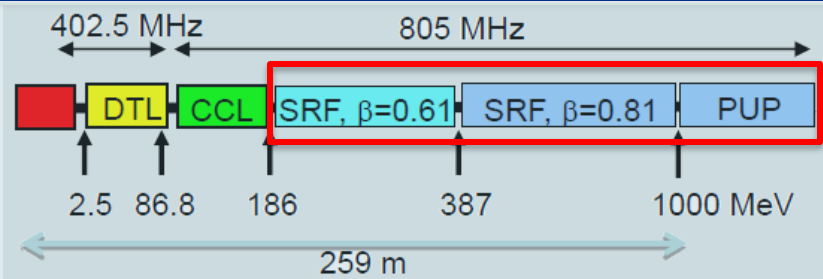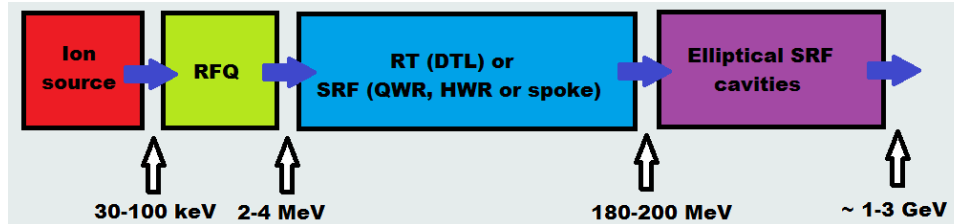
SNS (ORNL): H⁻ ,1 GeV, 6% DF, 1.44 MW to accumulator ring
In operation
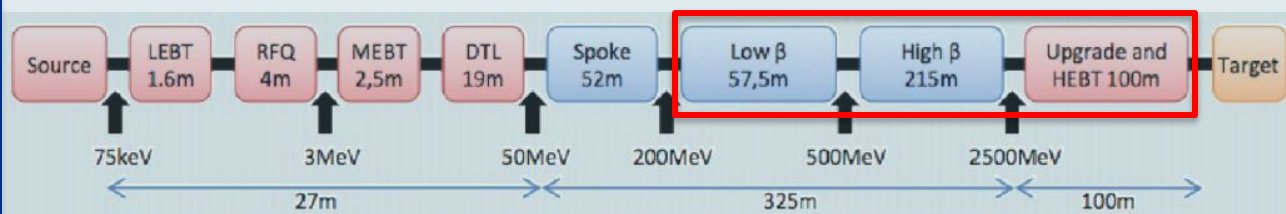
ESS (Lund): p⁺, 2.5 GeV, 4% DF, 5 MW to target
Under construction
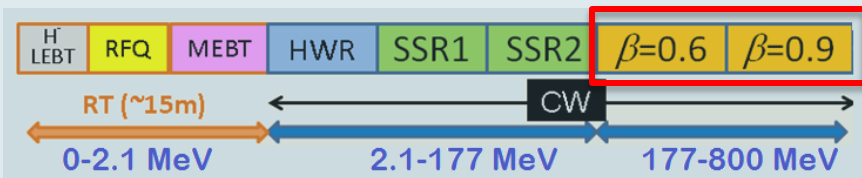
PIP II (FNAL): H⁻ ,800 MeV, up to 100% DF, up to 1.6 MW
Design

🔷 Fermilab

Linac Design Philosophy:

❑ RT or SRF frontend?

- For low duty factor RT frontend (up to ~200 MeV) may be used

- For high DF or CW SRF is necessary from the beginning

❑ Choice of beam line elements

- Accelerating RF Cavities

- Focusing Magnets

❑ Lattice Design

- Focusing Period

- Transition Energy between Sections

🛠 **Fermilab**
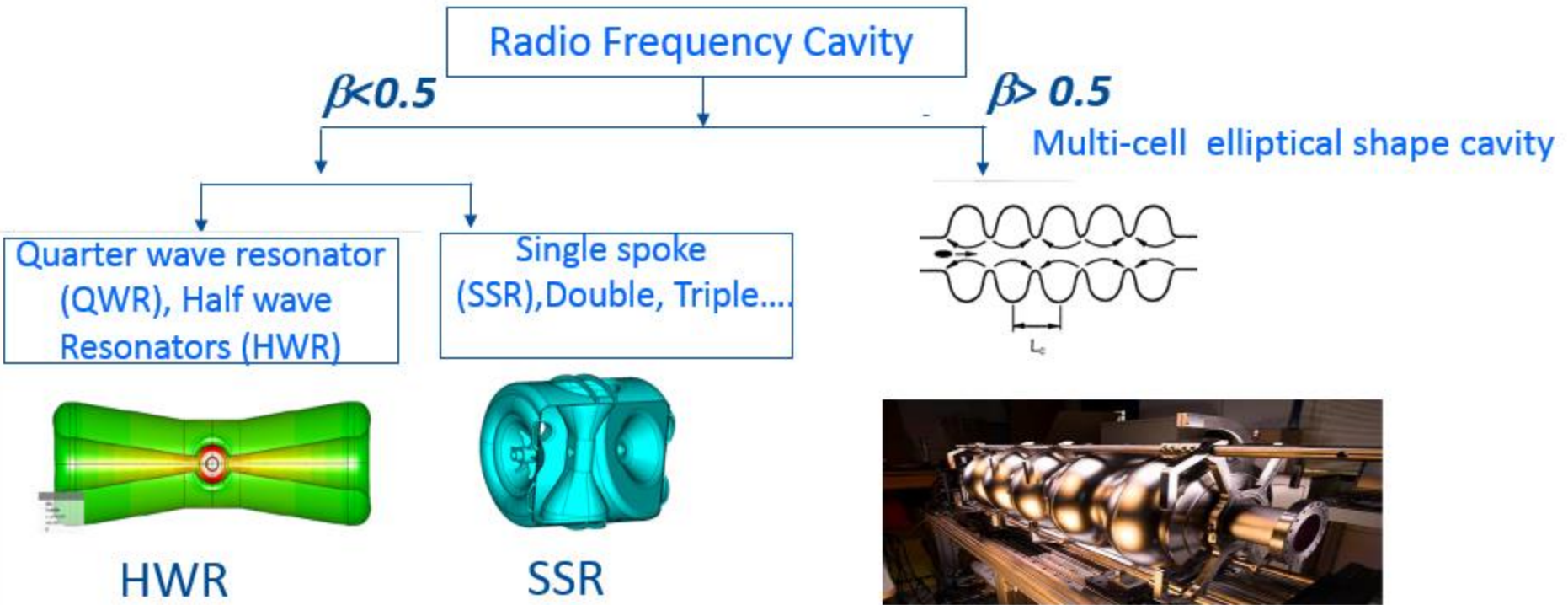
RF cavities:

- Lower RF frequency provides better interaction with beam.
- RF defocusing factor is inversely proportional to frequency.
- Lower frequency implies larger RF bucket and hence larger longitudinal acceptance.

RF cavities:

❑ The frequency choices for multi-cell:

- Cavity length is about the same for the same β_G (the same number of couplers, tuners, etc). Typical length ~0.8-1 m depending on β_G (from iris to iris)
- Lower frequencies → bigger size, higher cost, more difficult handling, microphonics
  but: lower losses per unit length (smaller R/Q, but lower R_s);
  larger aperture (current interception), smaller beam
  defocusing; smaller number of cells and therefore, smaller
  a/λ, smaller K_m and K_e and smaller numbers of cavity types.
- Typically , they use $650 - 800$ MHz, and 5-7 cells/cavity:
  SNS: 804 MHz, 6 cells/cavity (in operation)
  ESS: 704 MHZ, 5 cells/cavity (under construction)
  PIP II: 650 MHz, 5 cells/cavity (under development)

❑ The frequency choices for the front end:

- Subharmonics of the main frequency.

❑ Acceleration gradient choice (high DF, CW):

- Quench, $B_{peak} \gtrsim$ 70-80 mT
- Field emission, $E_{peak} \gtrsim$ 40 MV/m
- Thermal breakdown typically is not an issue for proton linacs.

🟦 **Fermilab**

RF cavities:

- Selection of the maximum accelerating gradients in cavities are made on the basis of :
  - Peak surface magnetic field
  - Peak surface Electrical field

- Choices of peak magnetic fields are derived from:
  - Dynamics heat load due to accelerating mode
  - Cavity quenching.

- Choices of peak surface field is made to avoid field emission

CW Linac assumptions:
- 162.5 MHz: $H_{pk} < 50$mT
- 325 MHz: $H_{pk} < 60$mT
- 650 MHz: $H_{pk} < 70$mT
- $E_{pk} < 40$ MV/m.

Accelerating Gradient in PIP-II Linac

	HWR	SSR1	SSR2	LB650	HB650
Gradient (MV/m)	9.7	10	11.4	15.9	17.8

🟦 **Fermilab**

Focusing elements:

❖ Normal conducting magnets are cheaper but superconducting magnets are:
  ➢ Compact in size
  ➢ Provide intense magnetic field with low power consumption.
❖ Low energy part of SRF linac typically has solenoidal focusing:
  ❖ Provide radial focusing
❖ Intermediate and high energy section of linac use normal conducting doublet focusing.
  ❖ Simplify cavity magnetic shielding requirements
❖ Correctors are built in each magnets.
❖ Solenoidal and doublet focussing keeps the beam round in transverse planes.

- *Focusing magnets in each section*

Section	HWR	SSR1	SSR2	LB650	HB650
Magnet	S	S	S	FD	FD

S – solenoid, FD – doublet (F : focusing and D: Defocusing quadrupole).

🔷 Fermilab

Focusing elements:

❏ Solenoid:

Solenoid focal length f:
(non-relativistic case, T is a particle kinetic energy, $T=mv^2/2$.)

$$\frac{1}{f} = \frac{q^2}{8Tm} \int B_z^2 dz$$

- Focal length is proportional to β^2;
- Focal length is inversed proportional to $B_z^2 L$, L is the solenoid length;
- Therefore, solenoid can be used for low β ($\beta<0.5$). For higher β quad is used.
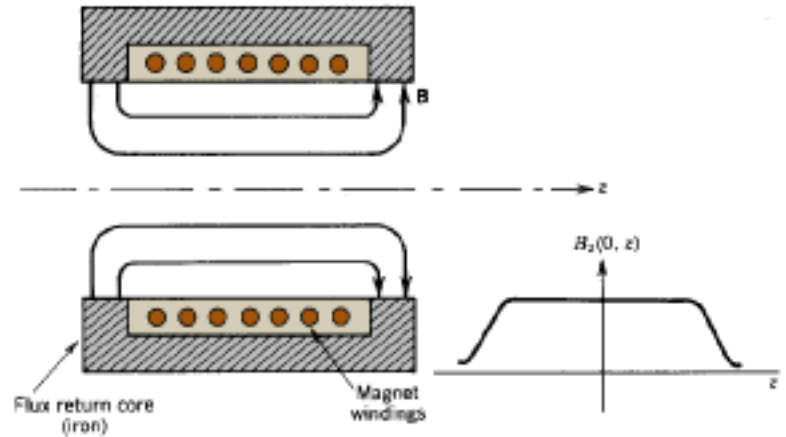
❏ Quadrupole lens:

Quad focal length f:

$$\frac{1}{f} = \frac{qB'L}{\gamma\beta mc}$$

🌠 Fermilab
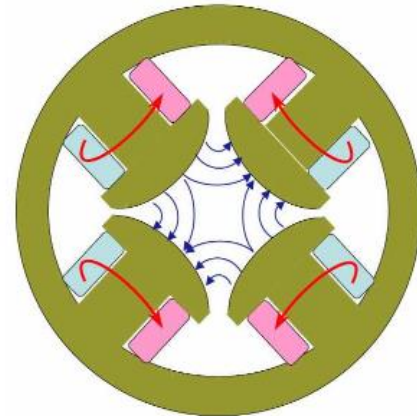
Focusing elements:

For low section SC solenoids are used.

- Simple and inexpensive;
- Filed up to 6-8 T;
- SRF cavity should have < 10 mT on the SRF cavity surface:
  remnant solenoid field should be compensated
- Solenoid contains correction coils (steering dipoles)
- Alignment (typically <0.3- 0.5 mm, <5 mrad tilt);
- Quench protection;
- Leads
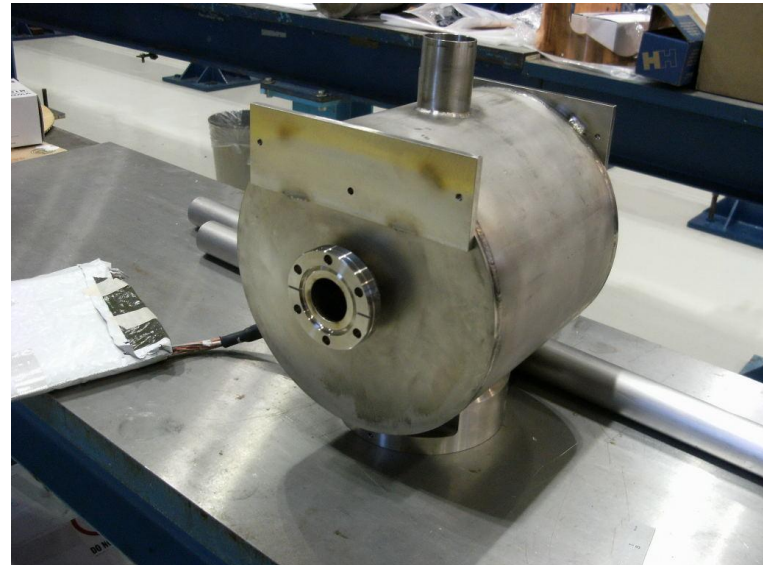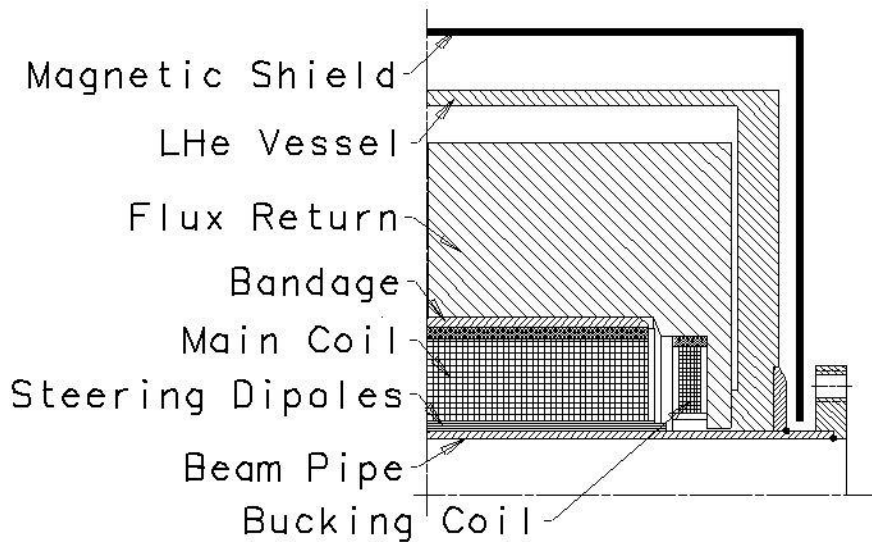
Lattice Design: Focusing Periods

- Length of the focusing period is kept short, especially in the low energy section where beam is non-relativistic and non-linear force may be significant .

Cryomodule Arrangement

HWR Section :

Solenoid	Drift	HWR Cavity	Drift
0.3 m	0.0806 m	0.25 m	0.0552m

0.6858 m
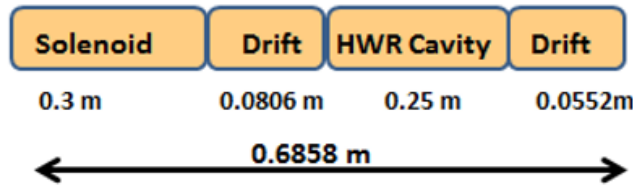
SC-SC-SC-SC-SC-SC-SC-SC

SSR1 Section :

0.3 m   0.3 m

SSR1 Cavity | Solenoid | SSR1 Cavity | SSR1 Cavity

0.4 m   0.45 m

1.25 m
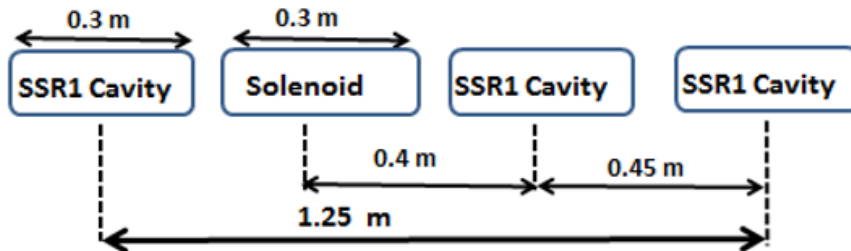
CSC-CSC-CSC-CSC

SSR2 Section :

0.32 m   0.4767 m

Solenoid | Cavity | Cavity | Solenoid

0.75 m   0.75 m

2.25 m

SCC-SCC-SC

‡ Fermilab
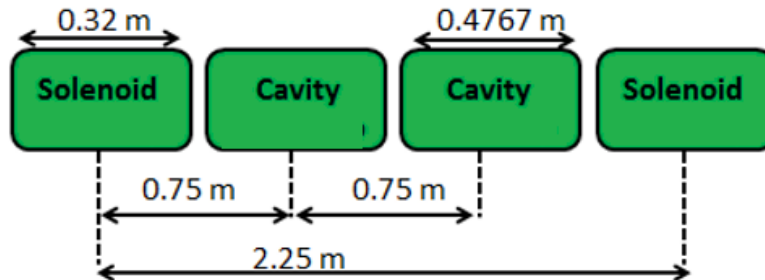
Lattice Design: Focusing Period in High Energy Section

- Frequency jump from 325 MHz to 650 MHz at LB650 MHz section
- Solenoidal focusing is replaced with quadrupole doublet.
- Same family of doublet is used in both LB650 and HB650 sections.

🔷 Fermilab
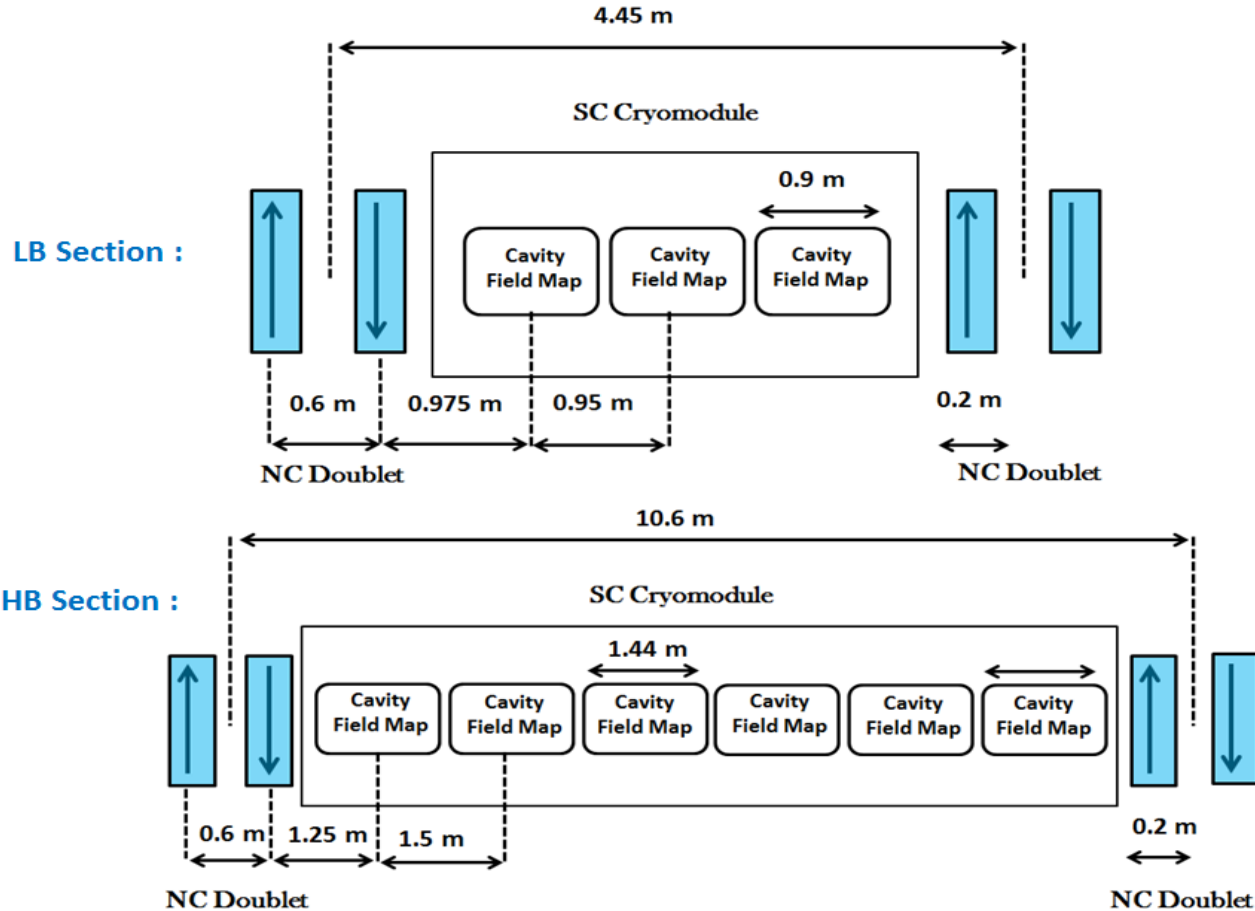
Transition Energy between Sections :

- Transition Energy between Sections (type cavity change). Optimization in order to minimize the number of cavities.
- Beam matching between sections and cryomodules are achieved using elements of each side of transitions. Avoiding abrupt changes in beam envelopes to reduce possibility of halo formations.
- Adiabatic variation in phase advance along linac. Reduces possibility of beam mismatch.
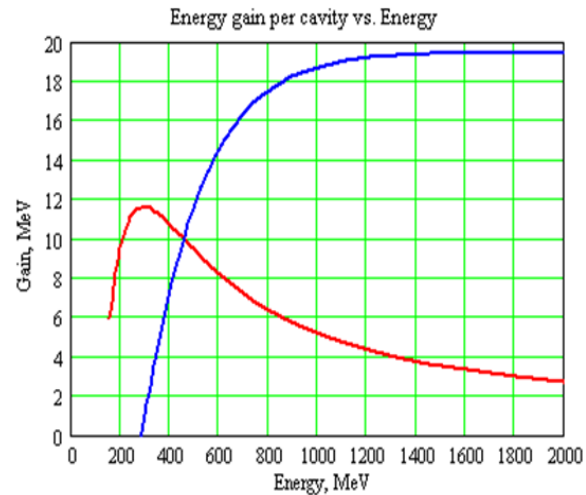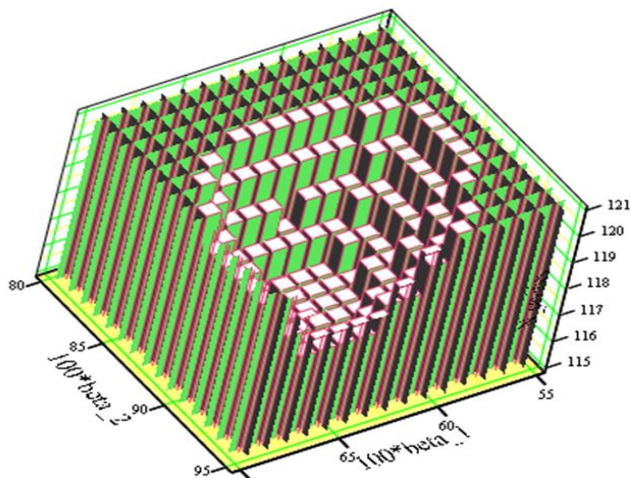
Number of cavities required for acceleration from 185 to 800 MeV versus cavity beta in the LB650 and HB650 sections (left) and the energy gain per cavity versus particle energy (right) for LB650 (red curve) and HB650 (blue curve) cavities.

🟦 **Fermilab**

Architecture of a GeV–range proton SRF accelerator:

Correct selections of transitional energy provide better optimization of real estate gradient and reduction in total number of beam line elements.

Transition time factor v/s beta
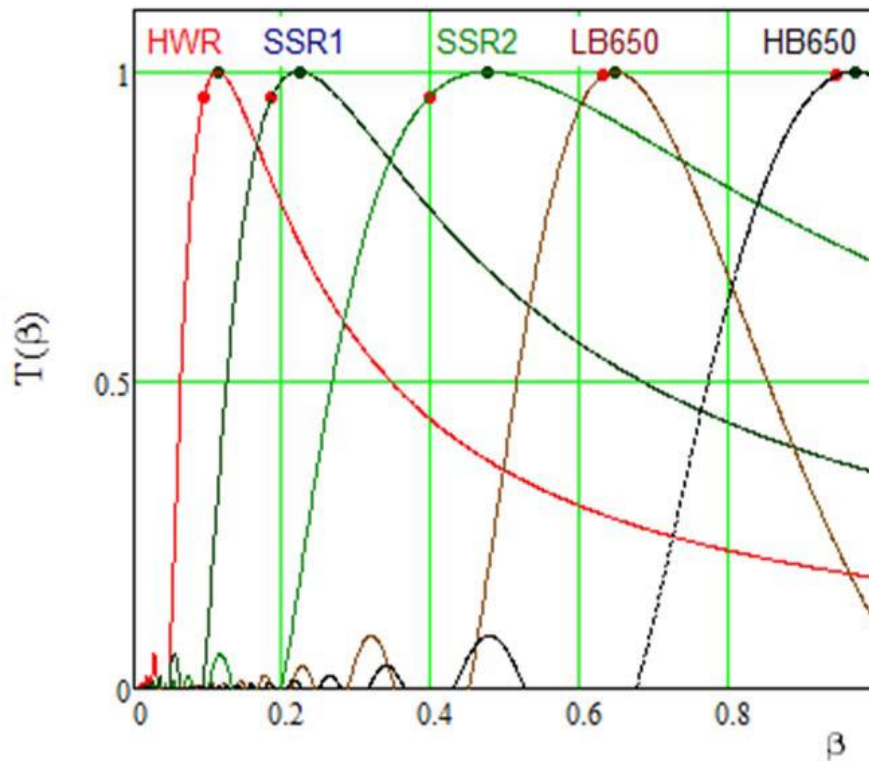
Sections	Initial Energy (MeV)	Design Beta	Beta range
HWR	2.1	0.094	0.067 -0.147
SSR1	10.3	0.186	0.147-0.266
SSR2	35	0.398	0.266-0.55
LB 650	185	0.61	0.55-0.758
HB 650	500	0.92	0.758-0.842

✳ Fermilab

Acceleration voltage distribution

Voltage Amplitude in Cavities
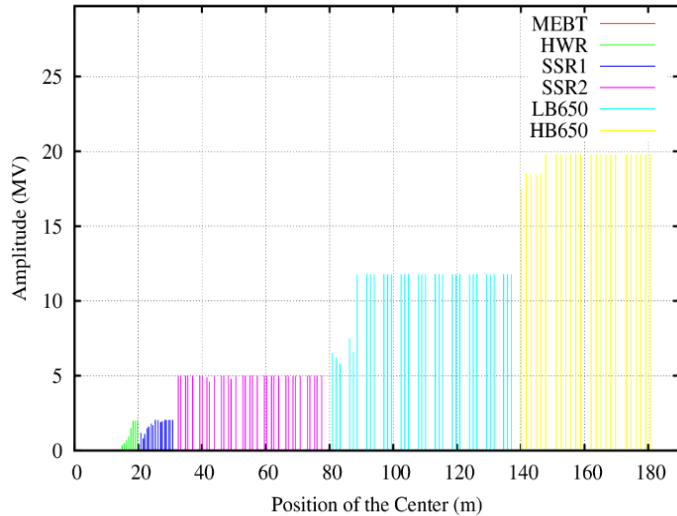
Voltage gain by beam
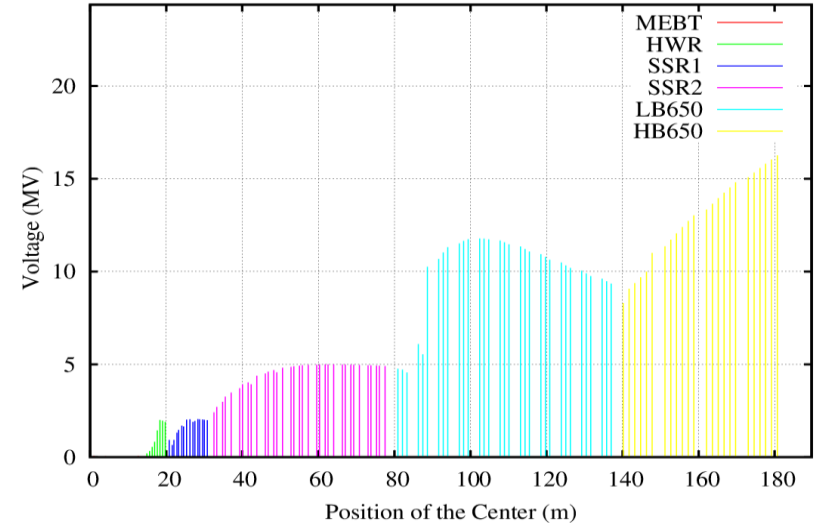
- Maximum Energy gain in PIP-II SC cavities

	HWR	SSR1	SSR2	LB650	HB650
Max. Egain (MeV)	2	2.05	5	11.9	19.9

🔷 Fermilab
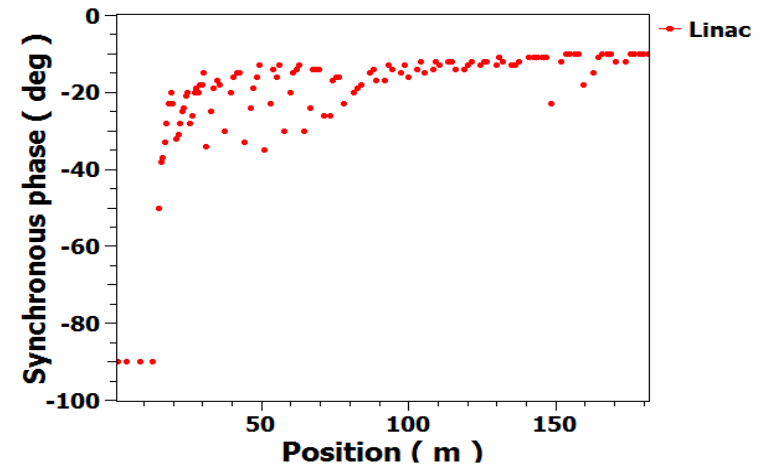
Summary:

- ❑ Architecture of a big SRF linac is determined by:
- • accelerated particles – electrons, protons or ions;
- • accelerator operation regime – pulsed or CW;
- • accelerator parameters – energy and power.
- ❑ For a proton accelerator the choice of the front end – RT or SRF – depends on the operation regime, pulsed or CW.
- ❑ The frequencies and cavity types for a proton or an ion accelerator should be determined;
- ❑ The types of the focusing elements should be selected.
- ❑ The lattice should be designed, which provides
- • acceleration
- • focusing
- • bunching.
- ❑ Break points between the section with different cavity types should be optimized;
- ❑ The sections should be matched to each other to provide required beam quality.

🔷 Fermilab

Chapter 12.

SRF around the world

V. Yakovlev | Cavity design. Linac archeticture, Lecture 14

SRF around the world
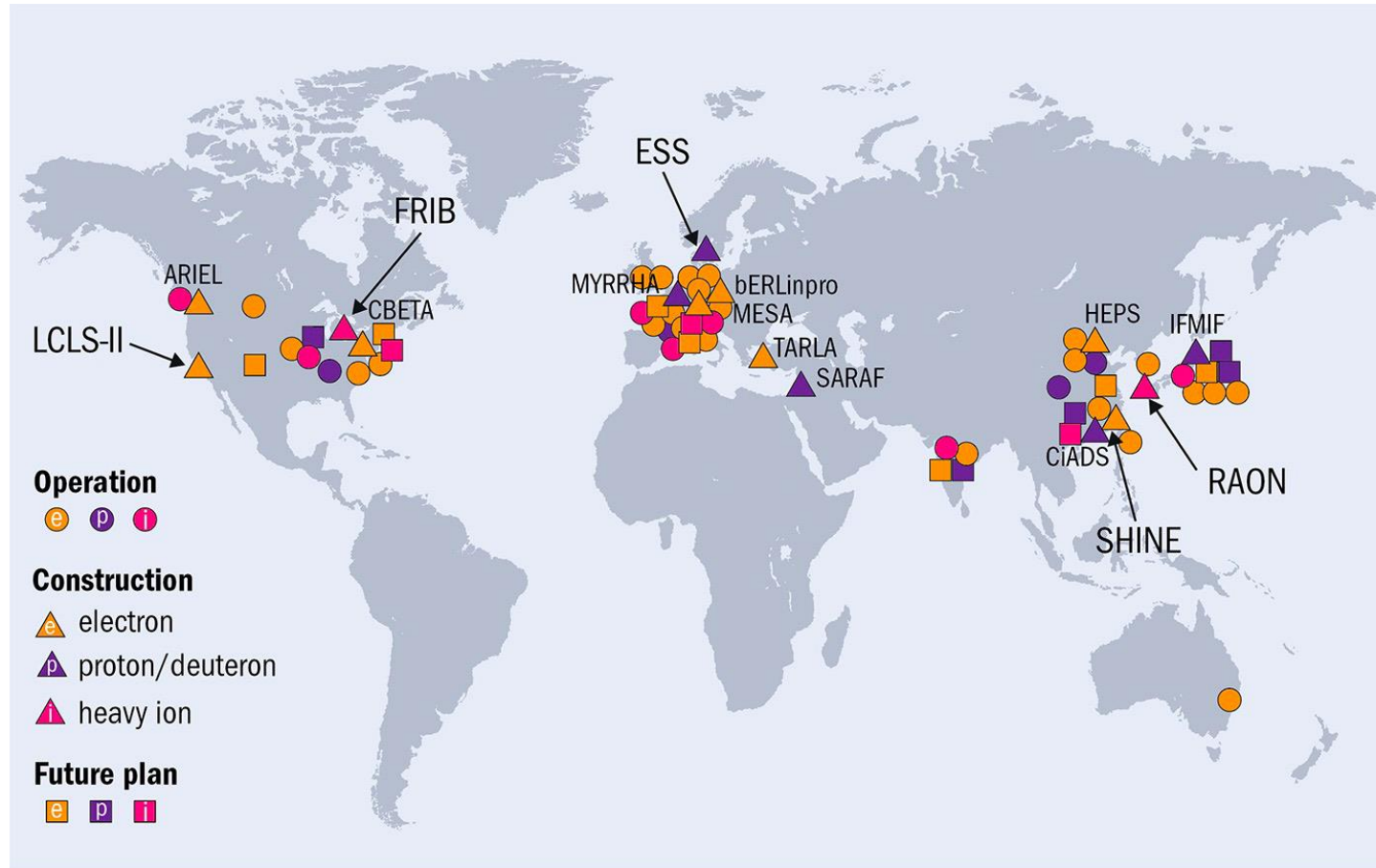
Global view Distribution of superconducting particle accelerators using SRF structures for electrons (orange), protons (purple) and heavy ions (pink). More than 30 SRF accelerators are in operation (circles), approximately 15 are presently under construction (triangles) and more than 10 future projects are under consideration (squares). *Credit: CERN*

Big SRF Accelerator Facilities:

Linac	Laboratory	Application	Acc. Particle	Operation	Status
SNS	ORNL, USA	Neutron Source	H$^-$	pulsed	Operation
ESS	ESS, Sweden	Neutron Source	p	pulsed	Construction
CIADS	IMP, China	ADS	p	CW	R&D
ISNS	Indore, India	Neutron Source	p	pulsed	R&D
ADSS	BARC, India	ADS	p	CW	R&D
PIP II	FNAL, USA	Neutrino/Muons	H$^-$	CW/pulsed	Construction
FRIB	MSU, USA	Nucellar physics	Ions	CW	Operation
RAON	RISP, S.Korea	Nucellar physics	Ions	CW	Construction
CEBAF	JLAB, USA	Nucellar physics	e$^-$	CW	Operation
XFEL	DESY, Germany	FEL	e$^-$	pulsed	Operation
SHINE	SINAP, China	FEL	e$^-$	CW	Construction
LCLS II	SLAC, USA	FEL	e$^-$	CW	Construction

🐝 Fermilab

New large SRF accelerator installations

CEBAF Upgrade - JLAB Upgrade 6.5 GeV => 12 GeV electrons	80 cavities	**Electrons**
XFEL – Hamburg, Germany 17.5 GeV electrons – Pulsed X-ray FEL	840 cavities	
LCLS-II (+ LCLS-II-HE) – SLAC 4 GeV electrons – CW X-ray FEL	296 (+184) cavities	
SPIRAL-II – France 30 MeV, 5 mA protons -> Heavy Ions	28 cavities	**Ions**
FRIB – MSU 400 kW, heavy ion beams for nuclear astrophysics	340 cavities	
RISP - Daejeon, South Korea 400 kW, heavy ion beams for nuclear astrophysics	340 cavities	
ESS – Sweden 1 – 2 GeV, 5 MW Pulsed spallation source	150 cavities	**Protons**
PIP-II – Fermilab 800 MV High intensity proton linac for neutrino beams	115 cavities	

Coming up: *SHINE* in China, *EIC* at BNL, *ILC* in Japan, *FCC-ee/FCC-hh* at CERN, *CEPC-SPPC* in China, *Accelerator complex upgrade to 2.4 MW* at Fermilab

🔷 **Fermilab**

SRF gradient achievements and applications

Credit: Source: R Geng/ORNL

Gradient growth SRF linac accelerating gradient achievements and application specifications since 1970.

CW SRF Linacs – SCA: Stanford Superconducting Accelerator; MUSL: llinois Microtron Using a Superconducting Linac; CEBAF: Continuous Electron Beam Accelerator Facility; JLab FEL: JLab Free Electron Laser; ELBE: HZDR Electron Linear accelerator with high Brillance and Low Emittance; ALICE: STFC Accelerators and Lasers In Combined Experiments; ARIEL: TRIUMF Advanced Rare IsotopE Laboratory; LCLS-II:

Linac Coherence Light Source extension; SHINE: Shanghai High Brightness Photon Facility.

Pulsed SRF Linacs – FAST: Fermilab Accelerator Science and Technology Facility; STF: KEK Superconducting RF Test Facility; E-XFEL: European Xray Free Electron Laser; ILC: International Linear Collider.

🐝 **Fermilab**

Fermilab PIP-II

| IS | LEBT | RFQ | MEBT | $\beta=0.11$ | $\beta=0.22$ | $\beta=0.51$ | $\beta=0.61$ | $\beta=0.9$ |

RT   SC

162.5 MHz   325 MHz   650 MHz
0.03-11 MeV   11-177 MeV   177-800 MeV

(115 Cavities)

Half Wave

Spokes

Medium-Beta Elliptical Cavities

High-Beta Elliptical Cavities

Architecture of Facility for Rare Isotope Beams (FRIB, MSU)

Beam Delivery System To Target

β=0.085 Matching Cryomodule   β=0.29 Matching Cryomodule   β=0.29 Matching Cryomodule

β=0.53 Matching Cryomodule   Superconducting Folding Segment

Li-Stripper Module

11 β=0.085 Cryomodules   3 β=0.041 Cryomodules   500 keV/u RFQ

Room-Temperature Folding Segment   β=0.085 Matching Cryomodule   12 β=0.29 Cryomodules   18 β=0.53 Cryomodules   10 m Vertical Drop from Ion Sources (above ground)

K. Saito, September 2014 LINAC14 THIOA02 ,

FRIB cavities

1- meter

$\beta_0 = 0.041$ $\beta_0 = 0.085$ $\beta_0 = 0.29$ $\beta_0 = 0.53$

N = 12   88   72   144
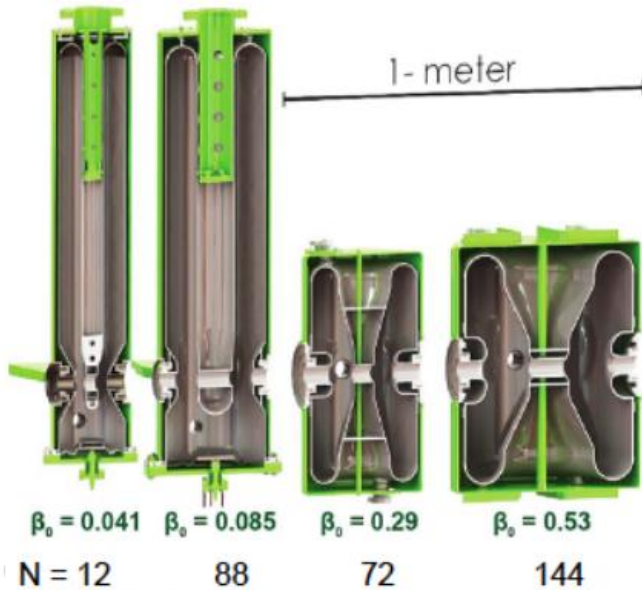
316 cavities need,
total 347 including matching module, spares

Cavity Type	QWR	QWR	HWR	HWR
β_0	0.041	0.085	0.285	0.53
f [MHz]	80.5	80.5	322	322
V_a [MV]	0.810	1.80	2.09	3.70
E_{acc} [MV/m]	5.29	5.68	7.89	7.51
E_p/E_{acc}	5.82	5.89	4.22	3.53
B_p/E_{acc} [mT/(MV/m)]	10.3	12.1	7.55	8.41
R/Q [Ω]	402	455	224	230
G [Ω]	15.3	22.3	77.9	107
Aperture [m]	0.036	0.036	0.040	0.040
$L_{eff} \equiv \beta\lambda$ [m]	0.153	0.317	0.265	0.493
Lorenz detuning [Hz/(MV/m)²]	< 4	< 4	< 4	< 4
Specific Q_0@VT	1.4E+9	2.0E+9	5.5e+9	9.2E+9
Q_L	6.3E+6	1.9E+6	5.6E+6	9.7E+6

🔷 **Fermilab**

FRIB linac is successfully commissioned in May 2021!

5-cell 644 MHz cavities for FRIB upgrade

Fermilab

Architecture of LCLS II (electron SRF Linac for FEL)

100-pC machine layout: Oct. 8, 2013; v21 ASTRA run; Bunch length L_b is FWHM
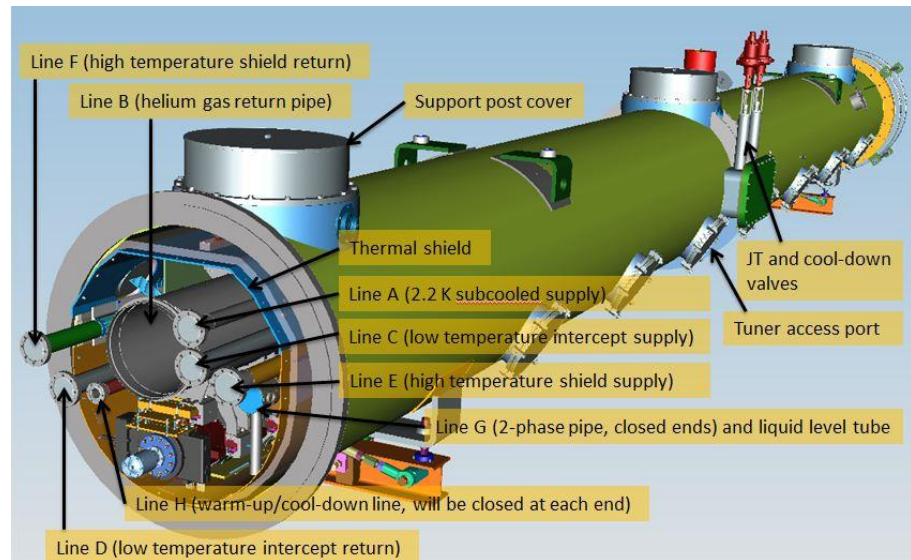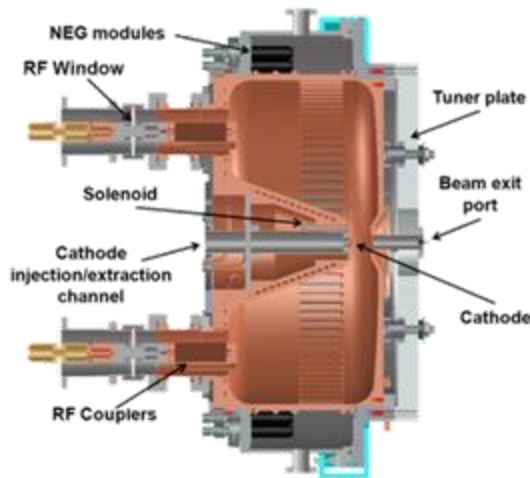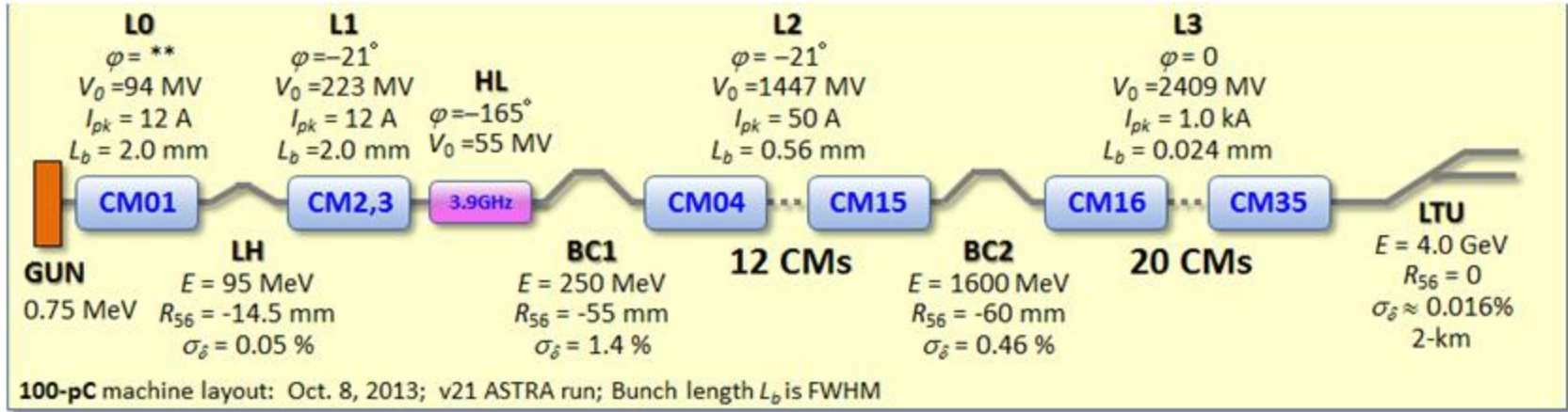
European XFEL

View Along the 1 km Long Superconducting Accelerator

- EXFEL is the world largest SRF application at 17.5 GeV (800 cavities).
- Operating gradient is 23.5 MV/m.
- Construction is complete, commissioning has started.
- First lasing in May 2017!

IPAC '17, 15.5.2017
Winni Decking, DESY

🟦 **Fermilab**

Επιλογος

❖ SRF Liner Accelerator is self-consistent system, parts of it strongly depend on each other. Deep understanding and careful analysis of subsystems and components as well as their interaction are necessary to achieve required beam parameters and facility reliability at minimal capital and operation cost.

❖ The design process will never be reduced to just a few simple rules or recipes. Using an existing design as a base for developing a new system is OK and can shorten the new system development time, but the system designers should be aware that even seemingly small changes could bring big consequences.

❖ As accelerator application demands continue to increase (higher energy, higher luminosity, brighter beams, more efficient accelerators, …) there will be no shortage of new challenges to tackle in the future.

❖ The field of RF superconductivity is very active. The SRF technology is the technology of choice for many types of accelerators.

V. Yakovlev | Cavity design. Linac archeticture, Lecture 14

🔷 Fermilab

There will always be ample opportunities for imagination, originality, and common sense.

The end

Appendixes

V. Yakovlev | Cavity design. Linac archeticture, Lecture 14

Appendix 1, Vector calculus

$\nabla \cdot (\psi \mathbf{A}) = \mathbf{A} \cdot \nabla \psi + \psi \nabla \cdot \mathbf{A}$	$\mathbf{div}(\psi \mathbf{A}) = \mathbf{A} \cdot \mathbf{grad}\psi + \psi \, \mathbf{div} \mathbf{A}$
$\nabla \times (\psi \mathbf{A}) = \nabla \psi \times \mathbf{A} + \psi \nabla \times \mathbf{A}$	$\mathbf{curl}(\psi \mathbf{A}) = \mathbf{grad}\psi \times \mathbf{A} + \psi \mathbf{curl} \mathbf{A}$
$\nabla(\mathbf{A} \cdot \mathbf{B}) = (\mathbf{A} \cdot \nabla)\mathbf{B} + (\mathbf{B} \cdot \nabla)\mathbf{A} +$ $+\mathbf{A} \times (\nabla \times \mathbf{B}) + \mathbf{B} \times (\nabla \times \mathbf{A})$	$\mathbf{grad}(\mathbf{A} \cdot \mathbf{B}) = (\mathbf{A} \cdot \nabla)\mathbf{B} + (\mathbf{B} \cdot \nabla)\mathbf{A} +$ $+\mathbf{A} \times \mathbf{curl} \mathbf{B} + \mathbf{B} \times \mathbf{curl} \mathbf{A}$
$\frac{1}{2}\nabla A^2 = \mathbf{A} \times (\nabla \times \mathbf{A}) + (\mathbf{A} \cdot \nabla)\mathbf{A}$	$\frac{1}{2}\mathbf{grad} A^2 = \mathbf{A} \times (\mathbf{curl} \mathbf{A}) + (\mathbf{A} \cdot \nabla)\mathbf{A}$
$\nabla \cdot (\mathbf{A} \times \mathbf{B}) = \mathbf{B} \cdot \nabla \times \mathbf{A} - \mathbf{A} \cdot \nabla \times \mathbf{B}$	$\mathbf{div}\,(\mathbf{A} \times \mathbf{B}) = \mathbf{B} \cdot \mathbf{curl}\,\mathbf{A} - \mathbf{A} \cdot \mathbf{curl}\,\mathbf{B}$
$\nabla \times (\mathbf{A} \times \mathbf{B}) = \mathbf{A}(\nabla \cdot \mathbf{B}) - \mathbf{B}(\nabla \cdot \mathbf{A}) +$ $+(\mathbf{B} \cdot \nabla)\mathbf{A} - (\mathbf{A} \cdot \nabla)\mathbf{B}$	$\mathbf{curl}\,(\mathbf{A} \times \mathbf{B}) = \mathbf{A}\,(\mathbf{div}\,\mathbf{B}) - \mathbf{B}\,(\mathbf{div}\,\mathbf{A}) +$ $+(\mathbf{B} \cdot \nabla)\mathbf{A} - (\mathbf{A} \cdot \nabla)\mathbf{B}$

P.W.

*

Fermilab

Appendix 1. Vector calculus

$$\nabla \psi = \text{grad } \psi$$

$$\nabla \cdot \mathbf{A} = \text{div} \mathbf{A}$$

$$\nabla \times \mathbf{A} = \mathbf{curl} \mathbf{A} \equiv \mathbf{rot} \mathbf{A}$$

$$\Delta = \nabla^2 = \nabla \cdot \nabla$$

$\nabla \times (\nabla \psi) = 0$	$\mathbf{curl}(\text{grad } \psi) = 0$
$\nabla \cdot (\nabla \times \mathbf{A}) = 0$	$\text{div} (\mathbf{curl} \mathbf{A}) = 0$
$\Delta \psi = \nabla \cdot (\nabla \psi) = \nabla^2 \psi$	$\Delta \psi = \text{div} (\text{grad } \psi)$
$\nabla \times \nabla \times \mathbf{A} = \nabla(\nabla \cdot \mathbf{A}) - \nabla^2 \mathbf{A}$	$\mathbf{curl}(\mathbf{curl} \mathbf{A}) = \text{grad} (\text{div} \mathbf{A}) - \Delta \mathbf{A}$

$$\nabla = \frac{\partial}{\partial x}\vec{i} + \frac{\partial}{\partial y}\vec{j} + \frac{\partial}{\partial z}\vec{k}, \qquad \int \mathbf{curl}\,\mathbf{F} \cdot d\mathbf{S} = \oint \mathbf{F} \cdot d\mathbf{l}\,, \qquad \int \text{div}\,\mathbf{F}\,dV = \int \mathbf{F} \cdot d\mathbf{S}$$

Stokes theorem   Gauss theorem

🎇 **Fermilab**

Appendix 1. Vector calculus

Differential operators in different coordinates:

	Cartesian	Cylindrical	Spherical
$\mathbf{A}$	$A_x\hat{\mathbf{x}} + A_y\hat{\mathbf{y}} + A_z\hat{\mathbf{z}}$	$A_\rho\hat{\boldsymbol{\rho}} + A_\varphi\hat{\boldsymbol{\varphi}} + A_z\hat{\mathbf{z}}$	$A_r\hat{\boldsymbol{r}} + A_\theta\hat{\boldsymbol{\theta}} + A_\varphi\hat{\boldsymbol{\varphi}}$
∇f	$\dfrac{\partial f}{\partial x}\hat{\mathbf{x}} + \dfrac{\partial f}{\partial y}\hat{\mathbf{y}} + \dfrac{\partial f}{\partial z}\hat{\mathbf{z}}$	$\dfrac{\partial f}{\partial \rho}\hat{\boldsymbol{\rho}} + \dfrac{1}{\rho}\dfrac{\partial f}{\partial \varphi}\hat{\boldsymbol{\varphi}} + \dfrac{\partial f}{\partial z}\hat{\mathbf{z}}$	$\dfrac{\partial f}{\partial r}\hat{\boldsymbol{r}} + \dfrac{1}{r}\dfrac{\partial f}{\partial \theta}\hat{\boldsymbol{\theta}} + \dfrac{1}{r\sin\theta}\dfrac{\partial f}{\partial \varphi}\hat{\boldsymbol{\varphi}}$
$\nabla \cdot \mathbf{A}$	$\dfrac{\partial A_x}{\partial x} + \dfrac{\partial A_y}{\partial y} + \dfrac{\partial A_z}{\partial z}$	$\dfrac{1}{\rho}\dfrac{\partial (\rho A_\rho)}{\partial \rho} + \dfrac{1}{\rho}\dfrac{\partial A_\varphi}{\partial \varphi} + \dfrac{\partial A_z}{\partial z}$	$\dfrac{1}{r^2}\dfrac{\partial (r^2 A_r)}{\partial r} + \dfrac{1}{r\sin\theta}\dfrac{\partial}{\partial \theta}(A_\theta \sin\theta) + \dfrac{1}{r\sin\theta}\dfrac{\partial A_\varphi}{\partial \varphi}$
$\nabla \times \mathbf{A}$	$\left(\dfrac{\partial A_z}{\partial y} - \dfrac{\partial A_y}{\partial z}\right)\hat{\mathbf{x}} \ +$ $\left(\dfrac{\partial A_x}{\partial z} - \dfrac{\partial A_z}{\partial x}\right)\hat{\mathbf{y}} \ +$ $\left(\dfrac{\partial A_y}{\partial x} - \dfrac{\partial A_x}{\partial y}\right)\hat{\mathbf{z}}$	$\left(\dfrac{1}{\rho}\dfrac{\partial A_z}{\partial \varphi} - \dfrac{\partial A_\varphi}{\partial z}\right)\hat{\boldsymbol{\rho}} \ +$ $\left(\dfrac{\partial A_\rho}{\partial z} - \dfrac{\partial A_z}{\partial \rho}\right)\hat{\boldsymbol{\varphi}} \ +$ $\dfrac{1}{\rho}\left(\dfrac{\partial(\rho A_\varphi)}{\partial \rho} - \dfrac{\partial A_\rho}{\partial \varphi}\right)\hat{\mathbf{z}}$	$\dfrac{1}{r\sin\theta}\left(\dfrac{\partial}{\partial \theta}(A_\varphi \sin\theta) - \dfrac{\partial A_\theta}{\partial \varphi}\right)\hat{\boldsymbol{r}} \ +$ $\dfrac{1}{r}\left(\dfrac{1}{\sin\theta}\dfrac{\partial A_r}{\partial \varphi} - \dfrac{\partial}{\partial r}(rA_\varphi)\right)\hat{\boldsymbol{\theta}} \ +$ $\dfrac{1}{r}\left(\dfrac{\partial}{\partial r}(rA_\theta) - \dfrac{\partial A_r}{\partial \theta}\right)\hat{\boldsymbol{\varphi}}$
$\Delta f = \nabla^2 f$	$\dfrac{\partial^2 f}{\partial x^2} + \dfrac{\partial^2 f}{\partial y^2} + \dfrac{\partial^2 f}{\partial z^2}$	$\dfrac{1}{\rho}\dfrac{\partial}{\partial \rho}\left(\rho\dfrac{\partial f}{\partial \rho}\right) + \dfrac{1}{\rho^2}\dfrac{\partial^2 f}{\partial \varphi^2} + \dfrac{\partial^2 f}{\partial z^2}$	$\dfrac{1}{r^2}\dfrac{\partial}{\partial r}\left(r^2\dfrac{\partial f}{\partial r}\right) + \dfrac{1}{r^2\sin\theta}\dfrac{\partial}{\partial \theta}\left(\sin\theta\dfrac{\partial f}{\partial \theta}\right) + \dfrac{1}{r^2\sin^2\theta}\dfrac{\partial^2 f}{\partial \varphi^2}$
$\Delta \mathbf{A}$	$\Delta A_x\hat{\mathbf{x}} + \Delta A_y\hat{\mathbf{y}} + \Delta A_z\hat{\mathbf{z}}$	$\left(\Delta A_\rho - \dfrac{A_\rho}{\rho^2} - \dfrac{2}{\rho^2}\dfrac{\partial A_\varphi}{\partial \varphi}\right)\hat{\boldsymbol{\rho}} \ +$ $\left(\Delta A_\varphi - \dfrac{A_\varphi}{\rho^2} + \dfrac{2}{\rho^2}\dfrac{\partial A_\rho}{\partial \varphi}\right)\hat{\boldsymbol{\varphi}} \ +$ $(\Delta A_z)\hat{\boldsymbol{z}}$	$\left(\Delta A_r - \dfrac{2A_r}{r^2} - \dfrac{2}{r^2\sin\theta}\dfrac{\partial(A_\theta \sin\theta)}{\partial \theta} - \dfrac{2}{r^2\sin\theta}\dfrac{\partial A_\varphi}{\partial \varphi}\right)\hat{\boldsymbol{r}} \ +$ $\left(\Delta A_\theta - \dfrac{A_\theta}{r^2\sin^2\theta} + \dfrac{2}{r^2}\dfrac{\partial A_r}{\partial \theta} - \dfrac{2\cos\theta}{r^2\sin^2\theta}\dfrac{\partial A_\varphi}{\partial \varphi}\right)\hat{\boldsymbol{\theta}} \ +$ $\left(\Delta A_\varphi - \dfrac{A_\varphi}{r^2\sin^2\theta} + \dfrac{2}{r^2\sin\theta}\dfrac{\partial A_r}{\partial \varphi} + \dfrac{2\cos\theta}{r^2\sin^2\theta}\dfrac{\partial A_\theta}{\partial \varphi}\right)\hat{\boldsymbol{\varphi}}$

V. Yakovlev | Cavity design. Linac archeticture, Lecture 14

Fermilab

Appendix 2

❑ Focusing. Panofsky-Wenzel theorem

Let's consider the particle transverse momentum change causes by the cavity RF field. The particle moves on the trajectory $z=vt$ parallel to the axis, but is displaced from it by $\vec{r}_\perp$.

Force acting on the particle is

$$\vec{F}(\vec{r}) = e\left[\vec{E}(\vec{r}) + \vec{v} \times \vec{B}(\vec{r})\right]e^{i\omega t}.$$

From Maxwell equation $curl\vec{E}(\vec{r}) = -i\omega\vec{B}(\vec{r})$ one has:

$$\vec{F}(\vec{r}) = e\left[\vec{E}(\vec{r}) + \vec{v} \times \frac{i}{\omega}curl\vec{E}(\vec{r})\right]e^{i\omega t} = e\left[\vec{E}(\vec{r}) + \frac{i}{\omega}\vec{\nabla}(\vec{v}\cdot\vec{E}(\vec{r})) - (\vec{v}\cdot\vec{\nabla})\cdot\vec{E}(\vec{r})\right]e^{i\omega t}.$$

If $\vec{v} = \vec{i}_z v$, then

$$F_z(\vec{r}) = eE_z(\vec{r})e^{i\omega t}$$

$$F_\perp(\vec{r}) = e\left[\vec{E}_\perp(\vec{r}) + v\frac{i}{\omega}\left(\vec{\nabla}_\perp E_z(\vec{r}) - \frac{\partial\vec{E}_\perp(\vec{r})}{\partial z}\right)\right]e^{i\omega t}$$

The differential operator $\vec{\nabla}_\perp$ acts on the transverse coordinates $\vec{r}_\perp$ only.

🎺 **Fermilab**

Appendix 2

If the particle velocity and particle transverse coordinates do not change significantly in the cavity, longitudinal and transverse momentum changes are:

$$\Delta p_{\parallel} = e \int_{-\infty}^{\infty} E_z(\vec{r}) e^{i\omega t} dt \, |_{t=z/v} = \frac{e}{v} \int_{-\infty}^{\infty} E_z(\vec{r}) e^{i\omega z/v} dz;$$

$$\Delta \vec{p}_{\perp} = e \int_{-\infty}^{\infty} \left[\vec{E}_{\perp}(\vec{r}) + \frac{iv}{\omega} \vec{\nabla}_{\perp} E_z(\vec{r}) - \frac{iv}{\omega} \frac{\partial \vec{E}_{\perp}(\vec{r})}{\partial z} \right] e^{i\omega t} dt \, |_{t=z/v}$$

However,

$$\frac{iv}{\omega} \int_{-\infty}^{\infty} \frac{\partial \vec{E}_{\perp}(\vec{r})}{\partial z} e^{i\omega t} dt \, |_{t=z/v} = \frac{i}{\omega} \int_{-\infty}^{\infty} \frac{\partial \vec{E}_{\perp}(\vec{r})}{\partial z} e^{i\omega z/v} dz = \frac{1}{v} \int_{-\infty}^{\infty} \vec{E}_{\perp}(\vec{r}) e^{i\omega z/v} dz = \int_{-\infty}^{\infty} \vec{E}_{\perp}(\vec{r}) e^{i\omega t} dt \, |_{t=z/v}$$

and

$$\Delta \vec{p}_{\perp} = e \frac{iv}{\omega} \int_{-\infty}^{\infty} \vec{\nabla}_{\perp} E_z(\vec{r}) e^{i\omega t} dt \, |_{t=z/v} = e \frac{i}{\omega} \int_{-\infty}^{\infty} \vec{\nabla}_{\perp} E_z(\vec{r}) e^{i\omega z/v} dz$$

Finally, we have:

$$\Delta \vec{p}_{\perp} = \frac{iv}{\omega} \vec{\nabla}_{\perp} (\Delta p_{\parallel}).$$

This relation between transverse and longitudinal momentum changes in an RF field is known as Panofsky – Wenzel theorem.

V. Yakovlev | Cavity design. Linac archeticture, Lecture 14   7/24/2024

Appendix 2.

❑ Bunching

Because a particle velocity depends on its energy, the cavity RF field provides the beam bunching. If the particle in the bunch center has the RF phase of ϕ_s (ϕ_s is a so-called synchronous phase), the particles next to the bunch center will have the same longitudinal coordinate at the same time at the distance L_z from the cavity (see Figure below), if

$$d\big(v(\phi) \cdot t(\phi)\big)/d\phi|_{\phi=\phi_s} = 0. \tag{1}$$
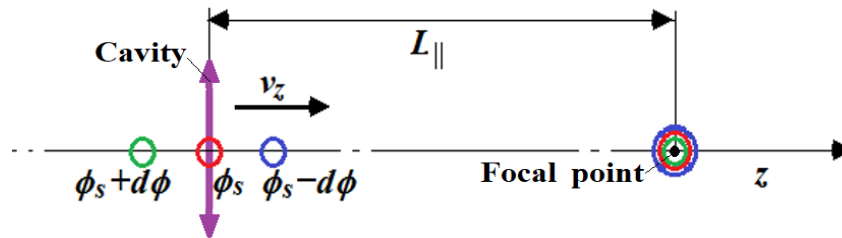
Here $v(\phi)$ is the particle velocity after it leaves the cavity, and $t(\phi)$ is time necessary for the particle to reach the distance $L_{//}$ – "longitudinal focusing distance":

$$t(\phi) = L_{//}/v(\phi_s) - (\phi - \phi_s)/\omega. \tag{2}$$

On the other hand, one has (Lecture 11, Slide 28):

$$\Delta W(r) = e\left|V_{0,z}\left(\frac{k}{\beta}\right)\right| I_0\left(\frac{kr}{\beta\gamma}\right)\cos\phi\,, \tag{3}$$

🔷 Fermilab

Appendix 2.

From (1), (2) and (3) it follows for the particle next to the axis ($kr/\beta\gamma <<1$) that

$$L_{||} = \left[\frac{v(\phi)^2}{\omega} \cdot \frac{dW/dv}{dW/d\phi}\right]_{\phi=\phi_s} = -\frac{v(\varphi_s)^2}{\omega} \cdot \frac{dW/dv|_{\phi=\phi_s}}{\Delta W_{max}(0) \cdot sin\phi_s} \qquad . \qquad (4)$$

For a linear accelerator one has

$$\frac{dW}{dv} = \frac{d(mc^2\gamma)}{dv} = mv\gamma^3, \qquad\qquad (5)$$

where m is the particle mass, and therefore

$$L_{||} = -\frac{(mc^2/e)\beta(\phi_s)^3\,\gamma(\phi_s)^3}{k\Delta W_{max}(0)\cdot sin\phi_s} = -\frac{(mc^2/e)\beta(\phi_s)^3\gamma(\phi_s)^3}{kV_{max}(0)\cdot sin\phi_s}. \qquad (6)$$

For bunching one needs $L_{//}>0$, and therefore, $\phi_s<0$. Note that $L_{//} \sim 1/k$. Note that for small energy (and therefore small β) the bunching may be too strong, and low RF frequency is to be used for acceleration.

🔷 **Fermilab**

Appendix 3. Eigen modes properties:

Eigenmodes in a cavity.

$$curl\vec{E} = -i\omega\mu_0\vec{H}, curl\vec{H} = i\omega\varepsilon_0\vec{E},$$
$$curlcurl\vec{E} - k^2\vec{E} = 0, curlcurl\vec{H} - k^2\vec{H} = 0, \qquad (1)$$

Here $k^2 = \omega^2\varepsilon_0\mu_0$

Boundary conditions: $\vec{E}_t = 0, \vec{H}_n = 0$ or $\vec{n} \times \vec{E} = 0, \vec{n} \cdot \vec{H} = 0$.

Equations (1) has non-trivial solutions only for defined k_m^2, eigenvalues.

Corresponding solutions $\vec{E}_m(x, y, z)$ and $\vec{H}_m(x, y, z)$ -eigenfunctions. There are infinite number of eigenvalues.

Eigenvalues are **real** and **positive.** From (1) and vector theorem (App.1)

$$div(\vec{A} \times \vec{B}) = \vec{B} \cdot curl\vec{A} - \vec{A} \cdot curl\vec{B} \qquad (2)$$

one has:

$$div(\vec{H}_m^* \times curl\vec{H}_m) = curl\vec{H}_m curlH_m^* - \vec{H}_m^* \cdot curlcurl\,\vec{H}_m = \left|curl\vec{H}_m\right|^2 - k_m^2\left|\vec{H}_m\right|^2$$

$$k_m^2 \int_0 \left|\vec{H}_m\right|^2 dV = \int_V \left|curl\vec{H}_m\right|^2 dV - \oint_S (\vec{H}_m^* \times curl\vec{H}_m)\,\vec{n}dS. \qquad \boxed{k_m^2 = \frac{\int_V \left|curl\vec{H}_m\right|^2 dV}{\int_V \left|\vec{H}_m\right|^2 dV}}$$

0

🎇 **Fermilab**

Appendix 3. Eigen modes properties

Eigenmodes are orthogonal:

$$curlcurl\vec{E}_m - k_m^2\vec{E}_m = 0, \qquad\qquad\qquad (3)$$

$$curlcurl\vec{E}_n - k_n^2\vec{E}_n = 0, \qquad k_m^2 \neq k_n^2$$

Let's calculate using (2)

$$div(\vec{E}_n \times curl\vec{E}_m) - div(\vec{E}_m \times curl\vec{E}_n) = curl\vec{E}_m \cdot curl\vec{E}_n - \vec{E}_n curlcurl\vec{E}_m -$$

$$curl\vec{E}_n \cdot curl\vec{E}_m + \vec{E}_m curlcurl\vec{E}_n = \vec{E}_m curlcurl\vec{E}_n - \vec{E}_n curlcurl\vec{E}_m.$$

Using (3) we have:

$$div(\vec{E}_n \times curl\vec{E}_m) - div(\vec{E}_m \times curl\vec{E}_n) = (k_n^2 - k_m^2)\,\vec{E}_m \cdot \vec{E}_n. \longrightarrow 0$$

$$(k_n^2 - k_m^2)\int_v \vec{E}_m \cdot \vec{E}_n dV = \oint_S \left(div(\vec{E}_n \times curl\vec{E}_m) - div(\vec{E}_m \times curl\vec{E}_n)\right)\vec{n}dS.$$

$$(k_n^2 - k_m^2)\int_V \vec{E}_m \cdot \vec{E}_n dV = 0, \quad \Longleftarrow \quad k_m^2 \neq k_n^2$$

$$\boxed{\int_V \vec{E}_m \cdot \vec{E}_n dV = 0,} \qquad \boxed{\int_V \vec{H}_m \cdot \vec{H}_n dV = 0,}$$

‡ Fermilab

Appendix 3. Eigen modes properties

Let's consider again the equation we got

$$k_m^2 \int_V |\vec{H}_m|^2 \, dV = \int_V |curl\vec{H}_m|^2 \, dV$$

Taking into account $curl\vec{H}_m = i\omega_m\varepsilon_0\vec{E}_m$ and $k_m^2 = \omega_m^2\varepsilon_0\mu_0$, we have:

$$\frac{1}{4}\int_V \mu_0|\vec{H}_m|^2 \, dV = \frac{1}{4}\int_V \varepsilon_0|\vec{E}_m|^2 \, dV$$

The time-average electrical stored energy is equal to the time-average magnetic stored energy.

🟦 **Fermilab**

Appendix 3. Eigen modes properties:

Variation properties of the eigenmvodes:

Let's consider expression for k^2:

$$k^2 = \frac{\int_V |curl\vec{H}|^2 dV}{\int_V |\vec{H}|^2 dV}. \qquad\qquad (1)$$

Variation of (1) gives:

$$\delta k^2 \int_V |\vec{H}|^2 dV + 2k^2 \int_V \vec{H} \cdot \delta\vec{H} dV = 2 \int_V curl\vec{H} \cdot curl\delta\vec{H} dV$$

Using the and vector theorem (2)

$$div(\delta\vec{H} \times curl\vec{H}) = curl\vec{H} \cdot curl\,\delta\vec{H} - \delta\vec{H} \cdot curlcurl\vec{H},\text{ we have}$$

$$\delta k^2 \int_V |\vec{H}|^2 dV = 2 \int_V (curlcurl\vec{H} - k^2\vec{H}) \cdot \delta\vec{H} dV + 2 \int_V div(\delta\vec{H} \times curl\vec{H}) dV.$$

Using Gauss theorem, we get

$$\delta k^2 \int_V |\vec{H}|^2 dV = 2 \int_V (curlcurl\vec{H} - k^2\vec{H}) \cdot \delta\vec{H} dV + 2 \oint_S (\delta\vec{H} \times curl\vec{H}) \cdot \vec{n} dS.$$
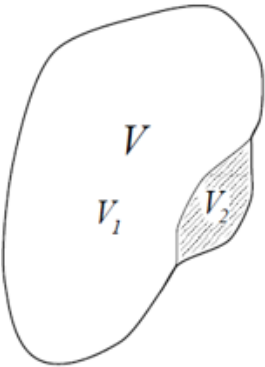
Taking into account that $curl\,curl\,\vec{H} - k^2\vec{H} = 0$ and boundary condition $\vec{n} \times curl\vec{H} = 0$ on S, and we finally get

$$\boxed{\delta k^2 = 0}$$

Appendix 3.

Small perturbations of the cavity geometry:

$$k^2 = \frac{\int\limits_{V_1} |\text{curl}\,\vec{H}^{(2)}|^2\, dV}{\int\limits_{V_1} |\vec{H}^{(2)}|^2\, dV} \approx \frac{\int\limits_{V_1} |\text{curl}\,\vec{H}^{(1)}|^2\, dV}{\int\limits_{V_1} |\vec{H}^{(1)}|^2\, dV} = \frac{\int\limits_{V} |\text{curl}\,\vec{H}^{(1)}|^2\, dV \;-\; \int\limits_{V_2} |\text{curl}\,\vec{H}^{(1)}|^2\, dV}{\int\limits_{V} |\vec{H}^{(1)}|^2\, dV \;-\; \int\limits_{V_2} |\vec{H}^{(1)}|^2\, dV} =$$

$$= k_1^2 \left\{ 1 + \frac{\int\limits_{V_2} |\vec{H}^{(1)}|^2\, dV}{\int\limits_{V} |\vec{H}^{(1)}|^2\, dV} - \frac{\int\limits_{V_2} |\text{curl}\,\vec{H}^{(1)}|^2\, dV}{\int\limits_{V} |\text{curl}\,\vec{H}^{(1)}|^2\, dV} \right\} = k_1^2 \left(1 + \frac{\Delta W_E - \Delta W_H}{W_0} \right)$$

$$\frac{k^2 - k_1^2}{k_1^2} = \frac{\Delta W_E - \Delta W_H}{W_0} \approx \frac{2\Delta\omega}{\omega_1} = \frac{(w_E - w_H) \cdot \Delta V}{W_0}.$$ ←Slater theorem

On the other hand, $\frac{1}{2}(w_H - w_E)\Delta V = p\,\Delta V = -\Delta W_0$ and

$$\frac{\Delta\omega}{\omega_0} = \frac{\Delta W_0}{W_0},$$

$$\boxed{\frac{W_0}{\omega_0} = \text{const}}$$ (compare to $E=vh$)

🔷 Fermilab

Appendix 4: Accelerating voltage and transit time factor:

For arbitrary axial distribution of the axisymmetric accelerating filed the voltage $V(\varphi)$ at arbitrary phase φ is the following:

$$V(\varphi) = Re \int_{-\infty}^{\infty} E_z(\rho = 0, z) e^{i(k_z z + \varphi)} dz =$$

$$= \int_{-\infty}^{\infty} Re[E_z(\rho = 0, z)] \cos(k_z z + \varphi) \, dz - \int_{-\infty}^{\infty} Im[E_z(\rho = 0, z)] \sin(k_z z + \varphi) \, dz =$$

$$= \int_{-\infty}^{\infty} Re[E_z(\rho = 0, z)] \cos(k_z z + \varphi) \, dz - \int_{-\infty}^{\infty} Im[E_z(\rho = 0, z)] \sin(k_z z + \varphi) \, dz =$$

$$= \cos(\varphi) \left(\int_{-\infty}^{\infty} Re[E_z(\rho = 0, z)] \cos(k_z z) \, dz - \int_{-\infty}^{\infty} Im[E_z(\rho = 0, z)] \sin(k_z z) \, dz \right) -$$

$$- \sin(\varphi) \left(\int_{-\infty}^{\infty} Re[E_z(\rho = 0, z)] \sin(k_z z) \, dz - \int_{-\infty}^{\infty} Im[E_z(\rho = 0, z)] \cos(k_z z) \, dz \right)$$

Maximal voltage V is, therefore,

$$V = \left[\left(\int_{-\infty}^{\infty} Re[E_z(\rho = 0, z)] \cos(k_z z) \, dz - \int_{-\infty}^{\infty} Im[E_z(\rho = 0, z)] \sin(k_z z) \, dz \right)^2 \right.$$

$$\left. + \left(\int_{-\infty}^{\infty} Re[E_z(\rho = 0, z)] \sin(k_z z) \, dz - \int_{-\infty}^{\infty} Im[E_z(\rho = 0, z)] \cos(k_z z) \, dz \right)^2 \right]^{1/2}$$

If $E_z(\rho, z)$ is real, $\quad V = \left[\left(\int_{-\infty}^{\infty} E_z(\rho = 0, z) \cos(k_z z) \, dz \right)^2 + \left(\int_{-\infty}^{\infty} E_z(\rho = 0, z) \sin(k_z z) \, dz \right)^2 \right]^{1/2}$

🔷 Fermilab

Appendix 5. Modes in a pillbox cavity:

In a pillbox cavities resonance field satisfies wave equations:

$$\Delta\vec{E} + k^2\,\vec{E} = 0, \Delta\vec{H} + k^2\,\vec{H} = 0, \text{ where } k = \frac{\omega}{c} \text{ - wavenumber.}$$

For an ideally conductive wall components of electric field tangential to the surface is zero. The pillbox cavity may be considered as a part of a waveguide having circular cross section, shortened at both ends. The fields in this waveguide may be described in cylindrical coordinates, (r,φ,z). In cylindrical coordinates longitudinal field components satisfy scalar wave equations:

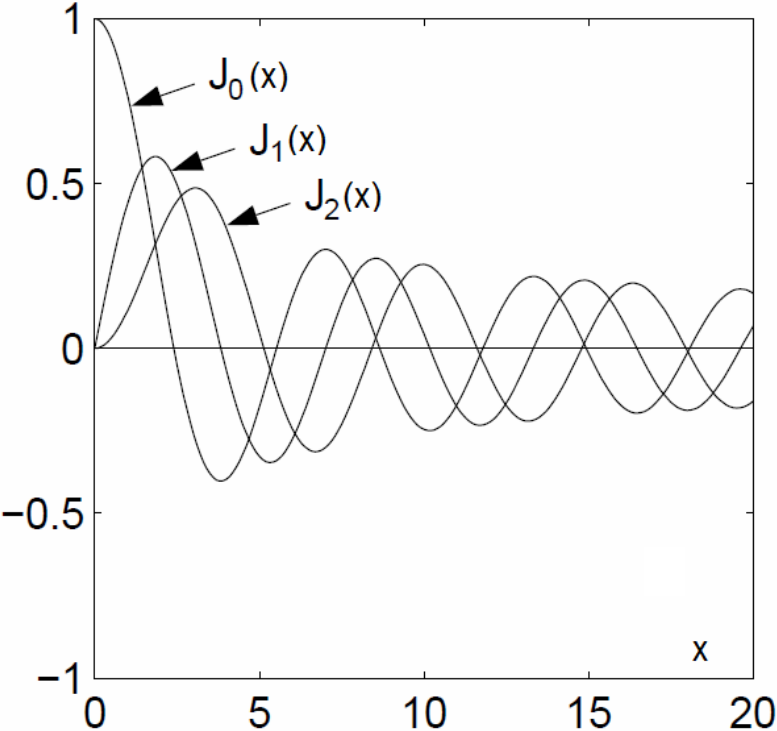$$\Delta E_z + k^2 E_z = 0, \Delta H_z + k^2 H_z = 0 \qquad\qquad (1)$$

For the waveguide, the fields have translation symmetry along $\vec{z}$, i.e., in two points having the same transverse coordinate, but different z, the fields differ by phase $\psi = k_z z$; *i.e.,* $\vec{E}, \vec{H} \sim e^{ik_z z}$. In this case:
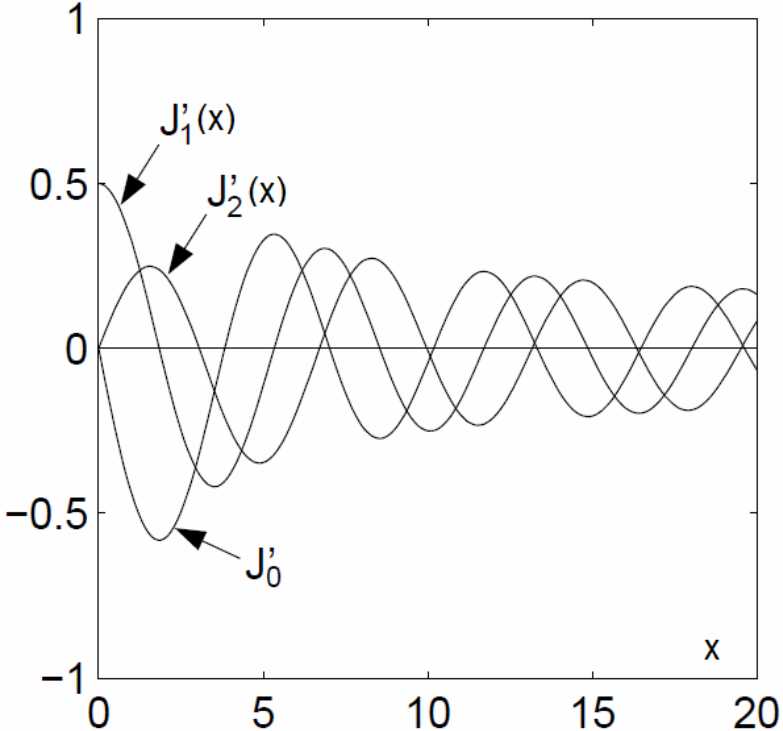
- Equations (1) have solution
$$E_z(r, \varphi, z), H_z(r, \varphi, z) = J_m(k_r r)e^{im\varphi}e^{ik_z z}; J_m(k_r r) \text{ are Bessel functions;}$$
- $k_r^2 + k_z^2 = k^2;$
- All transverse components (E_r, E_φ, H_r and H_φ)may be expressed through the longitudinal field components, E_z and H_z ;
- At $r=b$ (b is the waveguide radius) $E_z=0$ and $\frac{\partial H_z}{\partial n} = 0$. $\vec{n}$ is normal to the waveguide surface.

🎇 **Fermilab**

86   7/24/2024   V. Yakovlev | Cavity design. Linac archeticture, Lecture 14

Bessel functions and their derivatives

Appendix 5.

E_z and H_z satisfy the same equation, but have different boundary conditions, and therefore, different k_r :

	Electric field:	**Magnetic field:**
Equation:	$\Delta E_z + k^2 E_z = 0$	$\Delta H_z + k^2 H_z = 0$
Boundary condition:	$E_z(r, \varphi, z) = 0, r = a;$	$\partial H_z(r, \varphi, z)/\partial r = 0, r = a$
or	$J_m(k_r b) = 0;$	$J'_m(k_r b) = 0,$
and	$k_r = \frac{\nu_{mn}}{b}; J_m(\nu_{mn}) = 0;$	$k_r = \frac{\mu_{mn}}{b}; J'_m(\mu_{mn}) = 0.$

For the pillbox cavity having end walls at z=0 and z=d; therefore $k_z d = \pi p$ and

$$E_z = C J_m(k_r r) e^{im\varphi} \cos(\pi p z/d); \quad H_z = J_m(k_r r) e^{im\varphi} \sin(\pi p z/d),$$

and resonant frequencies are:

$$\frac{\omega}{c} = \sqrt{\left(\frac{\nu_{mn}}{b}\right)^2 + \left(\frac{\pi p}{d}\right)^2} \;; \qquad \frac{\omega}{c} = \sqrt{\left(\frac{\mu_{mn}}{b}\right)^2 + \left(\frac{\pi p}{d}\right)^2}$$

$$m = 0,1,\dots,\infty; \qquad\qquad m = 0,1,\dots,\infty;$$
$$n = 1,2,\dots,\infty; \qquad\qquad n = 1,2,\dots,\infty;$$
$$p = 0,1,\dots,\infty; \qquad\qquad p = 1,2,\dots,\infty;$$

TM_{mnp}-modes   TE_{mnp}-modes

$\text{TM}_{mnp}\text{-modes}$ $\text{TE}_{mnp}\text{-modes}$

🔷 **Fermilab**

Appendix 5.

Roots of $J'_m(x) = 0$.

m	μ_{m1}	μ_{m2}	μ_{m3}	μ_{m4}
0	3.832	7.016	10.174	13.324
1	1.841	5.331	8.536	11.706
2	3.054	6.706	9.970	13.170
3	4.201	8.015	11.346	14.586
4	5.318	9.282	12.682	15.964
5	6.416	10.520	13.987	17.313

$\mu_{0n} = \nu_{1n}!$

Roots of $J_m(x) = 0$.

m	ν_{m1}	ν_{m2}	ν_{m3}	ν_{m4}
0	2.405	5.520	8.654	11.792
1	3.832	7.016	10.174	13.324
2	5.135	8.417	11.620	14.796
3	6.380	9.761	13.015	16.223
4	7.588	11.065	14.373	17.616
5	8.771	12.339	15.700	18.980

TM$_{1np}$ and TE$_{0np}$ are degenerated!
n=1,2,…, ∞;
p=1,2,…, ∞*

*Note that TE$_{0n0}$ does not exist because of boundary conditions for magnetic field on the end walls.

Fermilab
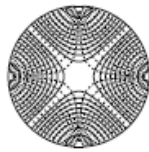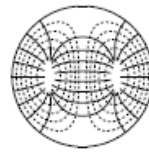
Appendix 5.

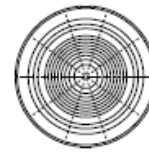Field plots for the pillbox modes
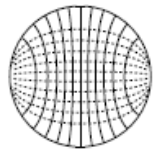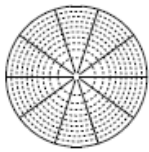
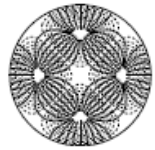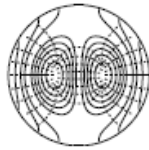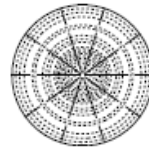(1) TE_{11} (2) TM_{01} (3) TE_{21} (4) TM_{11} (5) TE_{01} (6) TE_{31}
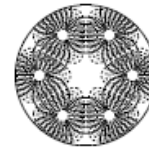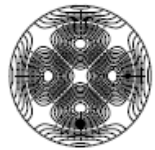
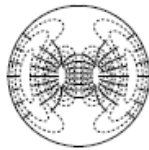(7) TM_{21} (8) TE_{41} (9) TE_{12} (10) TM_{02} (11) TM_{31} (12) TE_{51}
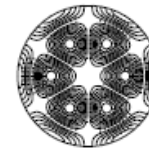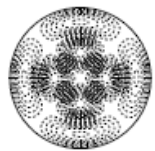
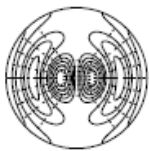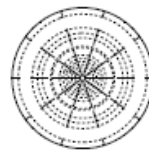(13) TE_{22} (14) TE_{02} (15) TM_{12} (16) TE_{61} (17) TM_{41} (18) TE_{32}
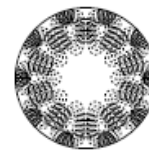
(19) TM_{22} (20) TE_{13} (21) TE_{71} (22) TM_{03} (23) TM_{51} (24) TE_{42}

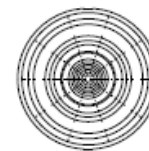(25) TE_{81} (26) TM_{32} (27) TM_{61} (28) TE_{23} (29) TM_{13} (30) TE_{03}

🔷 **Fermilab**

Appendix 6: RF cavity excitation by the beam:

- RF cavity having eigenmodes: eigen fields satisfy Maxwell equations:

$$\mathrm{curl}\,\mathbf{E}_s = -i\omega_s\mu\mathbf{H}_s, \quad \mathrm{curl}\,\mathbf{H}_s = i\omega_s\varepsilon\mathbf{E}_s. \qquad (1)$$

- The field excited by the beam:

$$\mathrm{curl}\,\mathbf{E} = -i\omega\mu\mathbf{H}, \qquad (2)$$

$$\mathrm{curl}\,\mathbf{H} = i\omega\varepsilon\mathbf{E} + \mathbf{J}_e$$

$\mathbf{J}_e$ – the beam current density spectrum component oscillating at the frequency ω

- The excited field may be expanded over the eigenmodes:

$$\mathbf{E} = \sum_s A_s\mathbf{E}_s - \mathrm{grad}\,\varphi_e, \quad \mathbf{H} = \sum_s B_s\mathbf{H}_s \qquad (3)$$

Here φ_e is space charge potential, typically its impact is small.

- From (1) and (2) one has:

$$\mathrm{div}\,(\mathbf{E}_s^* \times \mathbf{H}) = \mathbf{H}\cdot(i\omega_s\mu\mathbf{H}_s^*) - \mathbf{E}_s^*\cdot(i\omega\varepsilon\mathbf{E} + \mathbf{J}_e) =$$
$$= i\omega_s\mu\mathbf{H}\cdot\mathbf{H}_s^* - i\omega\varepsilon\mathbf{E}\cdot\mathbf{E}_s^* - \mathbf{J}_e\cdot\mathbf{E}_s^*, \qquad (4)$$
$$\mathrm{div}\,(\mathbf{E} \times \mathbf{H}_s^*) = \mathbf{H}_s^*\cdot(-i\omega\mu\mathbf{H}) - \mathbf{E}\cdot(-i\omega_s\varepsilon\mathbf{E}_s^*) =$$
$$= -i\omega\mu\mathbf{H}\cdot\mathbf{H}_s + i\omega\varepsilon\mathbf{E}\cdot\mathbf{E}_s^*.$$

All the fields have zero tangential electric field components on the wall.

‍🟦 **Fermilab**

Appendix 6:

Substituting (3) to (4) one has:

$$A_s = -\frac{\omega}{i(\omega^2 - \omega_s^2)} \cdot \frac{\int_V \mathbf{J}_e \mathbf{E}_s^* \, dV}{\mu \int_V \mathbf{H}_s \cdot \mathbf{H}_s^* \, dV}, \qquad B_s = -\frac{\omega_s}{i(\omega^2 - \omega_s^2)} \cdot \frac{\int_V \mathbf{J}_e \mathbf{E}_s^* \, dV}{\mu \int_V \mathbf{H}_s \cdot \mathbf{H}_s^* \, dV},$$

Note that

$$\mu \int_V \mathbf{H}_s \cdot \mathbf{H}_s^* \, dV = 2W_s$$

If there are wall losses, $\qquad \omega_s^2 \rightarrow \omega_s^2 \left(1 + \frac{i}{Q_0}\right)$

and for thin beam having the <u>average</u> current I_0 on the axis one has:

$$A_s = -\frac{i\omega}{\omega^2 - \omega_s^2 - i\frac{\omega\omega_s}{Q_s}} \times \frac{\int \mathbf{J}_e \mathbf{E}_s \, dV}{2W_s} = -\frac{i\omega}{\omega^2 - \omega_s^2 - i\frac{\omega\omega_s}{Q_s}} \times \frac{I_0 \left| \int_{-\infty}^{\infty} E_{sz}(z) e^{ikz} \, dz \right|}{W_s}, \quad k = \frac{\omega_s}{c} \qquad (5)$$

From (5) and (3) one has for the cavity voltage on the axis for the sth mode:

$$V_s = \frac{\Delta p_{\parallel} c}{e} = \int_{-\infty}^{\infty} E_{sz} e^{ikz} \, dz \approx \frac{i\omega_s^2}{\omega^2 - \omega_s^2 - i\frac{\omega\omega_s}{Q_s}} \cdot \frac{I_0 \left| \int_{-\infty}^{\infty} E_{sz}(z) e^{ikz} \, dz \right|^2}{\omega_s W_s} = \frac{i\omega_s^2}{\omega^2 - \omega_s^2 - i\frac{\omega\omega_s}{Q_s}} \cdot I_0 \left(\frac{R}{Q}\right)_s,$$

Appendix 6:

here

$$\left(\frac{R}{Q}\right)_s = \frac{\left|\int_{-\infty}^{\infty} E_{sz}(z)e^{ikz}dz\right|^2}{\omega_s W_s}$$

At the resonance one has

$$V_s = -Q_s I_0 \left(\frac{R}{Q}\right)_s = -I_0 R_s$$

where

$$R_s = Q_s \left(\frac{R}{Q}\right)_s$$

is a shunt impedance of the sth mode.

Fermilab

Appendix 6:

- This coincides to the voltage excited by the AC current $I = -2I_0$ in a parallel resonance circuit.
- Note that for a short bunch the beam current spectrum is

  $I(\omega) \approx I_0 + 2I_0 \sum \delta(\omega_s),$

  ω_s is the bunch sequence frequency; the equivalent circuit describes the cavity excitation by imaginary current, it gives the sign "-".
- From Kirchhoff theorem one has

  $I_C + I_L + I_R = iV\omega C + V/R + V/i\omega L = -2I_0,$

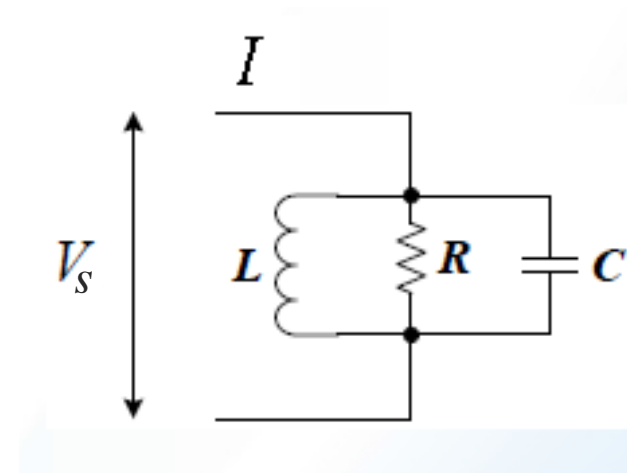 and taking into account that $\omega_s = (LC)^{-1/2}$, we get

$$V_s = \frac{i\omega_s^2}{\omega^2 - \omega_s^2 - i\frac{\omega\omega_s}{Q_s}} \cdot I_0 \left(\frac{R}{Q}\right)_s,$$

if $\omega_s \approx \omega$. Here are the equivalent circuit parameters:

$L = (R/Q)_s/2\omega;$
$C = 2/\omega(R/Q)_s;$
$R = (R/Q)Q_s/2.$

Appendix 7: The cavity coupled to the line.

Let's consider the cavity coupled to the feeding line:

Coupling slot

Cavity   line
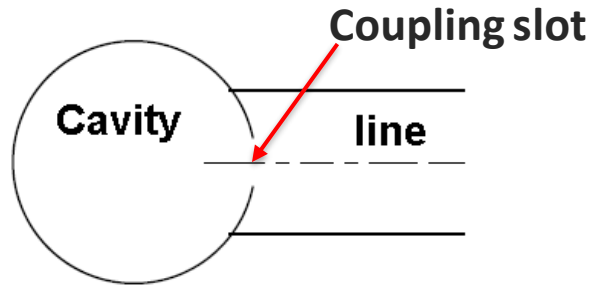
Consider another problem – the cavity coupled to the line shortened by a perfectly conducting plane S_1 placed such a way, that the electric field at the coupling slot has no tangential component:

Coupling slot S_1

Cavity   line   Cavity   line

(1)   (2) $E_t=0$
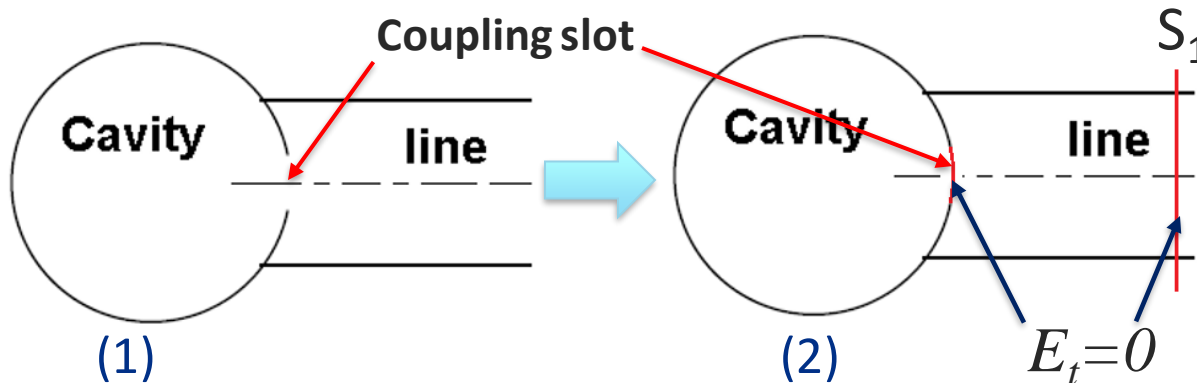
- The eigenfrequency of the new problem will be the same as for uncoupled cavity;
- The fields inside the cavity will be the same as for uncoupled cavity;
- The magnetic field on will be proportional to WG magnetic transverse eigenfunction $\boldsymbol{h}$, $H_t=ik\boldsymbol{h}(x,y)$; k is coefficient (real for convenience). Tangential electric field is zero.

≇ Fermilab

Appendix 7:

For the cavity excited by the line (problem 1) one has on S_1 for transverse fields:

$$E_t = U \cdot e(x,y), \quad H_t = I \cdot h(x,y), \qquad (1)$$

where $e(x,y)$ and $h(x,y)$ are the electric and magnetic WG transverse eigenfunction, $\int_{S_1} (e \times h) dS = 1$.

The field in the cavity H is proportional to the eigenfunction H_s of the cavity coupled to the shortened line (see previous slide):

$$H = B \cdot H_s = ikBh(x,y) \qquad (2)$$

From (1) and (2) one can find that

$$I = ikB \qquad (3)$$

Following the procedure from Appendix 11, we have, see Formulas 1,2 and 3 from this Appendix 11 and (1-3):

$$B = \frac{i\omega_s}{\omega^2 - \omega_s^2} \cdot \frac{\int_{S_1} \left(\vec{E} \times \vec{H}_s^* \right) \cdot dS}{2W_s} = - \frac{\omega_s}{\omega^2 - \omega_s^2} \cdot \frac{Uk}{2W_s}$$

and

$$(4)$$

$$I = - \frac{i\omega_s}{\omega^2 - \omega_s^2} \cdot \frac{Uk^2}{2W_s}$$

Appendix 7:

If there is wall loss in the cavity, $\omega_s^2 \to \omega_s^2 \left(1 + \frac{i}{Q_0}\right)$ and

$$I = -\frac{i\omega_s}{\omega^2 - \omega_s^2 - \frac{i\omega_s^2}{Q_0}} \cdot \frac{Uk^2}{2W_s}.$$

The cavity impedance at S_1 is therefore

$$Z_1 = \frac{U}{I} = -R_1 Q_0 \left(\frac{\omega^2 - \omega_s^2 - \frac{i\omega_s^2}{Q_0}}{i\omega_s^2}\right) \approx R_1(1 + iQ_0 x), \qquad (5)$$

where

$$R_1 = \frac{2\omega_s W_s}{Q_0 k^2}, x = \frac{\omega^2}{\omega_s^2} - 1 \approx \frac{2(\omega - \omega_s)}{\omega_s}.$$

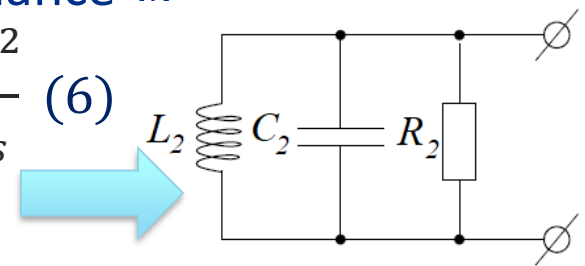The impedance (5) coincides to the impedance of a serial resonance circuit . At the distance of $\Lambda/4$ (Λ is wavelength in the WG) the cavity impedance is

$$Z_2 = \frac{Z_0^2}{Z_1} = \frac{Z_0^2}{R_1(1 + iQ_0 x)} = \frac{R_2}{(1 + iQ_0 x)}, R_2 = \frac{Z_0^2 Q_0 k^2}{2\omega_s W_s} \quad (6)$$

It is the impedance of a parallel resonance circuit (Z_0 is the WG impedance).

🔷 **Fermilab**
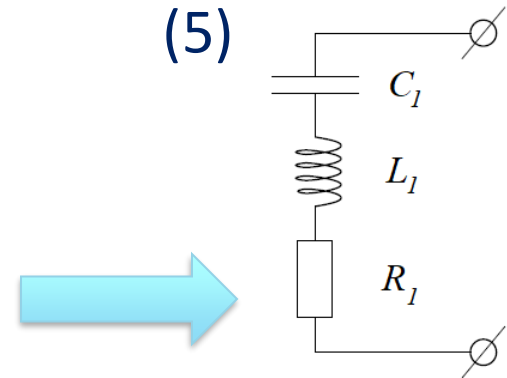
Appendix 7:

If the line is matched, the equivalent circuit is
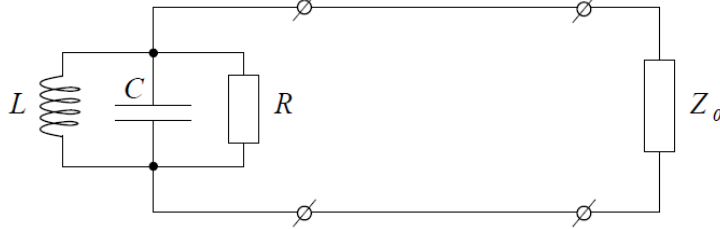
- Power P_R dissipated in R corresponds to the Ohmic losses in the cavity walls;
- Power P_{Z_0} dissipated in Z_0 corresponds to radiation in the line.

One can see:

$$\frac{P_{Z_0}}{P_R} = \frac{R}{Z_0} = \frac{Q_0}{Q_{ext}},$$

External quality factor, Q_{ext} describes radiation to the line:

$$Q_{ext} = \frac{\omega_s W_s}{P_{Z_0}}$$

Note that $Q_0 = \frac{\omega_s W_s}{P_R}$. The total loss is described by the loaded quality factor, Q_{load}

$$\frac{1}{Q_{load}} = \frac{P_{Z_0} + P_R}{\omega_s W_s} = \frac{1}{Q_{ext}} + \frac{1}{Q_0} \qquad (7)$$

Ratio of Q_0 to Q_{ext} is called coupling, β :

$$\frac{Q_0}{Q_{ext}} = \frac{R}{Z_0} \equiv \beta \qquad (8)$$

🔷 Fermilab

Appendix 7:

Let's estimate the reflection coefficient Γ of the parallel resonance circuit connected to the line:

$$\Gamma = \frac{Z - Z_0}{Z + Z_0},$$

According to (6)

$$Z = \frac{R}{(1 + iQ_0 x)}$$

At resonance (x=0)

$$\Gamma_0 = \frac{R - Z_0}{R + Z_0} = \frac{\frac{R}{Z_0} - 1}{\frac{R}{Z_0} + 1} = \frac{\beta - 1}{\beta + 1}.$$

For $x \neq 0$ one has

$$\Gamma = \frac{R - Z_0(1 + iQ_0 x)}{R + Z_0(1 + iQ_0 x)} = \frac{\Gamma_0 + 1}{1 + iQ_0 x/(1 + \beta)} - 1 = \frac{\Gamma_0 + 1}{1 + iQ_{load} x} - 1$$

(from (7) and (8) it follows that $Q_0/(1 + \beta) = Q_{load}$).
The power P dissipated in the cavity exited by the input power P_{in} is the following:

$$P = P_{in}(1 - |\Gamma|^2) = P_{in} \frac{1 - \Gamma_0^2}{1 + Q_{load}^2 x^2}.$$

‡ Fermilab

Appendix 8: Beam Loading

Power from RF source P_g

Input line

Coupling element

Beam I_b
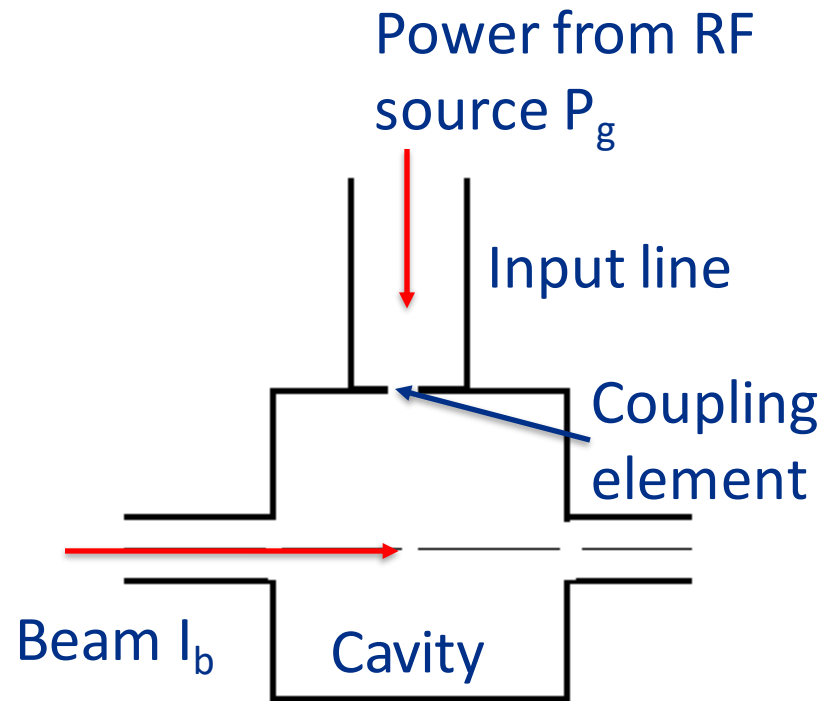
Cavity

- RF source and beam $\omega_g = \omega_b = \omega$;
- Cavity: ω_0
- Cavity voltage : V_c
- Shunt impedance: R_{sh}
- Losses: $P_c = V_c^2/R_{sh} = V_c^2/(Q_0 \cdot R/Q)$
- Radiation to the line: $V_c^2/(Q_{ext} \cdot R/Q)$
- Coupling: $\beta = Q_0 / Q_{ext}$
- Loaded Q: $Q_L = Q_0/(1 + \beta)$
- Average beam current: I_b
- Synchronous phase: φ
- Power consumed by the beam: $P_b = = I_b V_c cos\varphi$
- Input power P_g
- Reflected power: $P_r = P_g - P_c - P_b$

Fermilab

Appendix 8:

Equivalent circuit for the cavity excited by a WG and loaded by the beam (transformed to the cavity):

WG   Cavity   Beam
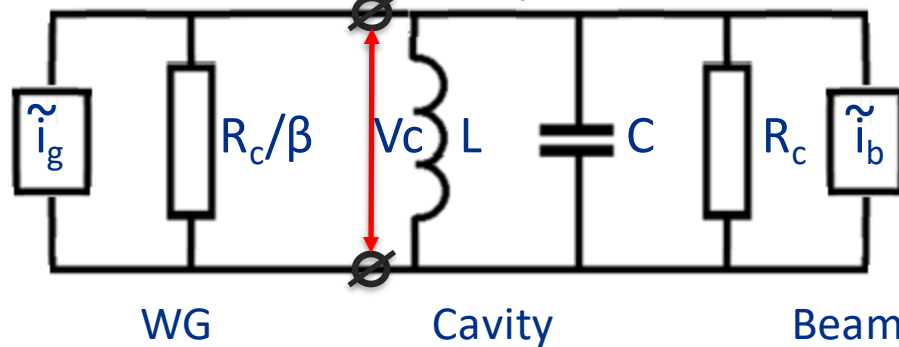
$L=R/Q/(2\omega_0)$
$C=2/(R/Q\cdot\omega_0)$
$R_c=R/Q\cdot Q_0/2$
$\tilde{\iota}_b=-2I_b$
$\beta = Q_0/Q_{ext}$

- The WG impedance transformed to the cavity is $Z_{WG}=R_c/\beta$ (radiated power is $\frac{V_c^2}{R_c/\beta}$);

- The WG is terminated by the cavity impedance* $Z_0 = \frac{R_c}{1+iQ_0x}$ in parallel to the beam impedance $Z_b = \frac{V_c}{I_b e^{i\varphi}}$, φ is the beam phase versus the voltage V_c.

- The total load impedance is $Z = \left(\frac{1}{Z_0}+\frac{1}{Z_b}\right)^{-1} = \left(\frac{1+iQ_0x}{R_c} + \frac{I_b e^{i\varphi}}{V_c}\right)^{-1}$.

- Reflection for this load is $\Gamma = \frac{V_{ref}}{V_{forw}} = \frac{Z-Z_{WG}}{Z+Z_{WG}} = \frac{1-Z_{WG}/Z}{1+Z_{WG}/Z}$.

- The cavity voltage is $V_c = V_{ref}+V_{forw} = V_{forw}(1+\Gamma) = V_{forw}\frac{2}{1+Z_{WG}/Z}$ and

$V_{forw} = \frac{V_c}{(1+\Gamma)} = \frac{V_c}{2}\left(1+Z_{WG}/Z\right)$.

*See Formulas (5-6), Appendix 7

‡ Fermilab

Appendix 8:

Therefore, the input power is:

$$P_g = \frac{\left|V_{forw}\right|^2}{Z_{WG}} = \frac{V_c^2}{4Z_{WG}}\left|1 + \frac{Z_{WG}}{Z}\right|^2 =$$

$$\approx \frac{V_c^2(1+\beta)^2}{4\left(\frac{R}{Q}\right)\beta Q_0}\left[\left(1 + \frac{I_b\cos\varphi\left(\frac{R}{Q}\right)Q_0}{(1+\beta)V_c}\right)^2 + \left(\frac{Q_0}{1+\beta}\cdot\frac{2\Delta f}{f} + \frac{I_b\sin\varphi\left(\frac{R}{Q}\right)Q_0}{1+\beta}\right)^2\right].$$

The formula works next to resonance: approximation is used for x:

$$x = \frac{\omega^2}{\omega_0^2} - 1 \approx \frac{2(\omega - \omega_0)}{\omega_0} = \frac{2(f - f_0)}{f_0} \approx \frac{2(f - f_0)}{f} = \frac{2\Delta f}{f}.$$

Note that $P_g = \frac{\left|V_{forw}\right|^2}{Z_{WG}}$ does not contain factor of 2 in the denominator

because of the cavity impedance $\left(\frac{R}{Q}\right)$ definition.

Fermilab

Appendix 9: Transverse impedance:

Let's consider a cavity excited by a beam current I_0 having offset x_0. If $\vec{E}$ is a dipole eigenmode, the field $\vec{\mathbf{E}}$ in the cavity in one-mode approximation may be expressed as $\vec{\mathbf{E}} \approx A(\omega, \omega_0)\vec{E}$, where ω is the bunch sequence harmonic frequency, ω_0 is the resonant frequency, and

$$A = -\frac{i\omega}{\omega^2 - \omega_0^2 - i\frac{\omega\omega_0}{Q}} \times \frac{\int \vec{j} \cdot \vec{\mathbf{E}} dV}{2W} = -\frac{i\omega}{\omega^2 - \omega_0^2 - i\frac{\omega\omega_0}{Q}} \times \frac{I_0\left|\int_{-\infty}^{\infty} E_z(x,y,z)e^{ikz} dz\right|}{W}.$$

where $W = \frac{\varepsilon_0}{2}\int |\vec{E}|^2 dV$ and I_0 is <u>an average </u>current

Appendix 10:

RF-kick at $x = x_0$ and $y=0$ may be obtained using Panofsky-Wenzel theorem:

$$U_{kick} = \frac{\Delta p_\perp c}{e} = \frac{ic}{\omega}\left|\nabla_\perp \int_{-\infty}^{\infty} E_z \, e^{ikz} dz\right| \approx \frac{c}{x_0\left(\omega^2 - \omega_0^2 - i\frac{\omega\omega_0}{Q}\right)} \times \frac{I_0\left|\int_{-\infty}^{\infty} E_z(x_0,0,z)e^{ikz}dz\right|^2}{W}$$

$$\approx \frac{c\omega_0}{\left(\omega^2 - \omega_0^2 - i\frac{\omega\omega_0}{Q}\right)} \times \frac{x_0 I_0\left|\int_{-\infty}^{\infty}\left(\frac{\partial E_z(x,0,z)}{\partial x}\right)_{x=x_0} e^{ikz} dz\right|^2}{W\omega_0} = \frac{\omega_0^2}{\left(\omega^2 - \omega_0^2 - i\frac{\omega\omega_0}{Q}\right)} \times \left(\frac{x_0}{k}\right) I_0 \left(\frac{r_\parallel}{Q}\right)$$

where $\left(\dfrac{r_\parallel}{Q}\right) \equiv \dfrac{\left|\int_{-\infty}^{\infty}\left(\frac{\partial E_z(x,0,z)}{\partial x}\right)_{x=x_0} e^{ikz} dz\right|^2}{W\omega_0}$

is dipole longitudinal impedance. and $k = \omega_0/c$. **Dipole** $\left(\dfrac{r_\parallel}{Q}\right)$ **is measured in Ohm/m².**

V. Yakovlev | Cavity design. Linac archeticture, Lecture 14

🎇 **Fermilab**

Appendix 10:

RF-kick may be expressed through the transverse impedance:

$$U_{kick} = \frac{\omega_0^2}{\left(\omega^2 - \omega_0^2 - i\frac{\omega\omega_0}{Q}\right)} \times x_0 I_0 \left(\frac{r_\perp}{Q}\right),$$

where $\left(\dfrac{r_\perp}{Q}\right) \equiv \left(\dfrac{r_\parallel}{Q}\right) \times \dfrac{1}{k} = \dfrac{\left|\int_{-\infty}^{\infty} \left(\dfrac{\partial E_z(x,0,z)}{\partial x}\right)_{x=x_0} e^{ikz} dz\right|^2}{kW\omega_0}.$

Note that $\left(\dfrac{\mathbf{r_\perp}}{\mathbf{Q}}\right)$ is measured in <u>Ohm/m</u>.

At resonance

$$U_{kick} = i\left(\frac{x_0}{k}\right) I_0 Q \left(\frac{r_\parallel}{Q}\right) = i x_0 I_0 Q \left(\frac{r_\perp}{Q}\right).$$

Appendix 10:

Sometimes they use other transverse impedance, that is determined as:

$$\left(\frac{r_\perp}{Q}\right)_1 = \frac{|U_{kick}|^2}{\omega_0 W_0},$$

where W_0 is the energy, stored in the cavity at the RF field amplitude which provides given transverse kick U_{kick}, $W_0 = |A|^2 W$. At the resonance one has

$$|A|^2 = \frac{\left|x_0 I_0 Q \int_{-\infty}^{\infty} \left(\frac{\partial E_z(x,0,z)}{\partial x}\right)_{x=x_0} e^{ikz} dz\right|^2}{(W\omega_0)^2} = \left(\frac{r_\parallel}{Q}\right) \frac{(x_0 I_0 Q)^2}{W\omega_0}$$

and

$$\omega_0 W_0 = \omega_0 W |A|^2 = \left(\frac{r_\parallel}{Q}\right)(x_0 I_0 Q)^2 .$$ On the other hand, $\quad |U_{kick}|^2 = \frac{1}{k^2}\left(x_0 I_0 Q \left(\frac{r_\parallel}{Q}\right)\right)^2$
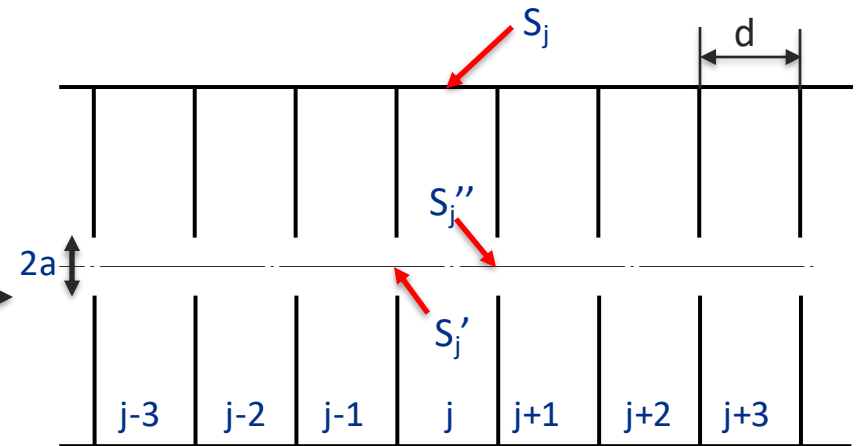
and

$$\left(\frac{r_\perp}{Q}\right)_1 = \frac{|U_{kick}|^2}{\omega_0 W_0} = \left(\frac{r_\parallel}{Q}\right) \times \frac{1}{k^2}.$$

$\left(\frac{r_\perp}{Q}\right)_1$ **is measured in <u>Ohm</u>.** Note that $\quad U_{kick} = i(kx_0)I_0 Q \left(\frac{r_\perp}{Q}\right)_1$

🔷 Fermilab

Appendix 11: Travelling–Wave acceleration structures:

- Each previous cell exits EM filed in a current cell, which in turn excites the field in the next cell.

- Pillbox cells with thin walls

S_i is the cell metallic surface, S_j' and S_j'' are the coupling holes; V is the cell volume.

$\vec{E}_j, \vec{H}_j$ - fields in the jth pillbox cell oscillate at frequency ω;

$\vec{E}_{j,n}, \vec{H}_{j,n}$ - eigenmodes in the jth pillbox cell oscillate at frequency ω_n;

All the fields satisfy Maxwell Equations. Boundary conditions:

$\vec{E}_j \times n = 0$ on S_i; $\vec{E}_{j,n} \times n = 0$ on $S_i + S_j' + S_j''$.

🔷 **Fermilab**

Appendix 11: Travelling–Wave acceleration structures.

We consider the following:

$$\int_{V_j} \vec{\nabla} \cdot \left(\vec{E}_j \times \vec{H}^*_{j,n} \right) dV = \int_{V_j} [\vec{H}^*_{j,n} \cdot \left(\vec{\nabla} \times \vec{E}_j \right) - \vec{E}_j \cdot \left(\vec{\nabla} \times \vec{H}^*_{j,n} \right)] dV$$

$$= \int_{V_j} [-i\omega\mu_0 \vec{H}_j \cdot \vec{H}^*_{j,n} - i\omega_n\varepsilon_0 \cdot \vec{E}^*_{j,n} \cdot \vec{E}_j] dV$$

Using Gauss theorem and boundary conditions we have

$$\omega_n\varepsilon_0 \int_{V_j} \vec{E}^*_{j,n} \cdot \vec{E}_j \, dV - \omega\mu_0 \int_{V_j} \vec{H}_j \cdot \vec{H}^*_{j,n} \, dV = \frac{1}{i} \int_{S'_j + S''_j} \left(\vec{E}_j \times \vec{H}^*_{j,n} \right) \cdot dS \qquad (1)$$

Similarly, by considering

$$\int_{V_j} \vec{\nabla} \cdot \left(\vec{H}_j \times \vec{E}^*_{j,n} \right) dV$$

we have

$$\omega\varepsilon_0 \int_{V_j} \vec{E}^*_{j,n} \cdot \vec{E}_j \, dV - \omega_n\mu_0 \int_{V_j} \vec{H}_j \cdot \vec{H}^*_{j,n} \, dV = 0 \qquad (2)$$

The eigenmode expansion:

$$\vec{E}_j = \sum X_{j,n} \vec{E}_{j,n}$$

$$\vec{H}_j = \sum Y_{j,n} \vec{H}_{j,n}$$

V. Yakovlev | Cavity design. Linac archeticture, Lecture 14

🫱 **Fermilab**

Appendix 11: Travelling–Wave acceleration structures:

By using (1) and (2) we obtain

$$X_{j,n} = -\frac{i\omega_n}{\omega^2 - \omega_n^2} \cdot \frac{\int_{S'_j + S''_j}\left(\vec{E}_j \times \vec{H}_{j,n}^*\right) \cdot dS}{2W_{j,n}} \qquad (3)$$

$$Y_{j,n} = \frac{i\omega}{\omega^2 - \omega_n^2} \cdot \frac{\int_{S'_j + S''_j}\left(\vec{E}_j \times \vec{H}_{j,n}^*\right) \cdot dS}{2W_{j,n}}$$

The eigenmode amplitudes are determined by tangential electric field on the holes, E_{rj}

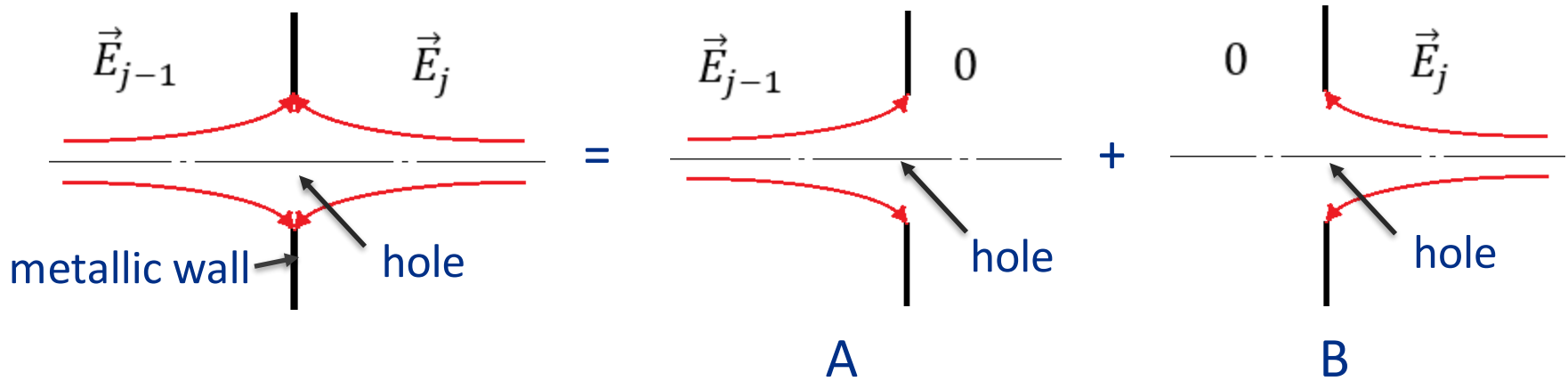How to find E_{rj} for small holes?
1. Quasi-static approximation:
We have: $\Delta\vec{E}_j + k^2\vec{E}_j = 0, \quad k^2 = \frac{\omega^2}{c^2}$
For a small hole, $a \ll \lambda_n$. It means that $\Delta\vec{E}_j \sim \frac{\vec{E}_j}{a^2} \gg k^2\vec{E}_j = \left(\frac{\omega}{c}\right)^2 \vec{E}_j$ and $\Delta\vec{E}_j \approx 0$
i.e., it means that $\vec{E}_j = \vec{\nabla}\Phi, \quad \Delta\Phi = 0$ or electric field is quasi-static.
Far from the holes electric field has only longitudinal (accelerating) component!

‡ Fermilab

Appendix 11: Travelling–Wave acceleration structures:

2. Superposition:

3. Electrostatic problem: conducting sheet at $z=0$ with a circular hole of the radius a, at $z=-\infty$ the field is homogeneous, $E_z=E_0$; at $z=\infty$ the field $E=0$: problem A above. The problem has analytical solution.*

We need to define the radial electric field at the hole, or at $z=0$.

* W.R. Smythe, Static and Dynamic Electricity, 1939, p. 159

🟦 **Fermilab**

Appendix 11: Travelling–Wave acceleration structures:

Oblate spheroidal coordinates:

$$\frac{z^2}{\zeta^2} + \frac{r^2}{1 + \zeta^2} = a^2 \qquad \text{spheroids}$$

$$-\frac{z^2}{\xi^2} + \frac{r^2}{1 - \xi^2} = a^2 \qquad \text{hyperboloids}$$

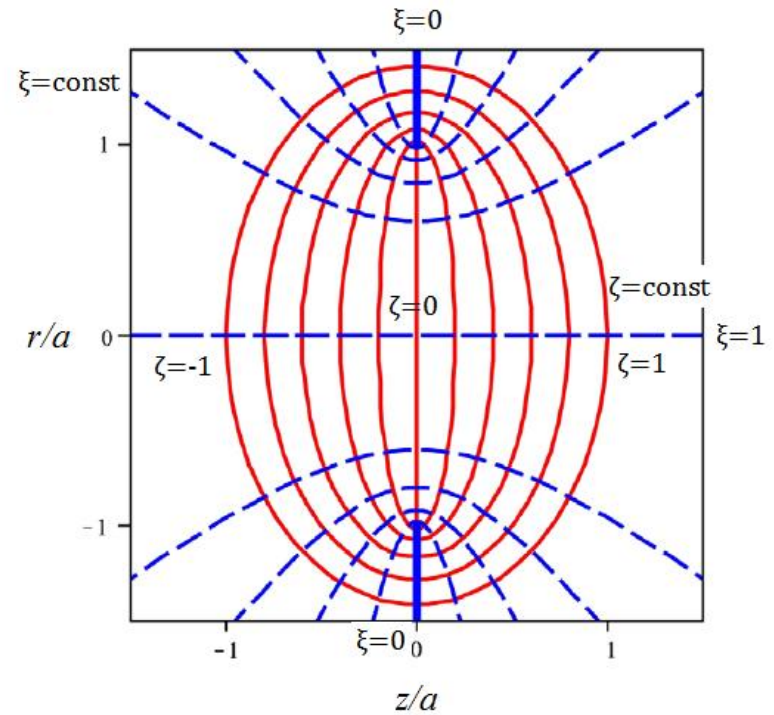$$r = a[(1 + \zeta^2)(1 - \xi^2)]^{1/2}$$

$$z = a\zeta\xi$$

$$\Delta\Phi = 0$$

$$\Phi(\xi, \zeta) = aE_0\xi\left[\zeta - \frac{1}{\pi}(\zeta\cot^{-1}\zeta - 1)\right]$$

$$E_r(r, 0) = \frac{1}{h_1}\nabla_\xi(\Phi(\xi, \zeta)|_{\zeta=0} = E_0\frac{(1 - \xi^2)^{\frac{1}{2}}}{\pi\xi} = E_0\frac{r}{\pi(a^2 - r^2)^{1/2}}$$

$$E_z(r, 0) = \frac{1}{h_2}\nabla_\zeta(\Phi(\xi, \zeta)|_{\zeta=0} = \frac{1}{2}E_0$$

Lamet coefficients

$$h_1 = a\left(\frac{\xi^2 - \zeta^2}{1 - \xi^2}\right)^{1/2}$$

$$h_2 = a\left(\frac{\xi^2 - \zeta^2}{1 + \zeta^2}\right)^{1/2}$$

🔷 **Fermilab**

Appendix 11: Travelling–Wave acceleration structures:

For TM_{010} mode in a pillbox near the axis (see slide 110):

$$E_{j,r}(r)|_{S_j'} = E_0 \frac{r}{\pi(a^2 - r^2)^{1/2}}[X_{j-1} - X_j]$$

$$E_{j,r}(r)|_{S_j''} = E_0 \frac{r}{\pi(a^2 - r^2)^{1/2}}[X_j - X_{j+1}]$$

$$H_{j,\varphi}(r) \approx -iE_0 \frac{(\frac{\omega_0}{c})r}{2Z_0}$$

and from (3), slide 108, we have:

$$X_j\left[1 - (1 + K)\frac{\omega_0^2}{\omega^2}\right] + \frac{1}{2}K\frac{\omega_0^2}{\omega^2}[X_{j-1} + X_{j+1}] = 0 \qquad (4)$$

where K is the coupling. dimensionless parameter:

$$K = \frac{2E_0^2 a^3}{3Z_0 W_0 c} = \frac{2}{3} \cdot \frac{R/Q}{Z_0} \cdot \frac{k_0 a^3}{d^2 T^2} \qquad k_0 = \frac{\omega_0}{c}$$

$K \sim a^3$. For a thick wall $K \sim a^\eta$, $\eta > 3$ *(field decays in the coupling hole).*

Appendix 11: Travelling–Wave acceleration structures:

In the infinite chain of cavities equation (4) has solution (travelling wave):

$$X_j = X e^{ij\varphi}$$
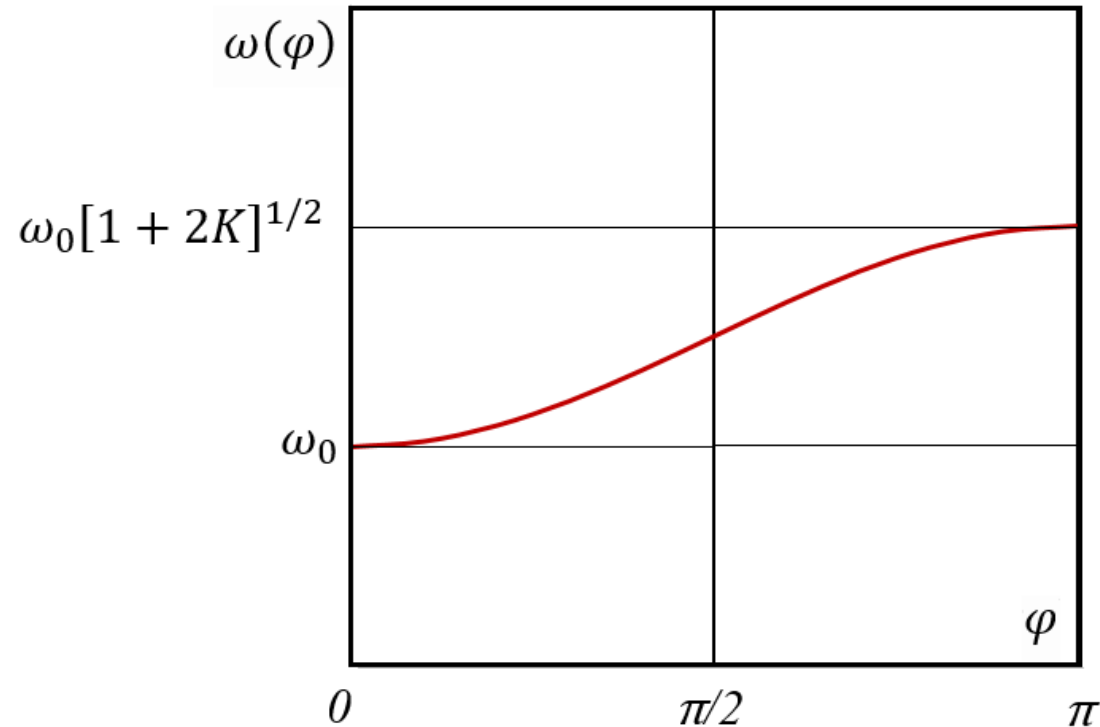
and

$$\omega(\varphi) = \omega_0 [1 + K(1 - cos\varphi)]^{1/2}$$

For small K we have:

$$\omega(\varphi) \approx \omega_0 [1 + \tfrac{1}{2} K(1 - cos\varphi)]$$

One can see that

$$K = \frac{\omega(\pi) - \omega(0)}{\omega(0)}$$

Appendix 11: Travelling–Wave acceleration structures.
The 2d Bell theorem, illustration:

For a pillbox structure:

The fields on the hole are equal to

$$E_{j,r}(r)|_{S'_j} = E_0 \frac{r}{\pi(a^2 - r^2)^{1/2}}[X_{j-1} - X_j]$$
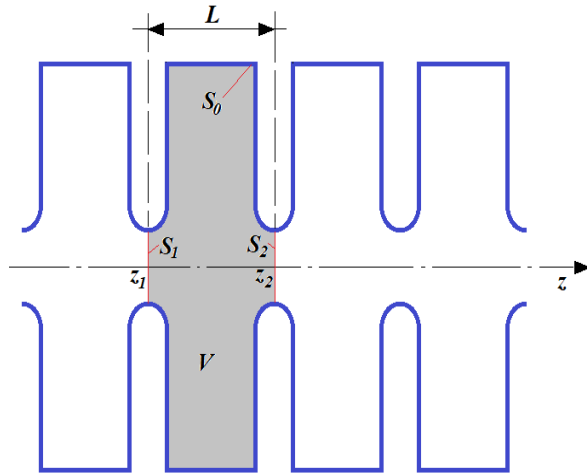
$$H_{j,\varphi}(r)|_{S'_j} \approx -iE_0 \frac{\left(\frac{\omega_0}{c}\right)r}{4Z_0}[X_{j-1} + X_j]$$

(E_z and H_ϕ on the hole are two times smaller than in the cell center, see slides 110-111).

Therefore, we have

$$v_{gr} = \frac{P}{\frac{|X_j|^2 W_0}{d}} = \frac{\frac{1}{2}Re \int E_r H^*_\varphi dS}{\frac{|X_j|^2 W_0}{d}} = \frac{\omega_0 E_0^2 a^3 d}{6Z_0 W_0 c} Re\left[i(X_{j-1} - X_j)(X^*_{j-1} + X^*_j)\right] =$$

$$= \frac{\omega_0 E_0^2 a^3 d}{3Z_0 W_0 c} sin(\varphi) = \frac{\omega_0 d}{2} K sin(\varphi) = c\frac{\pi K d}{\lambda} sin(\varphi) = \frac{d\omega}{dk_z}$$

🔷 **Fermilab**

Bell theorems for periodic acceleration structures, proof

I. Floquet Theorem

"For a given mode of propagation in a periodic system at given steady-state frequency the fields at one cross section differ from that one period away only by complex constant".

$$\vec{E}(x, y, z_2) = \vec{E}(x, y, z_1)e^{-ik_z L}$$
$$\vec{H}(x, y, z_2) = \vec{H}(x, y, z_1)e^{-ik_z L} \qquad (1)$$
$$z_2 = z_1 + L$$

II. 1st Bell Theorem

"The time-average electrical stored energy per period is equal to the time-average magnetic stored energy per period in the passband".

Consider the periodic structure to be divided by a series of surfaces perpendicular to the axis spaced by the periodic distance L. One cell of the structure having the volume V is surrounded by these surfaces S_1 and S_2 and the ideal metal boundary S_0. Let's consider the integral over the surface surrounding the cell, which equals to zero:

$$\oint \vec{E} \times \vec{H}^* \cdot d\vec{s} = \int_{S_0} \vec{E} \times \vec{H}^* \cdot d\vec{s} + \int_{S_1} \vec{E} \times \vec{H}^* \cdot d\vec{s} + \int_{S_2} \vec{E} \times \vec{H}^* \cdot d\vec{s} = 0 \qquad (2)$$

This is because we have

$$\int_{S_0} \vec{E} \times \vec{H}^* \cdot d\vec{s} = 0 \text{ because } E_t = 0 \text{ on } S_0$$

and $\int_{S_1} \vec{E} \times \vec{H}^* \cdot d\vec{s} + \int_{S_2} \vec{E} \times \vec{H}^* \cdot d\vec{s} = 0$ because of (1) and $d\vec{s}_2 = -d\vec{s}_1$

Bell theorems for periodic acceleration structures, proof

From Maxwell equations

$$curl\vec{E} = -i\omega\mu_0\vec{H} \tag{3}$$
$$curl\vec{E}^* = i\omega\mu_0\vec{H}^*$$

and (2) we have

$$\oint \vec{E} \times curl\vec{E}^* \cdot d\vec{s} = 0$$

Applying Gauss's theorem, we get:

$$\int_V div(\vec{E} \times curl\vec{E}^*)dv = 0 . \tag{4}$$

Using the vector theorem (see Appendix 1)

$$div(\vec{A} \times \vec{B}) = \vec{B} \cdot curl\vec{A} - \vec{A} \cdot curl\vec{B}, \tag{5}$$

we get:

$$\int_V (curl\vec{E}^*) \cdot (curl\vec{E})dv - \int_V \vec{E} \cdot (curl(curl\vec{E}^*))dv = 0 .$$

Using Maxwell's equations (3) and the homogenous wave equation derived therefrom (see Lecture 10)

$$curl(curl\vec{E}^*)) = \omega^2\mu_0\varepsilon_0\vec{E}^* \tag{6}$$

we get

$$\int_V (-i\omega\mu_0\vec{H}) \cdot (i\omega\mu_0\vec{H}^*)dv - \int_V \vec{E} \cdot (\omega^2\mu_0\varepsilon_0\vec{E}^*)dv = 0$$

Dividing through $4\omega^2\mu_0$ yields:

$$\boxed{\frac{1}{4}\int_V \mu_0|\vec{H}|^2 dv = \frac{1}{4}\int_V \varepsilon_0|E|^2 dv = W/2,}$$

quod erat demonstrandum.

Here W is total energy of electromagnetic field per period,

$$W = \frac{1}{2}\int_V \varepsilon_0\vec{E} \cdot \vec{E}^* dv = \frac{1}{2}\int_V \mu_0\vec{H} \cdot \vec{H}^* dv$$

‡ Fermilab

Bell theorems for periodic acceleration structures, proof

III. 2^d Bell Theorem

"The time-average power flow in the pass band is equal to the group velocity times time-average electro-magnetic stored energy per period divided by the period."

Consider (4) wherein $\vec{E}$ and $\vec{E}^*$ are functions of frequency ω. Differentiate with respect to frequency:

$$\frac{\partial}{\partial \omega} \int_V div(\vec{E} \times curl\vec{E}^*) dv = 0.$$

It gives:

$$\int_V div\left(\frac{\partial \vec{E}}{\partial \omega} \times curl\vec{E}^*\right) dv + \int_V div\left(\vec{E} \times curl\frac{\partial \vec{E}^*}{\partial \omega}\right) dv = 0.$$

Using the vector identity equation (5), we get

$$\int_V (curl\vec{E}^*) \cdot \left(curl\frac{\partial \vec{E}}{\partial \omega}\right) dv - \int_V \frac{\partial \vec{E}}{\partial \omega} \cdot (curl(curl\vec{E}^*)) dv + .$$

$$+ \int_V (curl\vec{E}) \cdot \left(curl\frac{\partial \vec{E}^*}{\partial \omega}\right) dv - \int_V \vec{E} \cdot \left(curl(curl\frac{\partial \vec{E}^*}{\partial \omega})\right) dv = 0 \, (7)$$

Differentiation (6) with respect to ω gives

$$curl(curl\frac{\partial \vec{E}^*}{\partial \omega})) = 2\omega\mu_0\varepsilon_0\vec{E}^* + \omega^2\mu_0\varepsilon_0\frac{\partial \vec{E}^*}{\partial \omega}$$

Using this in the second and fourth integrals of (7)

$$\int_V (curl\vec{E}^*) \cdot \left(curl\frac{\partial \vec{E}}{\partial \omega}\right) dv - \omega^2\mu_0\varepsilon_0 \int_V \frac{\partial \vec{E}}{\partial \omega} \cdot \vec{E}^* dv +$$

$$+ \int_V (curl\vec{E}) \cdot \left(curl\frac{\partial \vec{E}^*}{\partial \omega}\right) dv - 2\omega\mu_0\varepsilon_0 \int_V \vec{E} \cdot \vec{E}^* dv - \omega^2\mu_0\varepsilon_0 \int_V \frac{\partial \vec{E}^*}{\partial \omega}\vec{E} \cdot dv = 0$$

which is

$$2Re\left\{\int_V (curl\vec{E}^*) \cdot \left(curl\frac{\partial \vec{E}}{\partial \omega}\right) dv - \int_V \frac{\partial \vec{E}}{\partial \omega} \cdot (curl(curl\vec{E}^*)) dv\right\} - 2\omega\mu_0\varepsilon_0 \int_V \vec{E} \cdot \vec{E}^* dv = 0.$$

Bell theorems for periodic acceleration structures, proof

Using (5) in reverse,

$$2Re\left\{\int_V div\left(\frac{\partial\vec{E}}{\partial\omega}\times curl\vec{E}^*\right)dv\right\} - 2\omega\mu_0\varepsilon_0\int_V \vec{E}\cdot\vec{E}^*dv = 0.$$

and using Gauss's theorem on the first term,

$$2Re\left\{\oint\frac{\partial\vec{E}}{\partial\omega}\times curl\vec{E}^*\cdot d\vec{s}\right\} - 2\omega\mu_0\varepsilon_0\int_V \vec{E}\cdot\vec{E}^*dv = 0. \qquad (8)$$

Integral $\int_{S_0}\frac{\partial\vec{E}}{\partial\omega}\times curl\vec{E}^*\cdot d\vec{s} = 0$ because of boundary conditions on the ideal metal surface.

From Floquet theorem (1) the following relation hold:

$$\vec{E}(x,y,z_2) = \vec{E}(x,y,z_1)e^{-ik_zL}$$
$$curl\vec{E}^*(x,y,z)|_{z=z_2} = curl\vec{E}^*(x,y,z)|_{z=z_1}e^{ik_zL} \qquad (9)$$
$$\vec{E}^*(x,y,z_2) = \vec{E}^*(x,y,z_1)e^{ik_zL}$$
$$\frac{\partial\vec{E}(x,y,z_2)}{\partial\omega} = \frac{\partial\vec{E}(x,y,z_1)}{\partial\omega}e^{-ik_zL} - iL\frac{dk_z}{d\omega}\vec{E}(x,y,z_1)e^{-ik_zL}$$

Separating the surface integral of (8)

$$2Re\left\{\int_{S_1}\frac{\partial\vec{E}(x,y,z_1)}{\partial\omega}\times curl\vec{E}^*(x,y,z)|_{z=z_1}\cdot d\vec{s} + \int_{S_2}\frac{\partial\vec{E}(x,y,z_2)}{\partial\omega}\times curl\vec{E}^*(x,y,z)|_{z=z_2}\cdot d\vec{s}\right\} -$$

$$2\omega\mu_0\varepsilon_0\int_V \vec{E}\cdot\vec{E}^*dv = 0$$

and substituting equations (9)

$$2Re\left\{\int_{S_1}\frac{\partial\vec{E}(x,y,z_1)}{\partial\omega}\times curl\vec{E}^*(x,y,z)|_{z=z_1}\cdot d\vec{s} +\right.$$

$$\left.\int_{S_2}\frac{\partial\vec{E}(x,y,z_1)}{\partial\omega}\times curl\vec{E}^*(x,y,z)|_{z=z_1}\cdot d\vec{s} - iL\frac{dk_z}{d\omega}\int_{S_2}\vec{E}(x,y,z_1)\times curl\vec{E}^*(x,y,z)|_{z=z_1}\cdot d\vec{s}\right\} -$$

$$2\omega\mu_0\varepsilon_0\int_V \vec{E}\cdot\vec{E}^*dv = 0$$

☼ Fermilab

Bell theorems for periodic acceleration structures, proof

Since $d\vec{s}_2 = -d\vec{s}_1$ the first two integrals cancel. Using Maxwell equation (3) and condition s (9) we get

$$2Re\left\{\omega\mu_0 L \frac{dk_z}{d\omega}\int_{S_2} \vec{E}(x,y,z_2) \times \vec{H}^*(x,y,z_2) \cdot d\vec{s}\right\} - 2\omega\mu_0\varepsilon_0\int_V \vec{E}\cdot\vec{E}^* dv = 0$$

Multiplying by $\frac{1}{4\omega\mu_0 L}\frac{d\omega}{dk_z}$ we finally have

$$\frac{1}{2}Re\left\{\int_{S_2} \vec{E}(x,y,z_2) \times \vec{H}^*(x,y,z_2) \cdot d\vec{s}\right\} = \frac{d\omega}{dk_z}\cdot\frac{1}{L}\cdot\frac{1}{2}\int_V \varepsilon_0\vec{E}\cdot\vec{E}^* dv = 0$$

or

$$\boxed{P = v_{gr}w,}$$

here

$P = \frac{1}{2}Re\left\{\int_{S_2} \vec{E}(x,y,z_2) \times \vec{H}^*(x,y,z_2) \cdot d\vec{s}\right\}$ is the time averaged power flaw in the passbands;

$v_{gr} = \frac{d\omega}{dk_z}$ is a group velocity;

$w = \frac{1}{L}\cdot\frac{1}{2}\int_V \varepsilon_0\vec{E}\cdot\vec{E}^* dv = \frac{1}{L}\cdot\frac{1}{2}\int_V \mu_0\vec{H}\cdot\vec{H}^* dv = \frac{W}{L}$ is the time-averaged stored electromagnetic energy per unit length.

[1] J.S. Bell, "Group velocity and energy velocity in periodic waveguides," Harwell, AERE-T-R-858 (1952)
[2] D.A. Watkins, Topics in Electromagnetic Theory, John Willey & Sons, Inc. London, 1958
[3] E. A. *Burshtein*, and G. B. *Voskresensky*, The Intensive Beam Electron Linear Accelerators, Atomizdat, Moscow, 1970.

🔷 **Fermilab**

Appendix 12: Standing –Wave acceleration structures. Perturbation theory.

In matrix form Eq(1), see Lecture 8, Slide 31:

$$M\hat{X} - \frac{\omega_0^2}{\omega^2}\hat{X} = 0$$

here $\quad M_{jj} = 1; \ j = 0,1,\dots N;$

$$M_{jj-1} = \frac{K}{2W(j)}; \ j = 1,2,\dots N; \ M_{jj+1} = \frac{K}{2W(j)}; j = 0,1,\dots N-1.$$

and $\quad W(j) = 1, j = 1,2,\dots N-1 \quad W(j) = \frac{1}{2}, j = 0,N$

Eigenvectors and eigenvalues:

$$\hat{X}_j^q = cos\frac{\pi qj}{N}; \ \omega_q^2 = \frac{\omega_0^2}{1 + Kcos\frac{\pi q}{N}}, q = 0,1,\dots N$$

Orthogonality:

$$\hat{X}^q \cdot \hat{X}^r \equiv \sum_{j=0}^{N} W(j)\,\hat{X}_j^q\hat{X}_j^r = \frac{N\delta_{qr}}{2W(q)}, \quad \delta_{qq} = 1, and \ \delta_{qr} = 0, if \ q \neq r$$

‡ Fermilab

Appendix 12: Standing –Wave acceleration structures. Perturbation theory

- Perturbation of the cell resonance frequencies causes perturbation of the mode resonance frequencies $\delta\omega_q$;
- the field distribution $\delta\hat{X}_q$.

$$\omega_{0j}^{2\prime} = \omega_0^2 + \delta\omega_{0j}^2 \quad \rightarrow \quad \hat{X}^{q\prime} = \hat{X}^q + \delta\hat{X}^q, \quad \hat{X}^q \cdot \delta\hat{X}^q$$

Variation of the equation (1), see previous slide, gives

$$M\delta\hat{X}^q = \frac{\omega_0^2}{\omega_q^2}\left[\delta\hat{X}^q + \Omega\hat{X}^q - \frac{\delta\omega_q^2}{\omega_q^2}\hat{X}^q\right], \quad \text{where} \quad \Omega = \begin{bmatrix} \dfrac{\delta\omega_{01}^2}{\omega_0^2} & \cdots & 0 \\ \vdots & \ddots & \vdots \\ 0 & \cdots & \dfrac{\delta\omega_{0N}^2}{\omega_0^2} \end{bmatrix}$$

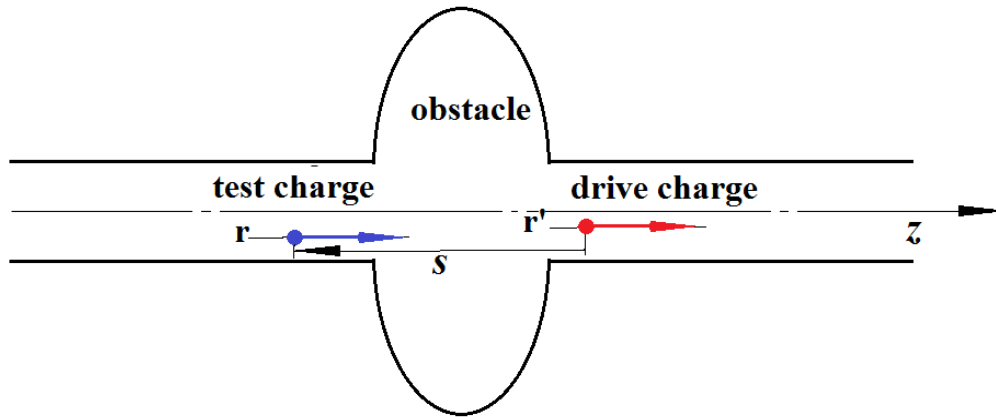$$\frac{\delta\omega_q^2}{\omega_q^2} = [2W(q)/N] \cdot \hat{X}^q\Omega\hat{X}^q;$$
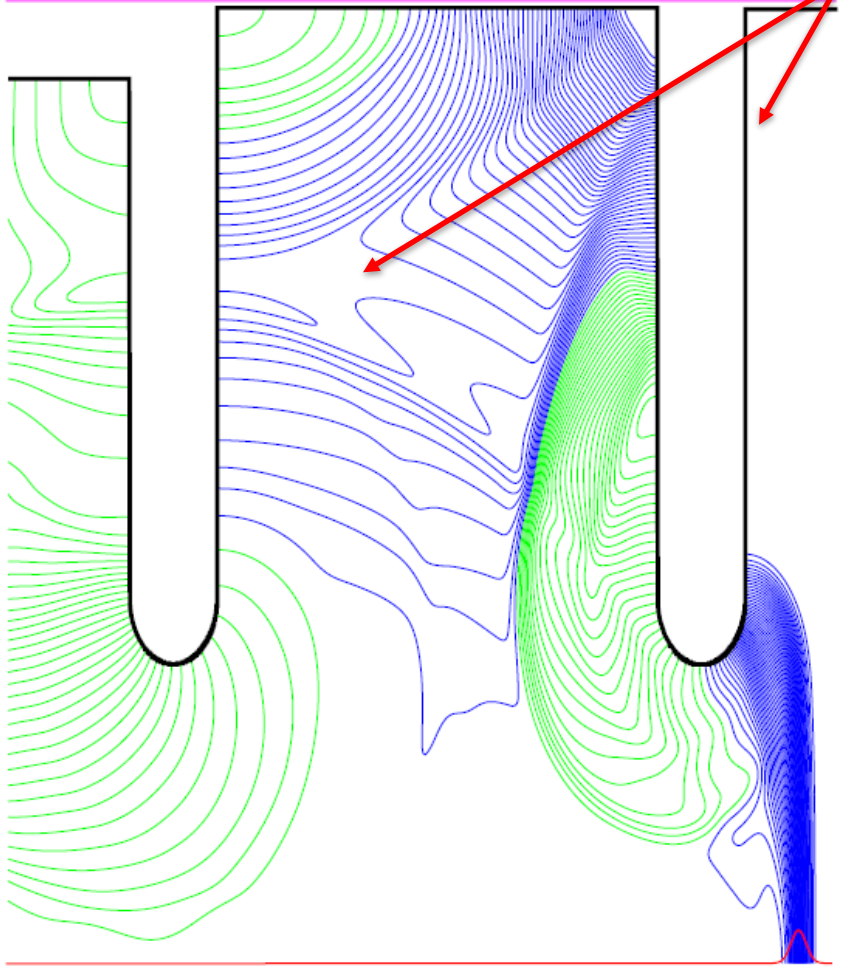
$$\delta\hat{X}^q = \sum_{q\prime \neq q} \frac{2W(q\prime)\hat{X}^q\Omega\hat{X}^q}{N\left(\dfrac{\omega_q^2}{\omega_{q\prime}^2} - 1\right)}\hat{X}^{q\prime}$$

$$\left|\delta\hat{X}^q\right| \sim \frac{\left|\delta\omega_{0j}\right|_{av}}{\left|\omega_q - \omega_{q\pm1}\right|}$$

‡ Fermilab

Appendix 13: Wake potentials

Acceleration cells

Radiation fields in the
TW acceleration structure

A. Novokhatski

Blue – deceleration
Green - acceleration

bunch

$$W_z(\vec{r}, \vec{r}', s) = -\frac{1}{q} \int_{z_1}^{z_2} dz \, [E_z(\vec{r}, z, t)]_{t=(z+s)/c} \ ,$$

$$\overrightarrow{W}_\perp(\vec{r}, \vec{r}', s) = \frac{1}{q} \int_{z_1}^{z_2} dz \, \left[\vec{E}_\perp + c(\hat{z} \times \vec{B})\right]_{t=(z+s)/c} .$$

$W_z=0, \ W_\perp =0 \ for \ s<0$

🟦 **Fermilab**

Appendix 13: Wake potentials

Loss and kick distribution along the bunch $V_z(s)$ and $V_\perp(s)$:

$$V_z(s) = \int_0^\infty ds' \, \lambda(s - s') \, W_z(s') = \int_{-\infty}^s ds' \, \lambda(s') \, W_z(s - s') \,,$$

$$\vec{V}_\perp(s) = \int_0^\infty ds' \, \lambda(s - s') \, \vec{W}_\perp(s') = \int_{-\infty}^s ds' \, \lambda(s') \, \vec{W}_\perp(s - s') \,.$$

$\lambda(s)$ is the charge distribution along the bunch.

Total losses and kick:

$$\Delta U = \int_{-\infty}^\infty ds \, \lambda(s) \, V_z(s), \quad k_\ell = \frac{\Delta U}{q^2} \equiv \frac{1}{q^2} \int_{-\infty}^\infty ds \, \lambda(s) \, V_z(s) \qquad k_l - \text{loss factor}$$

$$k_{HOM} = k_l - \frac{1}{4} \, R/Q \cdot \omega|_{acc. \, mode}$$

$$\vec{p}_\perp = q^2 \vec{k}_\perp / c \qquad \vec{k}_\perp \equiv \frac{1}{q^2} \int_{-\infty}^\infty ds \, \lambda(s) \, \vec{V}_\perp(s) \qquad \vec{k}_\perp - \text{kick factor}$$

🔷 Fermilab

Appendix 13: Wake potentials

Panofsky-Wenzel theorem for wakes:

$$\frac{\partial \overrightarrow{W}_\perp}{\partial s} = \frac{c}{eq}\frac{\partial \vec{p}_\perp}{\partial s} = -\frac{1}{q}\int_0^L dz \left[\overrightarrow{\nabla}_\perp E_z(z,t)\right]_{t=(s+z)/c} = \overrightarrow{\nabla}_\perp W_z.$$

Relation between wake and impedance:

$$Z(\omega) = \int_0^\infty W_z(\tau)\,\exp\{-i\omega\tau\}\,d\tau \equiv \widetilde{W}_z(\tau),$$

$$Z(k) = \int_0^\infty W_z(s)\,\exp\{-iks\}\,ds \equiv \widetilde{W}_z(s) = c\,[Z(\omega)]_{\omega=kc}$$

$$s = c\tau = ct - z$$

and

$$k_\ell = \frac{\Delta U}{q^2} = \frac{1}{\pi q^2}\int_0^\infty Z_R(\omega)\,I^2(\omega)\,d\omega.$$

Fermilab